# RADIOGENIC ISOTOPES: TRACERS OF PAST OCEAN CIRCULATION AND EROSIONAL INPUT

Martin Frank
*Department of Earth Sciences*
*Institute for Isotope Geology and Mineral Resources*
*Eidgenössische Technische Hochschule*
*Zürich, Switzerland*

Received 2 November 2000; revised 28 January 2002; accepted 1 February 2002; published 23 August 2002.

[1] The radiogenic isotope composition of dissolved trace metals in the ocean represents a set of relatively new and not yet fully exploited tracers with a large potential for oceanographic and paleoceanographic research on timescales from the present back to at least 60 Ma. The main topic of this review are those trace metals with oceanic residence times on the order of or shorter than the global mixing time of the ocean (Nd, Pb, Hf, and, in addition, Be). Their isotopic composition in the ocean has varied as a function of changes in paleocirculation, source provenances, style and intensity of weathering on the continents, as well as orogenic processes. The relative importance of these processes for each trace metal is evaluated, which is a prerequisite for reliable interpretation of their time series in terms of changes in paleocirculation or weathering inputs. This analysis of processes includes a discussion of the long-term isotopic evolution of Sr and Os, which are well mixed in the ocean and have thus not been influenced by circulation changes. The radiogenic isotope evolution of those trace metals with intermediate oceanic residence times can be used as paleoceanographic proxies to reconstruct paleocirculation and weathering inputs into the ocean. This is demonstrated by studies from different ocean basins, mainly carried out on ferromanganese crusts, which show that radiogenic trace metal isotopes provide important new insights and can complement results obtained by other well-established paleoceanographic tracers such as carbon isotopes. *INDEX TERMS:* 1040 Geochemistry: Isotopic composition/chemistry; 4267 Oceanography: General: Paleoceanography; 4283 Oceanography: General: Water masses; 4875 Oceanography: Biological and Chemical: Trace elements; 4885 Oceanography: Biological and Chemical: Trace elements; *KEYWORDS:* ocean circulation, weathering, trace elements, paleoceanography, isotope geochemistry, water masses

## 1. INTRODUCTION

### 1.1. Present-Day Ocean Circulation

[2] In a simplified model the modern global ocean circulation system is largely driven by the sinking of cold, saline (and therefore dense) water masses at high geographical latitudes [cf. *Gordon*, 1986; *Broecker*, 1991; *Schmitz*, 1995]. The most important location for deep-water production is the North Atlantic Ocean, where essentially four different sources (Iceland Scotland Ridge Overflow Water and Denmark Strait Overflow Water, which both originate from downwelling in the Norwegian/Greenland Seas, Labrador Seawater, and Lower Deep Water, which is derived from the Southern Ocean) produce a flow of some 15 ± 2 sverdrup (Sv) (1 Sv = $10^6$ $m^3$ $s^{-1}$) of North Atlantic Deep Water (NADW) according to latest estimates based on results of the World Ocean Circulation Experiment [*Ganachaud and Wunsch*, 2000] (Figure 1). NADW has a characteristic temperature and salinity and flows south, thereby entraining northward flowing Antarctic Bottom Water (AABW) from below and Antarctic Intermediate Water (AAIW) from above resulting in an increased flow of 23 ± 3 Sv when it leaves the South Atlantic at 30°S and joins the Antarctic Circumpolar Current (ACC) system and its main water mass Circumpolar Deep Water (CDW). The ACC flows eastward at a rate of 140–150 Sv, which makes it the largest current of the ocean in terms of volume transport.

[3] The Antarctic ice shelves represent a second important source of deep water. There, deep water is produced by formation of sea ice, which consists of freshwater and leaves a highly saline and cold brine behind, which sinks because of its high density. Through mixing of this water with other water masses, mainly CDW, 21 ± 6 Sv AABW are formed, which is denser than NADW. Bottom water originating from the Southern Ocean (eventually a mixture of AABW and NADW) flows northward in all three major ocean basins where the net inflow amounts to 6 ± 1.3 Sv into the Atlantic Ocean, 11 ± 4 Sv into the Indian Ocean, and 7 ± 2 Sv into the Pacific Ocean [*Ganachaud and Wunsch*, 2000].




8755-1209/02/2000RG000094
10.1029/2000RG000094

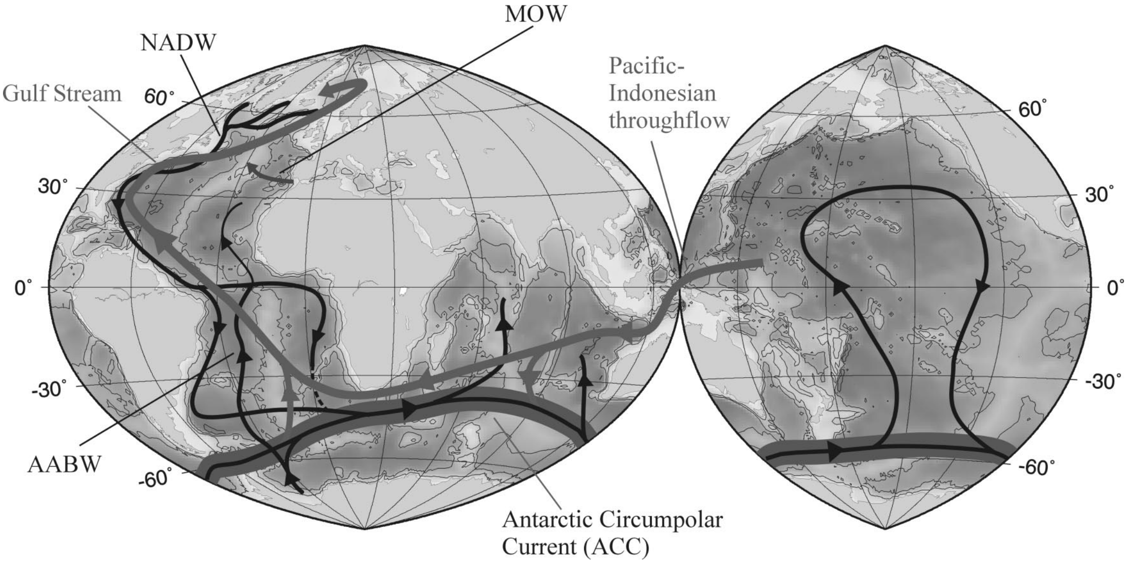


**Figure 1.** Simplified picture of the present-day global thermohaline circulation (single cell) following the two-layer conveyor belt model of *Schmitz* [1995]. Deep and bottom current flows are given as black lines (such as North Atlantic Deep Water (NADW) or Antarctic Bottom Water (AABW)), and surface flows are given as red lines (such as the Pacific-Indonesian throughflow or the Gulf Stream). The small purple arrow in the Atlantic marks the Mediterranean Outflow Water (MOW). The thick purple line marks the Antarctic Circumpolar Current (ACC), which flows eastward at all depth levels.

The northward flow of these deep and bottom water currents into the Pacific and Indian Oceans is mainly balanced by southward flowing intermediate and deep waters. Major upper level currents balancing mass flux at depth are the Pacific-Indonesian throughflow at a rate of 16 ± 5 Sv and thermocline waters from the Southern Ocean, which flow north in the Atlantic Ocean at a rate of 16 ± 3 Sv (AAIW and eventually the Gulf Stream surface current). Together these currents, whose detailed distribution and water mass exchange is much more complicated in detail, form the global thermohaline circulation. This system largely controls the transfer of heat and moisture on Earth and is thus one of the most important factors controlling global climate. There is evidence that the thermohaline circulation system is more complex than previously thought in that there may not only be one single global thermohaline circulation cell, but that two nearly independent cells coexist in which turbulent flow plays an important role [*Macdonald and Wunsch*, 1996]. In addition, it has recently been speculated that diapycnal mixing rates (vertical diffusive mixing across water mass boundaries) may have been overestimated in ocean circulation models, which is important with respect to air-sea gas exchange [*Archer et al.*, 2000]. Nevertheless, the overall general circulation patterns and amounts of water mass exchanged in the present-day ocean can be considered valid and will serve as a basis for the interpretation of the radiogenic isotope results.

## 1.2. Ocean Circulation in the Past

[4] The current mode of ocean circulation has gone through substantial changes in the past. On decadal timescales, for example, a strongly reduced deep-water production in the Greenland Sea was observed during the 1980s which might have been caused by anthropogenic perturbations of the climate system [*Schlosser et al.*, 1991]. For reconstructions of the distributions and flow patterns of water masses in the more distant past, classic tools of oceanographers, temperature and salinity, which are conservative in the ocean, as well as nutrient concentrations, such as phosphate, nitrate or silica, which are typical of certain water masses, are not preserved. Therefore a number of proxy tracers have been developed to extract information on water mass distribution and flow in the past from the marine sediments. The most commonly applied geochemical proxies to reconstruct past deep-water circulation have been the stable carbon isotope composition ($\delta^{13}C$) given in per mill:

$$\delta^{13}C = \left[\frac{\left(\frac{^{13}C}{^{12}C}\,\mathrm{SAMPLE}\right) - \left(\frac{^{13}C}{^{12}C}\,\mathrm{STD}\right)}{\frac{^{13}C}{^{12}C}\,\mathrm{STD}}\right] 1000$$

[cf. *Curry and Lohmann*, 1983; *Curry et al.*, 1988; *Woodruff and Savin*, 1989; *Raymo et al.*, 1992; *Sarnthein et al.*, 1994; *Ravelo and Andreasen*, 2000] and the Cd/Ca ratio [*Boyle*, 1988, 1992] as recorded and preserved by benthic foraminifera. The $\delta^{13}C$ of deep water is generally anticorrelated with nutrient (phosphate) concentration because of the preferential incorporation of $^{12}C$ into organic matter (thus low in $\delta^{13}C$) at the surface of the ocean which is released together with nutrients during organic matter remineralization at depth. Cd/Ca corre-

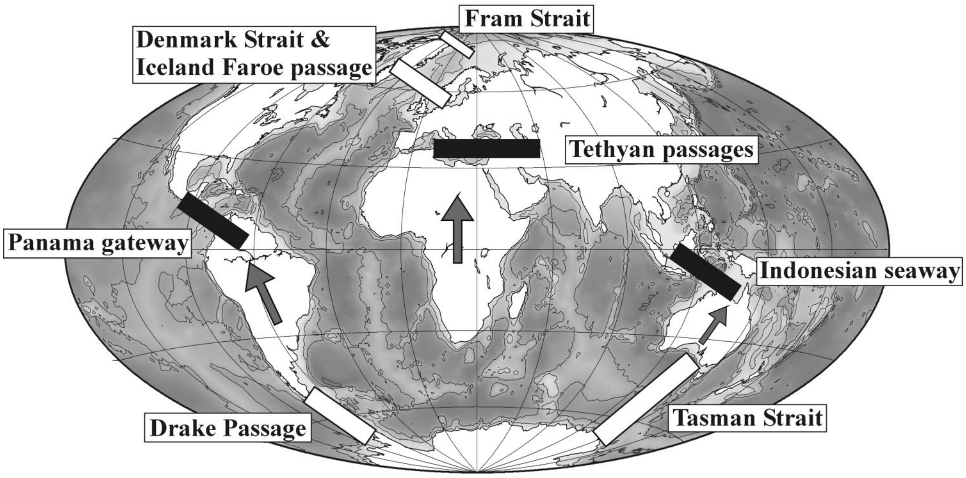


**Figure 2.** Locations of major paleogeographic changes over the past 50 Myr which have influenced the circulation pattern of the ocean. Ocean gateways which essentially closed over this period are indicated by solid bars, whereas the ones that opened up are indicated by open bars. Arrows indicate general directions of plate tectonic movements of the continents. Note that there has been a general trend to close low-latitude gateways, while high-latitude ones opened up.

lates positively with nutrient concentrations (phosphate, nitrate). This allows the distinction between low-nutrient (such as NADW) and high-nutrient deep waters (such as in the North Pacific) in the past. For example, comparison of the $\delta^{13}C$ gradients between the Atlantic and Pacific revealed a major reduction in the vigor of the global thermohaline during the glacial periods of the Pleistocene [*Raymo et al.*, 1990]. The same result was also obtained from reconstructions of the oceanic distribution of $^{14}C$ during the last glacial period [*Broecker et al.*, 1990].

[5] It is, however, difficult to make quantitative estimates of mixing between water masses on the basis of Cd/Ca or $\delta^{13}C$ data because neither of the two proxies may exclusively mirror the nutrient content of ambient deep water. In the case of $\delta^{13}C$, nonconservative effects of temperature and nutrient availability (see overview by *Broecker and Peng* [1982]) or variability in carbonate ion concentration [*Spero et al.*, 1997] are potentially superimposed. For Cd/Ca, problems arise from thermodynamic effects [*Boyle*, 1988]. Nevertheless, $\delta^{13}C$ and Cd/Ca have clearly been the most reliable proxies for past water mass distribution, which have been improved and refined over the past two decades. It is those tracers from which most of our present knowledge on past ocean circulation has been derived, and in most areas of the world ocean they yield consistent results. There are only few areas where results obtained from $\delta^{13}C$ and Cd/Ca are not consistent, which probably reflects some of the effects described above. One example is the Southern Ocean, where Cd/Ca shows no differences between the glacial and interglacial deep-water signal [*Boyle*, 1992], but $\delta^{13}C$ indicates a major decrease or even shut-down of glacial NADW input into the Southern Ocean [*Charles and Fairbanks*, 1992]. In addition, Cd/Ca and $\delta^{13}C$ are tracers of nutrient concentrations, which are controlled by processes in the surface ocean. Thus deep-water masses of different origins within an ocean basin may have essentially the same Cd/Ca and $\delta^{13}C$ signatures but cannot be distinguished further without additional information.

[6] An alternative approach to evaluate the strength of the global thermohaline circulation on glacial-interglacial timescales has involved the use of the $^{231}Pa/^{230}Th$ ratio adsorbed to marine sediment particles [*Yu et al.*, 1996]. From similar glacial and interglacial amounts of $^{231}Pa$ exported from the Atlantic basins into the Southern Ocean, *Yu et al.* [1996] concluded that there was no significant difference between glacial and interglacial strength of NADW production and thus thermohaline circulation. However, it was later suggested that the $^{231}Pa/^{230}Th$ ratio in the Southern Ocean may be less sensitive to changes in NADW export than previously suggested, thus preventing a quantitative reconstruction of water mass mixing with this proxy [*Asmus et al.*, 1999]. In addition, it has been claimed that the uncertainties of the mean Atlantic $^{231}Pa/^{230}Th$ ratios of the Holocene and the Last Glacial Maximum are too large to rule out even large changes in NADW export [*Marchal et al.*, 2000].

[7] On Cenozoic timescales, paleogeographic changes, such as openings and closings of oceanic gateways (Figure 2), have been responsible for large-scale reorganizations of the global ocean circulation and were intimately linked to global climate (see *Zachos et al.* [2001] for a recent summary). Tectonically induced initiation (cessation) of water mass exchange between ocean basins caused converging (diverging) evolution of organisms in the respective basins and was also recorded by changes of geochemical parameters such as the corrosiveness of deep waters to carbonate. One of the most important openings that led to dramatic changes of the

global ocean circulation in the course of the Tertiary was the stepwise establishment of the ACC. This started by rifting and subsequent northward drift of Australia away from the Antarctic at about 55 Ma and led to the establishment of a deep-water passage, the Tasman Strait, at about 30–25 Ma [*Weissel and Hayes*, 1972; *Kennett*, 1977]. The opening of Drake Passage between South America and the Antarctic at roughly 23 Ma [*Barker and Burrell*, 1977] completed this process, which eventually permitted unrestricted water mass exchange around the Antarctic, thermal isolation, and, ultimately, continuous Antarctic glaciation since about 14 Ma [cf. *Kennett*, 1977]. Over the period between 25 and 5 Ma other low-latitude gateways such as the Tethyan passages and the Indonesian seaway were closing with respect to deep-water circulation (Figure 2). The most recent major event was the progressive shallowing and closing of the Panama gateway, which was finalized by the emergence of the Isthmus of Panama, at about 3.5 Ma [*Keigwin*, 1982]. This stopped the direct exchange of Pacific and Atlantic water masses at low latitudes.

[8] Mechanisms of deep-water production prior to these paleogeographic changes (for example during the Eocene) were completely different than today. The global circulation system was dominated by meridional currents, and no significant ice caps at the poles existed. The ocean was ventilated by halothermal processes, whereby warm and highly saline oxygen-rich water masses sank at low latitudes, as evidenced by estimates of deep-water temperatures of up to 12°–14°C during the Eocene period at about 50 Ma [*Miller et al.*, 1987; *Lear et al.*, 2000]. The following paleogeographic reorganizations during the Tertiary caused a stepwise transition from a global ocean circulation system dominated by meridional currents at low latitudes toward the more latitudinally dominated circulation system of the present-day with its production of cold deep waters at high latitudes [cf. *Haq*, 1981].

[9] Related to these circulation changes, global climate has shown a general cooling since the Eocene climate optimum at circa 50 Ma. This general trend has been punctuated by steps during which the global climate exceeded thresholds permitting the first Antarctic glaciation at the Eocene-Oligocene boundary, the establishment of the present Asian monsoonal system at about 7 Ma, and the initiation of Northern Hemisphere glaciation and its glacial-interglacial cyclicity at 3 Ma [cf. *Zachos et al.*, 2001]. These steps were also related to the uplift of major orogens such as the Himalayas, with particular importance of the Tibetan Plateau, and the Andes, which had major consequences for the global atmospheric circulation patterns, the distribution of the climate zones, and the intensity and style of weathering on the continents [e.g., *Raymo and Ruddiman*, 1992].

### 1.3. Radiogenic Isotopes as Water Mass Proxies

[10] The radiogenic isotope ratios of trace metals dissolved in seawater discussed in this review are independent of fractionation induced by biological processes or evaporation. As a consequence, a change in the trace metal isotope composition of a water mass can only occur by addition from a reservoir of the respective trace metal with a different isotope composition. The factors other than mixing controlling the radiogenic isotope composition of a water mass are completely independent from the processes controlling $\delta^{13}C$ or Cd/Ca, and thus radiogenic isotopes can provide useful additional tracer information on past water mass exchange. The focus of this review will be on trace metals with an ocean residence time on the order of or shorter than the average circulation time of the global ocean, approximately 1500 years. If the residence time of a metal in the ocean is very short, for example, that of Th is only 5–20 years, it will not be suitable for this approach because water mass bodies will not be able to develop a typical signature which is traceable over longer distances. If, on the other hand, the residence time is too long, as is the case for U, Sr, and Os with oceanic residence times on the order of tens to hundreds of kiloyears or even million years, any water mass signatures will have been removed by mixing. In addition, the half-lives of any radioactive trace metal isotopes ($^{10}Be$) have to be long relative to the mixing times, at least within an ocean basin. The half-life obviously also has to be long enough to allow for the variability in trace metal isotope composition to be preserved on the timescales of the paleoceanographic reconstruction. These requirements leave the following metals suitable for this study: Nd, Pb, Hf (for these three metals all applied isotopes are stable), and the ratio between radioactive $^{10}Be$ and stable $^{9}Be$ (Table 1). For a reliable reconstruction of paleoceanographic changes using radiogenic isotopes, the evolution of the long residence time radiogenic isotope systems of Os and Sr provide valuable information on changes of the global weathering inputs, which have potentially also influenced the signals of the shorter residence time tracers. Os and Sr isotopes will therefore also be discussed.

### 1.4. Origin of Radiogenic Isotope Variability in the Ocean

[11] During extraction of the continental crust from the mantle and subsequent reworking during Earth's history, elements have been fractionated. Some of these elements are radioactive and produce daughter isotopes of other elements. As an example, Sm/Nd ratios in Earth's mantle and thus also mantle-derived rocks such as mid-ocean ridge basalts are generally higher than in the continental crust because Sm stays preferentially in the mantle during the formation of continental crust. $^{147}Sm$ is radioactive and produces stable $^{143}Nd$ at a very slow rate (the half-life of $^{147}Sm$ is 106 Gyr). Consequently, the abundance of $^{143}Nd$ in a rock relative to those of other stable isotopes of Nd, such as $^{144}Nd$, vary as a function of age and Sm/Nd ratio.

[12] Similar to Nd, there is a stable Hf isotope, $^{176}Hf$, which causes variations in the $^{176}Hf/^{177}Hf$ ratio ($^{177}Hf$ is

**TABLE 1. Radiogenic Isotope Systems Used as Tracers in the Ocean**

| Element | Radiogenic Isotopes | Parent Isotopes | Half-Life | Primordial Isotopes[a] | Average Elemental Deep-Water Concentration | Average Deep-Water Residence Time, years | Input Sources |
|---|---|---|---|---|---|---|---|
| Nd | $^{143}$Nd | $^{147}$Sm | 106 Gyr | $^{142}$Nd, **$^{144}$Nd**, $^{145}$Nd, $^{146}$Nd, $^{148}$Nd, $^{150}$Nd | 4 pg g$^{-1}$ | 600–2000 | erosion of continental crust |
| Pb | $^{206}$Pb | $^{238}$U | 4.47 Gyr | **$^{204}$Pb** | 1 pg g$^{-1}$ | ~50 (Atlantic) | erosion of continental crust |
| | $^{207}$Pb | $^{235}$U | 704 Myr | | | ~200–400 (Pacific) | minor hydrothermal inputs |
| | $^{208}$Pb | $^{232}$Th | 14 Gyr | | | | |
| Hf | $^{176}$Hf | $^{176}$Lu | 37.3 Gyr | $^{174}$Hf, **$^{177}$Hf**, $^{178}$Hf, $^{179}$Hf, $^{180}$Hf | 0.2 pg g$^{-1}$ | ~2000 | erosion of continental crust; hydrothermal inputs |
| Os | $^{187}$Os | $^{187}$Re | 43 Gyr | **$^{188}$Os**[b] ($^{186}$Os) | 10.8 fg g$^{-1}$ | 10,000–20,000 | erosion of continental crust; leaching of abyssal peridotites; cosmic particles |
| Sr | $^{87}$Sr | $^{87}$Rb | 48.8 Gyr | **$^{86}$Sr** | 7.6 μg g$^{-1}$ | Several Myrs | weathering of continental crust; hydrothermal inputs; dissolution of marine carbonates |
| Be | $^{10}$Be[c] | (cosmogenic) | 1.5 Myr | **$^{9}$Be** (stable) | $^{9}$Be: 0.25 pg g$^{-1}$ | 200–1000 | $^{10}$Be: atmospheric fallout |
| | | | | | $^{10}$Be: 1500–2000 atoms g$^{-1}$ | | $^{9}$Be: erosion of continental crust |

[a]The primordial isotopes printed in boldface are those commonly used for the radiogenic isotope ratios.
[b]The isotope $^{186}$Os has previously been used for the isotope ratios as well.
[c]The isotope $^{10}$Be is not formed by decay of a parent isotope but is radioactive itself. Nevertheless, the ratio between $^{10}$Be and $^{9}$Be in the ocean can be used in a similar way as the radiogenic isotope systems for the past 10 Myr.

primordial) between different rocks because of radiogenic ingrowth from decay of its parent isotope $^{176}$Lu (half-life is 37.3 Gyr). For Pb, there are three stable isotopes ($^{206}$Pb, $^{207}$Pb, $^{208}$Pb) which are the final products of the three U decay series with the parent isotopes $^{238}$U, $^{235}$U and $^{232}$Th (half-lives are 4.47 Gyr, 0.704 Gyr, and 14 Gyr, respectively). In addition, there is primordial $^{204}$Pb. Os shows variations in its $^{187}$Os/$^{188}$Os ratio ($^{188}$Os is primordial) between rocks due to decay of the parent isotope of $^{187}$Os, $^{187}$Re (half-life is 43 Gyr). Analogous to Nd, the isotope ratios of Pb, Hf, Os, and Sr in crustal rocks vary as a function of age and the ratios between daughter and parent isotope abundances.

[13] The release of trace metals with different isotope ratios from Earth's crust by weathering or hydrothermal processes is the basis for the observed variability in the ocean's water masses. Because of the very small differences among $^{143}$Nd/$^{144}$Nd ratios and $^{176}$Hf/$^{177}$Hf ratios, which are mostly at the fourth or even fifth decimal place, Nd isotope ratios are expressed as $\varepsilon_{Nd}$ values:

$$\varepsilon_{Nd}=\left[\frac{\left(\frac{^{143}\mathrm{Nd}}{^{144}\mathrm{Nd}}\,\mathrm{SAMPLE}\right)-\left(\frac{^{143}\mathrm{Nd}}{^{144}\mathrm{Nd}}\,\mathrm{CHUR}\right)}{\frac{^{143}\mathrm{Nd}}{^{144}\mathrm{Nd}}\,\mathrm{CHUR}}\right]10{,}000\,,$$

where CHUR is the $^{143}$Nd/$^{144}$Nd of the chondritic uniform reservoir (presently 0.512638). Analogous to Nd, Hf isotope ratios are given as $\varepsilon_{Hf}$ values, with a $^{176}$Hf/$^{177}$Hf for CHUR of 0.282769 [*Nowell et al.,* 1998]. CHUR stands for a model describing the terrestrial Nd and Hf isotope evolution from a uniform reservoir whose Sm/Nd and Lu/Hf ratios are equal to those of chondritic meteorites. All time series of $\varepsilon_{Nd}$ and $\varepsilon_{Hf}$ in this review have been corrected to the corresponding value of CHUR at the time of their deposition in the marine archives.

[14] The variability of the Be isotope ratio, $^{10}$Be/$^{9}$Be, in the ocean is mainly caused by oceanic processes (see section 3.5).

## 1.5. Analytical Techniques

[15] Following chemical separation, preconcentration, and purification, the radiogenic isotope ratios of the trace metals (on amounts as low as a few nanograms) are determined at high precision by various techniques of mass spectrometry. It is self-evident that measurement precision needs to be significantly better than the natural variability of isotope ratios. For many years, thermal ionization mass spectrometry (TIMS) has been the most commonly applied method to measure isotope ratios and metal concentrations at high precision (Nd, Sr, Pb). For some metals such as Pb the precision of the TIMS measurements has been greatly improved using double- or triple-spike methods [*Galer*, 1999], which is, however, very labor-intensive. Over the past few years, multiple-collector–inductively coupled plasma mass spectrometry

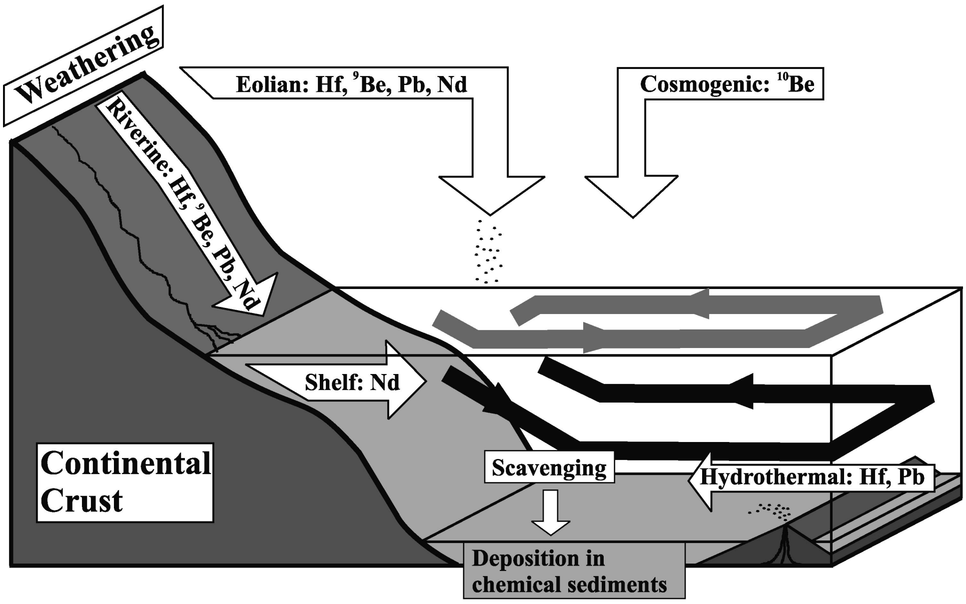


**Figure 3.** Pathways of different trace metals from their sources to their sinks. There are three major sources of particulate and dissolved trace metals for the ocean, which are eolian, riverine, and hydrothermal input. In addition, some metals such as Nd are probably supplied by partial dissolution of shelf sediments. The shaded and solid lines mark surface and deep-water circulation which causes mixing of the dissolved metals.

(MC-ICPMS) has facilitated the precise measurement of isotope ratios of metals which are difficult to ionize thermally, such as Hf [cf. *Rehkämper et al.*, 2001], and allows greater throughput of samples. In the case of metals that have only one or two stable or primordial isotopes, such as Cu or Pb, isotope ratios can be measured more precisely than by conventional TIMS techniques by correction for instrumental mass fractionation through addition of a spike of a different element with similar mass [*Belshaw et al.*, 1998]. Coupled to a laser system, isotope ratios of trace metals can also be measured directly from certain materials by MC-ICPMS without chemical pretreatment [cf. *Rehkämper et al.*, 2001]. Ratios and concentrations of other very low abundance isotopes such as $^{10}$Be are measured by accelerator mass spectrometry (AMS) [cf. *Suter*, 1992] or secondary ion mass spectrometry (SIMS) [*Belshaw et al.*, 1995].

## 2. SOURCES OF RADIOGENIC TRACE METALS IN THE OCEAN

[16] There are three main pathways by which trace metals with distinct isotope compositions can be made available as dissolved tracers in the ocean (Figure 3). The first possibility is the introduction via rivers, either in dissolved, colloidal, or particulate form. The second is eolian input of particles mobilized from the continental crust by erosion or volcanic activity. Particles introduced into the ocean partially dissolve, the relative amount depending on lithology of the dust and respective trace metal [e.g., *Duce et al.*, 1991], and release their trace metal isotope signature to the water column. Third, for some trace metals the release by hydrothermal activity on the seafloor is an important additional source. The relative importance of these sources is different for each trace metal and depends on factors such as their mobility during weathering and erosional processes and their chemical behavior in rivers and estuaries. For some dissolved trace metals the relative present-day budgets of the input sources are well known, while for others, there are considerable uncertainties.

### 2.1. Nd

[17] For Nd, there is clear evidence that hydrothermal sources do not contribute to the dissolved seawater Nd budget because of an immediate immobilization or scavenging (adsorption and subsequent removal to the sediments) of Nd by hydrothermal precipitates very close to or even within the hydrothermal sources [*German et al.*, 1990; *Halliday et al.*, 1992]. There is an ongoing discussion, however, about the input mechanisms of Nd, i.e., the relative importance of eolian and riverine input. From measurements of Nd isotopes and rare earth element (REE) concentrations in sediment trap material, *Tachikawa et al.* [1997, 1999] suggested that up to 20% of the Nd contained in dust particles is released to seawater and that eolian dust is an important contributor to the dissolved Nd budget in the Atlantic Ocean. *Goldstein et al.* [1984] arrived at a similar conclusion from isotope analyses of desert-derived dust. From REE patterns along an E-W transect across the Pacific Ocean, *Greaves et al.* [1999] showed that eolian inputs are important for the dissolved Nd budget of Pacific surface waters. In contrast, *Jones et al.* [1994] suggested that eolian sources do not play a major role from the appar-

ent missing imprint of the Asian dust plume on the dissolved Nd isotope composition of NW Pacific deep waters. It is quite likely, however, that very efficient mixing of Nd in Pacific thermocline waters prevents an identification of local eolian sources in the Pacific deep waters [*von Blanckenburg and Igel*, 1999; *Igel and von Blanckenburg*, 1999].

[18] Riverine input, particularly in regimes of strong chemical weathering, is a very important source for the dissolved Nd budget of water masses, although most of the dissolved Nd load of rivers is precipitated in the estuarine sediments [*Goldstein and Jacobsen*, 1988; *Elderfield et al.*, 1990; *Ingri et al.*, 2000]. It was shown, however, that more than 90% of the Nd, at least in high-latitude rivers, is transported to the ocean on colloids (particle size between 0.2 μm and 3000 Dalton molecular weight) [*Ingri et al.*, 2000; *Andersson et al.*, 2001]. Nd can also be released from resuspended sediments [*Goldstein and O'Nions*, 1981] or diagenesis of particles originating from rivers [*Elderfield and Sholkovitz*, 1987]. *Sholkovitz et al.* [1999] suggested that the Equatorial Undercurrent (EUC) in the Pacific Ocean is one example of the importance of riverine input, because this current apparently derives a large amount of its dissolved REE supply from Papua New Guinea rivers. The release of trace metals such as Nd to the ocean by leaching and mobilization from continental slope sediments has also been suggested to play a role for the Nd isotope signature of the EUC [*Lacan and Jeandel*, 2001] and other water masses in the vicinity of the Indonesian Island Arcs [*Jeandel et al.*, 1998].

[19] Nd isotopes are generally not influenced significantly by isotopic fractionation during weathering and dissolution processes of detrital material [e.g., *Goldstein et al.*, 1984], although it was recently proposed that there may be some fractionation effects, which preferentially release Nd with unradiogenic isotope composition (low $^{143}Nd/^{144}Nd$) owing to the more efficient dissolution of minerals with a corresponding isotope signature. Such observations have been reported for weathering of glacial tills [*Öhlander et al.*, 2000] and during erosion and partial dissolution of rocks that supply a boreal river in northern Scandinavia [*Andersson et al.*, 2001]. A similar conclusion was drawn from mild acid leaching experiments of Greenland river sediments [*von Blanckenburg and Nägler*, 2001]. It remains to be shown, however, that these fractionation effects are of quantitative importance for the Nd isotope budget of an ocean basin.

### 2.2. Pb

[20] For Pb in the ocean the importance of the sources is different (natural sources, not anthropogenic inputs). In contrast to Nd, hydrothermal input is of at least local importance for the dissolved Pb isotope signal [*Barrett et al.*, 1987], but it is considered to be a minor contributor (<2%) for the total oceanic budget [*Chen et al.*, 1986]. It was concluded that riverine input plays a very important role, while dust input can explain only about 10–12% of the preanthropogenic Pb budget of the ocean [*Chow and Patterson*, 1962]. *Chow and Patterson* [1962] also estimated a natural annual global input flux of $6.3 \times 10^7$ mol yr$^{-1}$ which, assuming steady state in the ocean, must equal the output (deposition in marine sediments, section 3.2). On the basis of estimates of the global flux of eolian material into the ocean and an average amount of about 8% of this material dissolving [*Duce et al.*, 1991], a 12% contribution by dust to the dissolved Pb budget of the ocean was estimated in accordance with the former estimate [*Henderson and Maier-Reimer*, 2002]. Given that a significant part of the dissolved riverine Pb is scavenged in the estuaries [cf. *Nozaki et al.*, 1976], it was suggested in a more recent study that dust may still be an important factor contributing to the budget of Pb and its isotope composition of seawater, particularly in ocean areas with low riverine inputs [*Jones et al.,* 2000].

[21] There is an additional process that is important for the evaluation of the sources of the Pb isotope composition of the ocean. Other than described for Nd isotopes above, Pb isotopes are fractionated during weathering of continental rocks, an effect that is also well known for Sr isotopes. In the case of Pb the radioactive decay of isotopes causes radiation damage to the crystal structure of a mineral and leaves the resulting daughter isotopes more loosely bound in the minerals or even causes a mobilization of the daughter isotopes to the mineral grain boundaries. The radiogenic isotopes of Pb ($^{206}Pb$, $^{207}Pb$, $^{208}Pb$), which have been produced within the rocks by decay of U and Th, are thus easier to mobilize from rocks and minerals during weathering than nonradiogenic $^{204}Pb$ [*Erel et al.*, 1994; *Jones et al.*, 2000]. This means that the Pb isotope composition of solutions produced during continental weathering and the dissolved Pb in the ocean may not reflect the isotope composition of the source rocks on the surrounding continents, as was demonstrated for the North Atlantic Ocean [*von Blanckenburg and Nägler*, 2001].

### 2.3. Hf

[22] The relative importance of different sources in controlling the dissolved Hf isotope composition of the oceans is still unclear at present, mainly because Hf isotope measurements of seawater are not available yet. As soon as such measurements are available, the whole potential of the isotopic composition of this element will be accessible. It is, nevertheless, obvious from ferromanganese crust/nodule data, which reflect the deep-water Hf isotope composition, that there is a strong effect of incongruent weathering on the dissolved Hf isotope composition of seawater. This is caused by the fractionation of Hf and Lu between sand and clay-sized particles. Lu/Hf ratios and thus also $^{176}Hf/^{177}Hf$ ratios are very low in weathering-resistant zircons, which are concentrated in the sand fraction of continental and near-shore marine sediments and turbidites. This results in much lower time-integrated $^{176}Hf/^{177}Hf$ ratios in sand

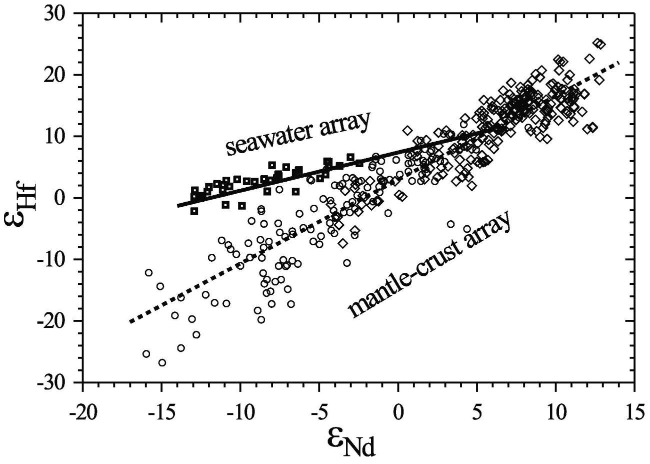


**Figure 4.** Values of $\varepsilon_{Nd}$ versus $\varepsilon_{Hf}$ for continental rocks (circles), oceanic basalts (diamonds), and surfaces of ferromanganese crusts and nodules (squares) which represent today's deep-water isotope composition. The isotope data for the rocks are compiled from various literature sources. The crust mantle array defined by the continental rocks and the basalts [*Vervoort et al.*, 1999] is the result of the differentiation of Earth's continental crust from its mantle, during which the parent isotopes of $^{143}$Nd and $^{176}$Hf ($^{147}$Sm and $^{176}$Lu, respectively) have preferentially stayed in the mantle and are thus enriched in basalts compared with continental rocks. The seawater array defined by the ferromanganese crust and nodule data [*Albarède et al.*, 1998; *David et al.*, 2001] shows the offset of the $\varepsilon_{Hf}$ values from the mantle-crust array for a given $\varepsilon_{Nd}$ value, which is a consequence of the incongruent realease of Hf to seawater during weathering of continental crust. Hf isotope data of the ferromanganese crusts and nodules are from different literature sources [*Godfrey et al.*, 1997; *Albarède et al.*, 1998; *David et al.*, 2001].

than in clay. The Hf in the zircons of the sand fraction is almost unavailable to weathering and is not introduced into seawater. Consequently, the seawater data, as represented by the ferromanganese crust/nodule data, are offset toward higher $\varepsilon_{Hf}$ for a given $\varepsilon_{Nd}$ compared with crustal rock data in plots of Nd versus Hf isotopes [*Albarède et al*., 1998; *David et al*., 2001] (Figure 4). In addition to this effect, it has been suggested that hydrothermal contributions may play an important role for the dissolved Hf budget of the ocean [*White et al*., 1986; *Godfrey et al*., 1997], whereas there is no information available on the importance of riverine sources because of the lack of measurements.

### 2.4. Os

[23] The Os isotope composition of the ocean is controlled by inputs derived from continental weathering, by alteration of abyssal peridotites, and to some extent by cosmic dust [*Pegram et al*., 1992; *Ravizza*, 1993]. The average $^{187}$Os/$^{188}$Os of these inputs varies between high values around 1.54 in average upper continental crust and low values around 0.126 in peridotites and cosmic dust as a consequence of fractionation between Re and Os during the formation of continental crust. Under the assumption that the ocean is at steady state with respect to Os, the unradiogenic input sources together contribute 30% to the dissolved Os in the ocean, of which ~14% (a total of 4% of the input) originate from cosmic dust. Seventy percent of the total budget is contributed from continental (riverine) sources to reach the present $^{187}$Os/$^{188}$Os of seawater (1.06) [*Levasseur et al*., 1999].

### 2.5. Sr

[24] As a consequence of fractionation of Rb and Sr during the formation of continental crust the Sr isotope ratios in crust and mantle differ strongly. Thus the Sr isotope budget in the ocean is mainly a balance between riverine inputs with radiogenic (high) $^{87}$Sr/$^{86}$Sr ratios (average ~ 0.7119) and mantle-derived high-temperature hydrothermal inputs at the mid-ocean ridges with unradiogenic (low) $^{87}$Sr/$^{86}$Sr ratios (average ~ 0.7035) [*Palmer and Edmond*, 1989]. The isotope composition of the riverine inputs can vary significantly, mainly as a function of the amount of old marine carbonates in the drainage area, which have a high Sr content and are easily dissolved. In addition, there is a small contribution (about 10% of the global riverine flux [*Elderfield and Gieskes*, 1982] remobilized from marine sediments via pore waters with an average isotopic composition similar to that of modern seawater (~ 0.7084). For the contemporaneous global oceanic mass balance of Sr (total inventory = $125 \times 10^{15}$ mol) it has been suggested that the most important source is the riverine flux amounting to approximately $33 \times 10^9$ mol yr$^{-1}$, followed by a hydrothermal contribution on the order of $15 \times 10^9$ mol yr$^{-1}$ and about $3.4 \times 10^9$ mol yr$^{-1}$ from marine pore waters [*Palmer and Edmond*, 1989]. Earlier estimates of the hydrothermal contribution were low (2 and $4 \times 10^9$ mol yr$^{-1}$) owing to low estimates of the global high-temperature hydrothermal water flux at the mid-ocean ridges [*Morton and Sleep*, 1985; *Goldstein and Jacobsen*, 1987]. These older estimates required correspondingly lower values for the average riverine Sr isotope composition (0.7095 to 0.7106) to achieve mass balance, assuming steady state of the oceans with respect to Sr concentration and isotopic composition.

## 3. PRESENT-DAY DISTRIBUTION OF RADIOGENIC TRACE METAL ISOTOPES IN THE OCEAN

### 3.1. Nd Isotopes

[25] The dissolved trace metals in this review differ in their oxidation states and chemical speciation in the oxygenated water column of the ocean, which determines their reactivities and oceanic residence times [*Turner et al*., 1981; *Bruland*, 1983]. Nd exists exclusively in the +3 state in oxygenated seawater similar to all other rare earth elements (except for Ce, which can be oxidized to the +4 state). Nd is most likely present as a

Nd-carbonate ($NdCO_3^+$) or Nd-sulfate ($NdSO_4^+$) complex together with traces of $Nd^{3+}$ [*Bruland*, 1983]. It is removed from the water column by particulate scavenging (adsorption), which explains its typical water column pattern of depleted surface concentrations, which increase with depth because of desorption/disaggregation processes. The global average ocean residence time of Nd in deep waters is between 600 and 2000 years [*Jeandel*, 1993; *Jeandel et al.*, 1995; *Tachikawa et al.*, 1999] and deep-water concentrations are around 4 pg $g^{-1}$. On ocean basin scales where the water mass mixing times are on the order of only few hundred years, Nd can be considered quasi-conservative. Nd is deposited in marine and estuarine sediments, which constitute its most important sink.

[26] The isotopic distribution of Nd in the world ocean has been examined in greater detail than other metals [*Piepgras et al.*, 1979; *Piepgras and Wasserburg*, 1980, 1982, 1983, 1987; *Stordal and Wasserburg*, 1986; *Piepgras and Jacobsen*, 1988; *Spivack and Wasserburg*, 1988; *Bertram and Elderfield*, 1993; *Jeandel*, 1993; *Shimizu et al.*, 1994; *Jeandel et al.*, 1995, 1998; *Tachikawa et al.*, 1999; *Amakawa et al.*, 2000]. These studies have revealed clear and well-resolved Nd isotope signatures for particular water masses, related to the weathering of Nd from different types and ages of continental crust. Continental rocks eroding in the areas surrounding the North Atlantic are mainly Proterozoic or Archean in age and have $\varepsilon_{Nd}$ as low as −40, which is a function of their low Sm/Nd ratios ($^{147}Sm$ is the parent isotope of $^{143}Nd$) and the long period of time that these crustal units had to evolve. In contrast, the island arc rocks around the Pacific Ocean are composed of young mantle-derived material with high (radiogenic) $\varepsilon_{Nd}$ values up to +20.

[27] As a consequence, the most negative (least radiogenic, lowest $^{143}Nd/^{144}Nd$ ratios) $\varepsilon_{Nd}$ values are found in water masses closest to the weathering sites of old continental rocks, such as in the Baffin Bay, where $\varepsilon_{Nd}$ values as low as −26 have been measured in the seawater [*Stordal and Wasserburg*, 1986]. These waters mix with other water masses of different origin and with higher $\varepsilon_{Nd}$ in the North Atlantic (see section 1.1) to form NADW. This mixture results in a present-day typical value of –13.5 for NADW, whereas water masses originating in the southern Atlantic and Southern Ocean (AAIW, CDW, or AABW) have $\varepsilon_{Nd}$ values between –7 and –9 [*Piepgras and Wasserburg*, 1982, 1987; *Jeandel*, 1993]. This is a consequence of mixing between Atlantic and Pacific water masses in the Southern Ocean. Figure 5 illustrates the relationship between water masses (defined by their salinities) and $\varepsilon_{Nd}$ on a N-S transect in the Atlantic Ocean. The tongue of southward flowing NADW with its high salinity and low $\varepsilon_{Nd}$ is distinct from northward flowing AAIW above and AABW below and can be identified until 49°S. The water column of the Southern Ocean is quite homogenous in $\varepsilon_{Nd}$ owing to efficient vertical and horizontal mixing [*Piepgras and Wasserburg*, 1982]. Another water mass with distinct Nd isotope composition in the Atlantic Ocean is Mediterranean Outflow Water with an $\varepsilon_{Nd}$ value of –9.4 [*Spivack and Wasserburg*, 1988]. Pacific intermediate and surface waters are much more positive in $\varepsilon_{Nd}$ (between 0 and −4), while deep and bottom water masses vary around lower values between –3 and −6 [*Piepgras and Jacobsen*, 1988; *Shimizu et al.*, 1994]. This has been interpreted as the admixture of northward penetrating AABW. The Nd isotope composition of Indian Ocean water masses tends to be intermediate between the Atlantic and Pacific and is relatively homogenous at $\varepsilon_{Nd}$ values of about −7 to −8 [*Bertram and Elderfield*, 1993], whereas in the vicinity of the Indonesian throughflow water masses of Pacific origin are traceable by $\varepsilon_{Nd}$ values between −5 and −3 [*Jeandel et al.*, 1998].

### 3.2. Pb Isotopes

[28] Dissolved Pb exists in the ocean in a +2 state mainly as $Pb^{2+}$ ion or Pb carbonate complexes ($PbCO_3$ or $Pb(CO_3)_2^{2-}$), but biologically mediated reactions can change the speciation [*Bruland*, 1983]. The water column profiles of Pb concentration show increased surface water values due to atmospheric (to a large extent, anthropogenic) inputs and depleted concentrations at depth [e.g., *Schaule and Patterson*, 1981]. Pb is a highly particle-reactive element in the ocean [*Schaule and Patterson*, 1981; *Cochran et al.*, 1990], which has been shown from extensive studies of the short-lived radioactive Pb isotope $^{210}Pb$ ($^{210}Pb$ is produced at a relatively constant rate from the decay of $^{226}Ra$ in the oceans and $^{222}Rn$ in the atmosphere (see *Henderson and Maier-Reimer* [2002] for a compilation)). As a consequence of its particle reactivity the residence time of Pb in deep waters is only about 50 years in the Atlantic and up to 200–400 years in the Pacific with Pb concentrations around 1 pg $g^{-1}$ in the deep water. Pb is thus efficiently transferred to the ocean sediments, most likely by nonreversible particulate scavenging with some release at depth mainly by particle decomposition and remineralization.

[29] For Pb, there are no reliable natural isotope distributions in the water column available because of the atmospheric input with anthropogenically modified isotope composition [*Schaule and Patterson*, 1981; *Boyle et al.*, 1986; *Shen and Boyle*, 1988; *Alleman et al.*, 1999]. Information on preanthropogenic deep-water distribution of Pb isotopes can only be derived from the records preserved in authigenic marine sediments such as ferromanganese crusts and nodules [*Abouchami and Goldstein*, 1995; *von Blanckenburg et al.*, 1996b] (see section 5.2).

[30] Similar to Nd, weathering of continental crust is the main input source of preanthropogenic natural Pb into the ocean. The young mantle-derived end-member (similar to mid-ocean ridge basalt) has, for example, $^{206}Pb/^{204}Pb$ near 18.5. The continental crust end-member is difficult to define because of the effects of incongruent weathering (see section 2.2). Weathering of these rocks results in $^{206}Pb/^{204}Pb$ ratios around 19.3 for

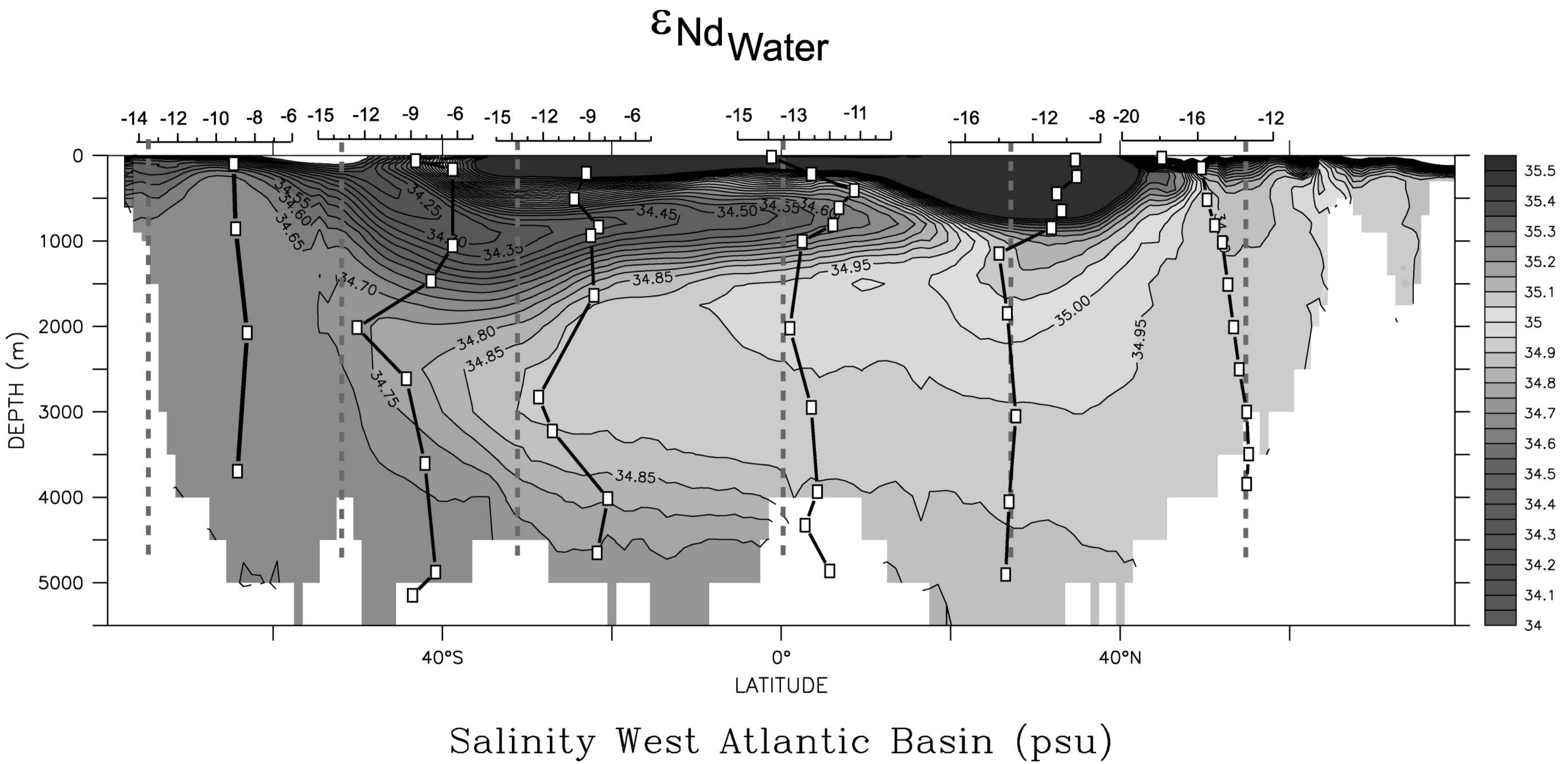


**Figure 5.** Water mass distribution on a N-S transect in the present-day Atlantic Ocean as characterized by salinity (in per mill) [*Levitus*, 1982]. NADW flowing south is characterized by its high salinity. This flow is compensated by northward flowing cold AABW and warmer low- salinity Antarctic Intermediate Water. Water column $\varepsilon_{Nd}$ data are shown (open squares and black lines) [*Piepgras and Wasserburg*, 1982, 1987; *Jeandel*, 1993], which clearly follow this distribution of water masses [*von Blanckenburg*, 1999]. (Reprinted with permission from *von Blanckenburg* [1999]. Copyright © 1999 American Association for the Advancement of Science.) The pink dashed vertical lines denote the $\varepsilon_{Nd}$ signature of NADW (−13.5) as measured in the North Atlantic [*Piepgras and Wasserburg*, 1987].

present NADW and between 18.5 and 18.8 for deep Pacific water masses. Water masses in the Indian and Southern Oceans are intermediate between those values. A similar separation between the main deep-water masses is also observed for the other radiogenic Pb isotope pairs. It must be noted that the ferromanganese crust surfaces average over several tens to hundreds of thousands of years, which includes glacial/interglacial variations. That means that the actual preanthropogenic deep-water Pb isotope composition may have had a larger range and more extreme values for particular water masses such as NADW.

### 3.3. Hf Isotopes

[31] Dissolved Hf in oxygenated seawater is present in the +4 state. It is one of the hydroxide-dominated elements which exists as hydrolysis products such as $Hf(OH)_5^-$ or $Hf(OH)_4$ [*Turner et al.*, 1981; *Bruland*, 1983]. The only reliable profiles of Hf concentrations indicate a surface water depletion and an increase with depth similar to Nd, which points to some effect of particulate scavenging [*Godfrey et al.*, 1996; *McKelvey and Orians*, 1998]. This suggests that, despite the lack of direct information, the major sink for Hf in the ocean is the marine sediments. The Hf residence time in seawater has been estimated from water column studies [*Godfrey et al.*, 1996; *McKelvey and Orians*, 1998]. Additional constraints have been derived from studies of ferromanganese crusts, which show a range of Hf isotope variations similar to those in Nd. Given that the range in Hf isotope values in the continental crust (the ultimate source of both Nd and Hf) is about double that of Nd, a residence time of Hf on the order of 1500–2000 years is indicated [*Godfrey et al.*, 1997; *Lee et al.*, 1999; *David et al.*, 2001]. Analytical difficulties and the low concentrations (0.04–0.2 pg $g^{-1}$ [*Godfrey et al.*, 1996; *McKelvey and Orians*, 1998]) have so far prevented the measurement of Hf isotopes in seawater. Therefore, as is the case for Pb, the distribution of Hf isotopes in the deep ocean can presently only be derived from records preserved in ferromanganese crust surfaces (see also section 5.2).

[32] Continental weathering and (to some extent) hydrothermal inputs control the isotopic composition of Hf in deep waters. There is a wide range in the Hf isotope composition of continental rocks which have $\varepsilon_{Hf}$ values as low as −30 and mantle rocks which can be as high as +25. Because of the strong incongruent weathering effects of zircons from the continental crust (see section 2.3), seawater $\varepsilon_{Hf}$ is higher than expected from comparison with the corresponding $\varepsilon_{Nd}$ data (Figure 4). The ferromanganese crust data indicate that Pacific deep waters have generally high $\varepsilon_{Hf}$ values between +3 and +9, while the deep North Atlantic values range between −2 and +3. Indian and Southern Ocean values are intermediate between +2 and +5.5. Analogous to the Pb isotopes, the ferromanganese crust and nodule Hf isotope data average over relatively long periods of time and the actual values of the water masses may have a somewhat wider range and more extreme values.

### 3.4. Os and Sr Isotopes

[33] Dissolved Os in the ocean is present in the +8 state and it has been suggested from thermodynamic modeling that the main chemical species are oxyanions such as $H_2OsO_5$ or $H_3OsO_6^-$, although it appears that a large part of the Os is present as organic complexes [*Levasseur et al.*, 1998]. Dissolved Os concentrations, which have only recently been measured successfully in seawater [*Levasseur et al.*, 1998], have been shown to be homogenous at 10.86 ± 0.07 fg $g^{-1}$, although evidence has been presented since for a somewhat lower Os concentration within the oxygen minimum zone of the Pacific water column [*Woodhouse et al.*, 1999]. A further measurement also suggested a slight deviation of the Pacific deep-water concentration from a homogenous value [*Sharma et al.*, 2000]. The most important sinks for Os in the ocean are reducing sediments, which are found beneath the major upwelling areas.

[34] The average residence time of Os in the ocean is significantly longer than the circulation time of the ocean [*Ravizza and Turekian*, 1992; *Sharma et al.*, 1997], but there is a discrepancy between the residence time calculated from the marine Os mass balance (>10 kyr) and that inferred from short-term glacial-interglacial Os isotope variations found in marine sediments (3–4 kyr) [*Oxburgh*, 1998]. This may partly arise from an underestimation of the osmium inputs into the ocean. The short-term isotopic variability observed may be related to a postglacial meltwater spike [*Oxburgh*, 2001]. Most recent estimates of the residence time (6.5–15 kyr) are at the lower end of the marine mass balance–based estimates [*Levasseur et al.*, 1998; *Oxburgh*, 2001]. This residence time implies that any differences from the present $^{187}Os/^{188}Os$ value of 1.06 [*Levasseur et al.*, 1998] between water masses or ocean basins must thus be very small [*Burton et al.*, 1999b].

[35] Sr is a major conservative component of seawater with a residence time on the order of several million years, which is the reason why it is homogenously distributed in seawater at a concentration of 7.6 $\mu g\ g^{-1}$ and the $^{87}Sr/^{86}Sr$ in the present-day ocean is uniform at 0.70918. Sr is present in the +2 state in the ocean as $Sr^{2+}$ ions. The only significant sink for Sr in the ocean is the incorporation into carbonate shells and subsequent burial in marine sediments.

### 3.5. Be Isotopes

[36] Be is present in the +2 state in the ocean, mainly as a hydrolysis product such as $Be(OH)^+$ or $Be(OH)_2$ [*Bruland*, 1983]. Because of its particle reactivity, Be shows nutrient-type concentration patterns with a generally strong surface water depletion and increased values at depth caused by particulate scavenging at the surface and release at depth through desorption and particle remineralization. Its residence time in the ocean

varies between about 100 years in high particle flux areas and up to 3000 years in the central Pacific gyres [*Lao et al.*, 1992; *von Blanckenburg and Igel*, 1999]. The global average oceanic residence time of Be in deep waters is about 500 to 1000 years [*Segl et al.*, 1987; *Ku et al.*, 1990; *von Blanckenburg et al.*, 1996a], which is similar to or somewhat shorter than that of Nd.

[37] Stable beryllium, $^9$Be, a common trace element in the continental crust, is supplied to the ocean by weathering. A radioactive beryllium isotope $^{10}$Be ($T_{1/2}$ = 1.5 Myr) is produced in the upper atmosphere at an approximately constant rate by interaction of atmospheric nitrogen and oxygen with the cosmic radiation. $^{10}$Be is mainly delivered to the ocean by wet precipitation. The main factor controlling the $^{10}$Be/$^9$Be ratio in the ocean's water column is the $^{10}$Be concentration, which increases with the "age" of the water masses owing to remineralization processes from values around 1000 atoms g$^{-1}$ water in the Atlantic to about 2000 atoms g$^{-1}$ in the the north Pacific [*Kusakabe et al.*, 1987; *Ku et al.*, 1990]. In contrast, $^9$Be concentrations in deep waters are quite homogenous at values around 0.25 pg g$^{-1}$. The result is a distinct $^{10}$Be/$^9$Be ratio of water masses. NADW has a typical $^{10}$Be/$^9$Be ratio around 0.5 × 10$^{-7}$, AABW and CDW have values of about 1 × 10$^{-7}$, AAIW has ratios around 1.2 × 10$^{-7}$, and Pacific deep waters range between 1 and 1.4 × 10$^{-7}$ [*Ku et al.*, 1990; *Xu*, 1994; *Measures et al.*, 1996].

## 4. ISOTOPIC EVOLUTION OF THE LONG-RESIDENCE TIME TRACERS Sr AND Os IN THE OCEAN

[38] The isotope composition of trace metals in seawater has been reconstructed from authigenic chemical phases in the ocean. Because of their high Sr contents, (1) carbonate shells of different organisms (foraminifera, brachiopods, belemnites, conodonts) [cf. *Veizer et al.*, 1999]; (2) marine biogenic barite, which is produced in chemical microenvironments in the decaying organic matter of diatoms in the upper water column of the ocean [*Paytan et al.*, 1993]; (3) fish teeth [*Staudigel et al.*, 1985]; and (4) some phosphatic peloids [*Shaw and Wasserburg*, 1985] have been used for reconstructing the Sr isotope evolution of the world's ocean over the Phanerozoic (Figures 6a and 6b). For the past 60 Myr, foraminifera have been used almost exclusively [cf. *Hodell et al.*, 1991; *Veizer et al.*, 1999]. The evolution of the Sr isotope composition of the world ocean is characterized by an asymmetric trough-like shape over the Phanerozoic starting with $^{87}$Sr/$^{86}$Sr ratios similar to the present-day value in the Cambrian [cf. *Edmond*, 1992]. From the Cambrian to the late Jurassic the ratios showed a general decline to ratios as low as 0.7067, which was interrupted by large, relatively short term excursions, for example, at the end of the Ordovician, the middle Devonian, and most pronounced at the Permian/Triassic

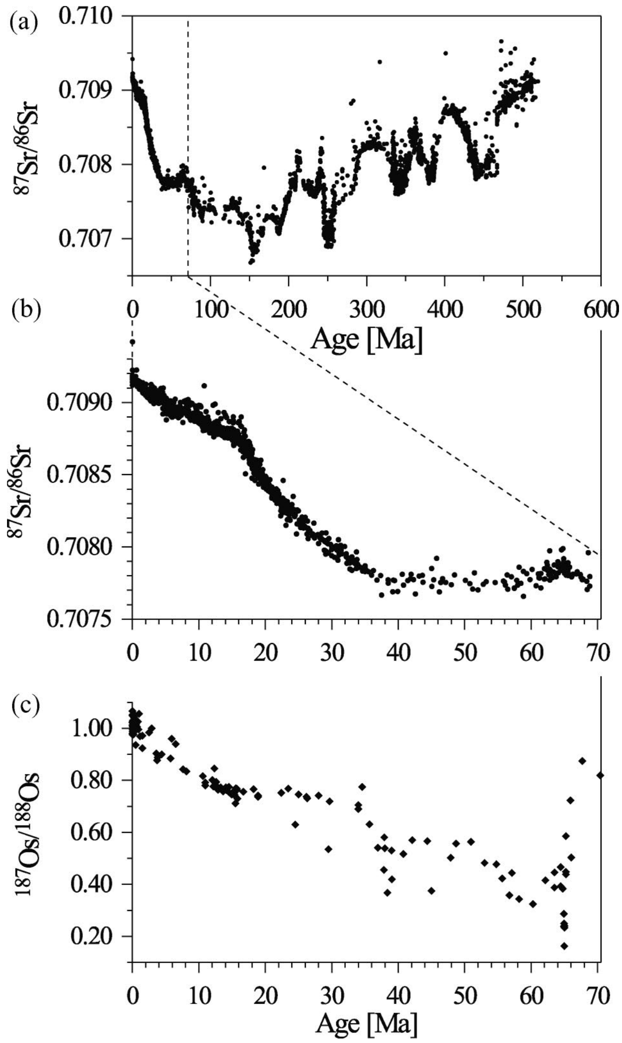


**Figure 6.** (a) Long-term evolution of the Sr isotope ratio ($^{87}$Sr/$^{86}$Sr) in seawater for the Phanerozoic (past 530 Ma) (as compiled by *Veizer et al.* [1999]; for particular literature sources, see references therein), (b) detail of the Sr isotope evolution for the past 70 Myr, and (c) the Os isotope ($^{187}$Os/$^{188}$Os) evolution for the past 70 Myr (as compiled by *Peucker-Ehrenbrink and Ravizza* [2000]; for particular literature sources and additional information, see references therein).

boundary. At the end of the Jurassic the trend reversed and the ratios have steadily risen since, with major steepenings between about 35 and 20 Ma and over the past 2.5 Myr. The reasons for these changes have been hotly debated, but it is clear that variations in the main input sources continental erosion and hydrothermal flux must be responsible. Such changes can be accomplished in different ways. In general, increased contributions from continental weathering via river runoff tend to raise the ocean $^{87}$Sr/$^{86}$Sr, whereas increased hydrothermal exchange at the mid-ocean ridges tends to lower it. This is the reason why major plate tectonic and paleogeographical changes have been invoked as a key factor in controlling the oceanic Sr isotope composition [cf. *Richter et al.*, 1992]. During periods of major continental breakup, increased hydrothermal activity at the ridges is expected, whereas during continental collisions and orogenies an increase in erosion rate and weathering occurs. This has led to the interpretation that major increases in the oceanic $^{87}Sr/^{86}Sr$ (such as the most pronounced rise between 35 Ma and present) have been caused by major orogenies such as Himalayan uplift and related changes in weathering regime and increases in erosional inputs [cf. *Richter et al.*, 1992]. For the Cenozoic curve it has also been suggested that contributions from the Himalayan metamorphic core complex with its extraordinarily high Sr isotope ratio and high Sr concentrations in the rivers have exerted control on the Cenozoic global oceanic Sr isotope budget [*Edmond*, 1992]. Erosional inputs from similar metamorphic complexes may have been involved in previous major orogenies and related excursions of the Sr isotope curve by supplying Sr with extreme isotopic composition to the ocean.

[39] The evolution of the Os isotopes provides complementary insight into the processes that control the isotope budget of long residence time tracers in the ocean. In the case of Os, which has a much shorter oceanic residence time than Sr, there is some evidence for isotopic variations on short timescales (10,000 years) extracted from metalliferous sediments. These variations have been attributed to changes in weathering regime on glacial/interglacial timescales [*Oxburgh*, 1998] and during the Paleocene thermal maximum [*Ravizza et al.*, 2001]. Long-term Os isotope records have been obtained for the past 70 Myr [*Pegram et al.*, 1992; *Ravizza*, 1993; *Peucker-Ehrenbrink et al.*, 1995; *Pegram and Turekian*, 1999] (see also the recent review by *Peucker-Ehrenbrink and Ravizza* [2000]) (Figure 6c). The Os isotope record looks similar to the Sr isotope evolution in that it shows a general increase between about 65 Ma and present. In contrast to the Sr isotope record, however, the Os isotopes show high values prior to 65 Ma, and there have been several excursions toward lower values in the Cenozoic, the most pronounced of which occurred at the Eocene/Oligocene boundary at about 33 Ma (see *Peucker-Ehrenbrink and Ravizza* [2000] for discussion of the timing). The major minimum at the Cretaceaous/Tertiary boundary has been interpreted as a consequence of the impact of a large extraterrestrial body which supplied significant amounts of Os with low $^{187}Os/^{188}Os$. The slow increase in the Os isotope ratio after the impact may be explained by weathering of impact material on the continents [*Peucker-Ehrenbrink et al.*, 1995]. The minimum at the Eocene/Oligocene boundary is less well constrained and occurred only in one core. An extraterrestrial origin cannot be excluded, but it is also possible that this feature is a leaching artifact of volcanic ash which requires verification by further records.

[40] Comparison of the general trend of the Os and Sr isotope records suggests that related processes have controlled the oceanic isotope budget for both elements. However, evidence has recently been presented that the changes in Os isotopes are unlikely to have originated from Himalayan riverine supply, because the dissolved Os concentrations are too low to have such a large impact on the Os isotope composition of the ocean [*Sharma et al.*, 1999]. This suggests that Himalayan weathering and erosion has probably not been the only factor controlling the global oceanic budget of both isotope systems during the Tertiary and that more global variations in weathering regime and intensity have been involved.

## 5. ISOTOPIC EVOLUTION OF SHORT AND INTERMEDIATE RESIDENCE TIME TRACE METALS (ND, HF, PB, BE): IMPLICATIONS FOR PALEOCEANOGRAPHY AND CONTINENTAL WEATHERING HISTORY

[41] The deep-water isotopic composition of short to intermediate residence time trace metals in the ocean (Nd, Hf, Pb, Be) is recorded by authigenic chemical precipitates in the ocean without significant fractionation processes. This is an important difference compared with classic nutrient-related isotopic water mass proxies, such as carbon isotopes. If a reliable age control for the authigenic deposits is available, the trace metal isotope composition of the ambient deep water in the past can be reconstructed.

[42] There have been attempts to extract the Nd isotope composition from the calcite of planktonic foraminifera as primary authigenic phase in the ocean, which contains only very low amounts of Nd (only few parts per million at maximum). There has been a debate as to the validity of these measurements due to potentially incomplete separation from postdepositional Mn-oxyhydroxide coatings, which contain much higher Nd concentrations than the foraminiferal calcite itself. With the advance of more reliable cleaning techniques, it has recently been suggested that the surface water Nd isotope composition can be extracted reliably from the calcite of planktonic foraminifera deposited in marine sediments. Such a record was obtained in the Labrador Sea for the past 2.5 Myr [*Vance and Burton*, 1999]. For the past 150 kyr, variations in a surface water Nd isotope record obtained from planktonic foraminfera from the Bay of Bengal were interpreted as changes in riverine inputs of Nd as a function of monsoonal circulation [*Burton and Vance*, 2000]. Although there are still uncertainties concerning the true Nd concentration of foraminiferal calcite prior to coating with the Mn-oxyhydroxides in the sediment [*Pomies and Davies*, 2000], which will require future studies, Nd isotopes in foraminferal calcite are a promising new tool for continuous reconstructions of surface ocean paleoceanography.

[43] For the present-day Atlantic Ocean [*Palmer and Elderfield*, 1985] (Figure 9a) and for the past 60 Myr at a location on the Rio Grande Rise in the South Atlantic

[*Palmer and Elderfield*, 1986] (Figure 11a), the deep-water Nd isotope composition has been reconstructed from the early diagenetic ferromanganese coatings of foraminifera. Potential problems are caused by the diagenetic mobility of Mn and REE in the sediments under reducing conditions. The coatings may not have only derived their Nd from the bottom water but may also contain contributions from pore waters, which may have a different isotope composition and may bias a true deep-water isotope signal [*Elderfield et al*., 1981]. More recently, glacial-interglacial Nd isotope records obtained from the Mn coatings of South Atlantic sediment cores, which have obviously remained oxidized for the past up to 70 kyr, were used to reconstruct the NADW export into the Southern Ocean [*Rutberg et al*., 2000; *Bayon et al*., 2002] (section 5.3.2 and Figure 15).

[44] Other authigenic materials, mostly discontinuous archives, that have been used to reconstruct the seawater Nd isotope composition are fish teeth [*Staudigel et al*., 1985; *Martin and Haley*, 2000], shark teeth [*Vennemann et al*., 1998], marine phosphates, carbonates, and other fish remains [*Staudigel et al*., 1985; *Stille and Fischer*, 1990; *Stille*, 1992; *Stille et al*., 1996].

[45] Reconstructions of the origin, strength, and flow paths of paleocurrents with radiogenic isotopes (Sr, Nd, Pb) have not only been derived from the dissolved water column signal but have also utilized the isotopic signatures of the detrital fraction carried by currents, which is ultimately deposited in marine sediments. It is obvious that the clay mineral fraction is most suitable for the reconstruction of certain water masses because of its slow sinking speed and thus long residence time within a water mass, whereas the larger grain size fractions have more likely recorded the detrital supplies from nearby outcropping terranes [*Innocent et al*., 2000]. Such studies have mainly focused on glacial-interglacial variations of bottom waters in the North Atlantic region where distinct isotopic differences of the source regions allow a detailed reconstruction of sources and mixing of different water masses [*Grousset et al*., 1988; *Revel et al*., 1996; *Bout-Roumazeilles et al*., 1998; *Hemming et al*., 1998; *Fagel et al*., 1999, *Innocent et al*., 2000], but there is also a study of the source provenances and circulation patterns in the Indian Ocean using Nd isotopes in the detrital fraction of marine sediment [*Dia et al*., 1992].

### 5.1. Ferromanganese Crusts: Genesis and Age Dating

[46] Recently, most attention has been devoted to extracting continuous radiogenic isotope time series from depth profiles of hydrogenous ferromanganese crusts which grow directly from the water column on outcrops of hard substrate such as hyaloclastite or basalt on the seafloor. The requirement for growth of crusts is the absence of particle sedimentation, which either occurs through bottom currents or steep slopes, for example, on seamounts (Figure 7). In addition, depth profiles of hydrogenous Mn nodules which grow on top of pelagic sediments in areas of very low sedimentation rates have been used. If these nodules get buried in oxygenated marine sediments, they preserve their radiogenic isotope composition and can be used to some extent for time series reconstructions on the megayear scale using the sediment stratigraphy [*Winter et al*., 1997; *Ito et al*., 1998].

**Figure 7.** Bottom view of a seamount slope in the Pacific Ocean. The basaltic rocks which have been kept clear of sediments by bottom currents and because of slope steepness are covered with a hydrogenous ferromanganese crust of up to 20 cm thickness. The distance across is about 3 m. Photograph was taken by J.R. Hein, U.S. Geological Survey.

[47] Trace metals are incorporated into crusts and nodules by a coprecipitation process. Although the exact mechanism of crust precipitation is unclear, it probably involves a two-stage process [*Koschinsky and Halbach*, 1995]. First, Mn and Fe from the water column form mixed colloids which scavenge trace metals by surface sorption. Second, these colloids precipitate together with the sorbed trace metals as amorphous oxide or oxihydroxide encrustations on any substrates on the seafloor. This process, in combination with the very slow growth rates, enriches the concentrations of trace metals in the crusts and nodules by up to 10 orders of magnitude compared with the seawater concentrations.

[48] The crusts and nodules precipitate at rates between 1 and 15 mm $Myr^{-1}$. The most precise growth rate estimates have been obtained using the U series nuclide $^{230}Th$ which is, however, restricted to the last about 400 kyr owing to its half-life of 75 kyr [*Segl et al*., 1984; *Banakar and Borole*, 1991; *Eisenhauer et al*., 1992; *Bollhöfer et al*, 1996; *Abouchami et al*., 1997; *Claude-Ivanaj et al*., 2001]. On longer timescales, depth profiles of $^{10}Be$, normalized to stable $^{9}Be$, make dating of crusts possible back to ~10 Ma [*Krishnaswami et al*., 1972; *Ku et al*., 1979; *Sharma and Somayajulu*, 1982; *Segl et al*., 1984; *McMurtry et al*., 1994; *Ling et al*., 1997; *O'Nions et al*., 1998; *Frank and O'Nions*, 1998; *Reynolds et al*., 1999; *Frank et al*., 1999b, 2002] (Figure 8a). Beyond 10 Ma, there are no other reliable isotopic dating methods available. Attempts have been made using magnetostratigra-

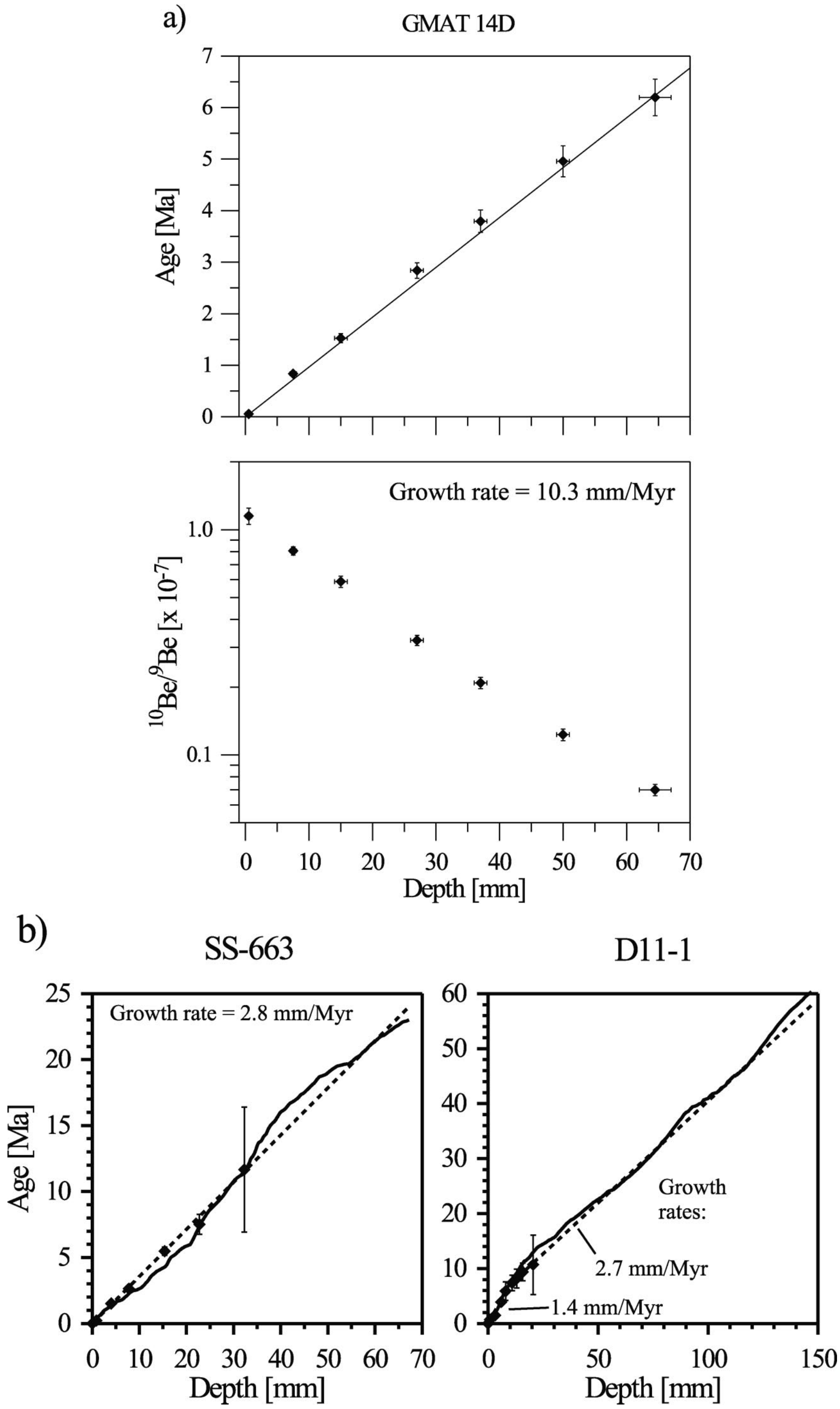


**Figure 8.** Examples for dating ferromanganese crusts using $^{10}Be/^{9}Be$ and Co chronology. (a) $^{10}Be/^{9}Be$ ratios and corresponding ages (Ma) versus depth (millimeters) for crust GMAT 14D from the eastern equatorial Pacific Ocean [after *Frank et al.*, 1999b]. The growth rate calculated for this crust is 10.3 mm $Myr^{-1}$. (b) Comparison of age-depth relationships based on $^{10}Be/^{9}Be$ and Co chronology for crusts SS663 from the deep central Indian Ocean and D11-1 from a seamount in the central equatorial Pacific Ocean [after *Frank et al.*, 1999a]. The dashed lines indicate the growth rates derived from $^{10}Be/^{9}Be$: 2.8 mm $Myr^{-1}$ for SS663, 1.4 mm $Myr^{-1}$ for the upper 9.5 mm, and 2.7 mm $Myr^{-1}$ for the part below 9.5 mm depth for D11-1. These growth rates were extrapolated to the base of the crusts assuming constant growth rate and the absence of any growth hiatus. In the case of crust SS663 the general relationship between Co content and growth rate of *Manheim* [1986] has been applied, whereas in the case of the Co-rich seamount crust D11-1 the relationship given by *Puteanus and Halbach* [1988] was used (solid bold lines). The good correspondance between the $^{10}Be/^{9}Be$ and Co-based approaches suggests that there have not been any major changes in growth rates beyond 10 Ma in both crusts. For all growth rates derived from Be isotopes it is assumed that the initial $^{10}Be/^{9}Be$ at the growth surface of the crust has remained constant over the past 10 Myr.

phy [*Joshima and Usui*, 1998] and biostratigraphy using microfossils which are sometimes incorporated into the crusts [*Harada and Nishida*, 1976; *Kadko and Burckle*, 1980]. The only other attempt that has been used successfully and more routinely is based on constant flux models of Co incorporation [*Halbach et al*., 1983; *Manheim*, 1986; *Puteanus and Halbach*, 1988; *Manheim and Lane-Bostwick*, 1988]. The most reliable results are presently obtained by a combination of the $^{10}Be/^{9}Be$ and Co constant-flux dating methods (Figure 8b), although in crust sections older than 10 Myr, hiatuses cannot be detected by this method [*Frank et al*., 1999a].

[49] It has recently been confirmed that isotope records of highly particle reactive elements (Th, Be, Pb, Nd) obtained from the highly porous ferromanganese crusts dating back millions of years are not significantly affected by diagenetic alterations or postdepositional exchange with present-day seawater. *Henderson and Burton* [1999] calculated the rates of postdepositional exchange of trace metals in crusts from a comparison with the mobility of U. For Hf and Os their calculated exchange rates are too high owing to erroneous seawater concentrations. Using the correct seawater concentrations for Hf [*McKelvey and Orians*, 1998] and Os [*Levasseur et al*., 1998], the (much lower) exchange rates indicate that long-term records of Hf and Os isotopes in ferromanganese crusts can also be considered reliable. Less particle reactive elements (U, Sr, Li) with long oceanic residence times are not reliable because of exchange processes with seawater after deposition. This prevents a direct comparison of time series of Sr isotopes with those of other isotopes in crusts and makes the Sr isotope dating of crusts impossible. Further evidence for the reliability of radiogenic isotope records in crusts comes from the existence of coherent and sharp changes in the high-resolution Pb isotope composition of even 30- to 50-Myr-old sections of ferromanganese crusts D11-1 and CD29-2 in the Pacific Ocean, which are separated by more than 3000 km [*Christensen et al*., 1997]. These changes cannot be correlated to a major period of phosphatization, confirming the robustness of the crust records. An additional argument is that datings of the same crusts obtained from profiles of different radioactive trace metals such as $^{230}Th$ or $^{10}Be$ give consistent results (see *Frank et al*. [1999a] for further discussion).

### 5.2. Present-Day Deep-Water Isotope Composition From Ferromanganese Crust Surfaces

[50] From comparisons of the isotope composition of Nd, Be, and Os in surface scrapings of crusts and nodules with deep-water data, and by inference also for Pb and Hf, for which no deep-water data are available, there is clear evidence that hydrogenous ferromanganese crusts and nodules have recorded the trace metal isotope composition of the ambient deep water [*O'Nions et al*., 1978; *Piepgras et al*., 1979; *Goldstein and O'Nions*, 1981; *Elderfield et al*., 1981; *Aplin et al*., 1986/1987; *Futa et al*., 1988; *Ben Othman et al*., 1989; *Amakawa et al*., 1991; *Albarède and Goldstein*, 1992; *Abouchami and Goldstein*, 1995; *von Blanckenburg et al*., 1996a, 1996b; *Albarède et al*., 1997, 1998; *Godfrey et al*., 1997; *Burton et al*., 1999b; *David et al*., 2001; *Vlastélic et al*., 2001]. From these studies a detailed global distribution of deep-water isotope compositions has emerged for most of the above mentioned trace metals and is shown in Figure 9 for Nd and Pb isotopes. Many of these data suffer from bad or even missing age control. However, even with a good chronology these crust/nodule samples will always integrate over periods of time on the order of $10^4$–$10^5$ years because of the very slow growth rates. This implies that shorter-term changes of ocean circulation, such as glacial-interglacial variability, will not be resolvable using ferromanganese crusts and nodules. There is, nevertheless, a clear and general provinciality between the deep Atlantic and Pacific basins (with the Indian basin being intermediate) in Nd, Pb, Hf, and Be isotopes. For Os isotopes the provinciality signal is very small, which is caused by its long ocean residence time [*Burton et al*., 1999b]. In the case of Pb and Nd, and probably also Hf, this provinciality is caused by differences in the weathering inputs from the surrounding continental crust, which is also reflected by intrabasin isotopic variability of Pb due to its short oceanic residence time [*Abouchami and Goldstein*, 1995; *Vlastélic et al*., 2001].

[51] Superimposed on the general provinciality are patterns ascribed to ocean circulation. In the case of Be the isotopic provinciality is almost exclusively a function of the nutrient-like behavior of $^{10}Be$ which gets enriched along the flow of deep water from the Atlantic into the Pacific [*von Blanckenburg et al.*, 1996a]. For Nd and Pb isotopes a tongue of low $\varepsilon_{Nd}$ ($-9$ to $-11$) and high $^{206}Pb/^{204}Pb$ (18.85 to 19.07) in the eastern sector of the Southern Atlantic has been attributed to the advection of NADW [*Albarède and Goldstein*, 1992; *Abouchami and Goldstein*, 1995; *Albarède et al*., 1997] (Figure 9). In the case of $^{206}Pb/^{204}Pb$ the NADW advection is apparently trackable into the SW Indian Ocean by high ratios (Figure 9b) [*Vlastélic et al*., 2001], whereas there is no indication for this in the Nd isotope data [*Albarède et al*., 1997]. Similarly, a tongue of low $^{206}Pb/^{204}Pb$ (18.7 to 18.8) and high $\varepsilon_{Nd}$ ($-5$ to $-7$) has been observed in the western sector of the Southern Atlantic and has been interpreted as inflowing Pacific waters. It was noted, however, that this is also the only major area where available deep-water $\varepsilon_{Nd}$ data do not agree with the nodule surface data, which was attributed to an integrated effect of decreased glacial NADW advection [*Albarède et al*., 1997] (see also section 5.3.2). In the Pacific Ocean a gradual northward increase in $\varepsilon_{Nd}$ [*Albarède and Goldstein*, 1992] and a clear relationship between water depth and Nd isotope composition at least for the central Pacific Ocean [*Aplin et al*., 1986/1987] are observed, which mirrors the northward advection of AABW with its lower $\varepsilon_{Nd}$ signature [*Piepgras and Jacobsen*, 1988; *Shimizu et al*., 1994]. Similarly, there is a

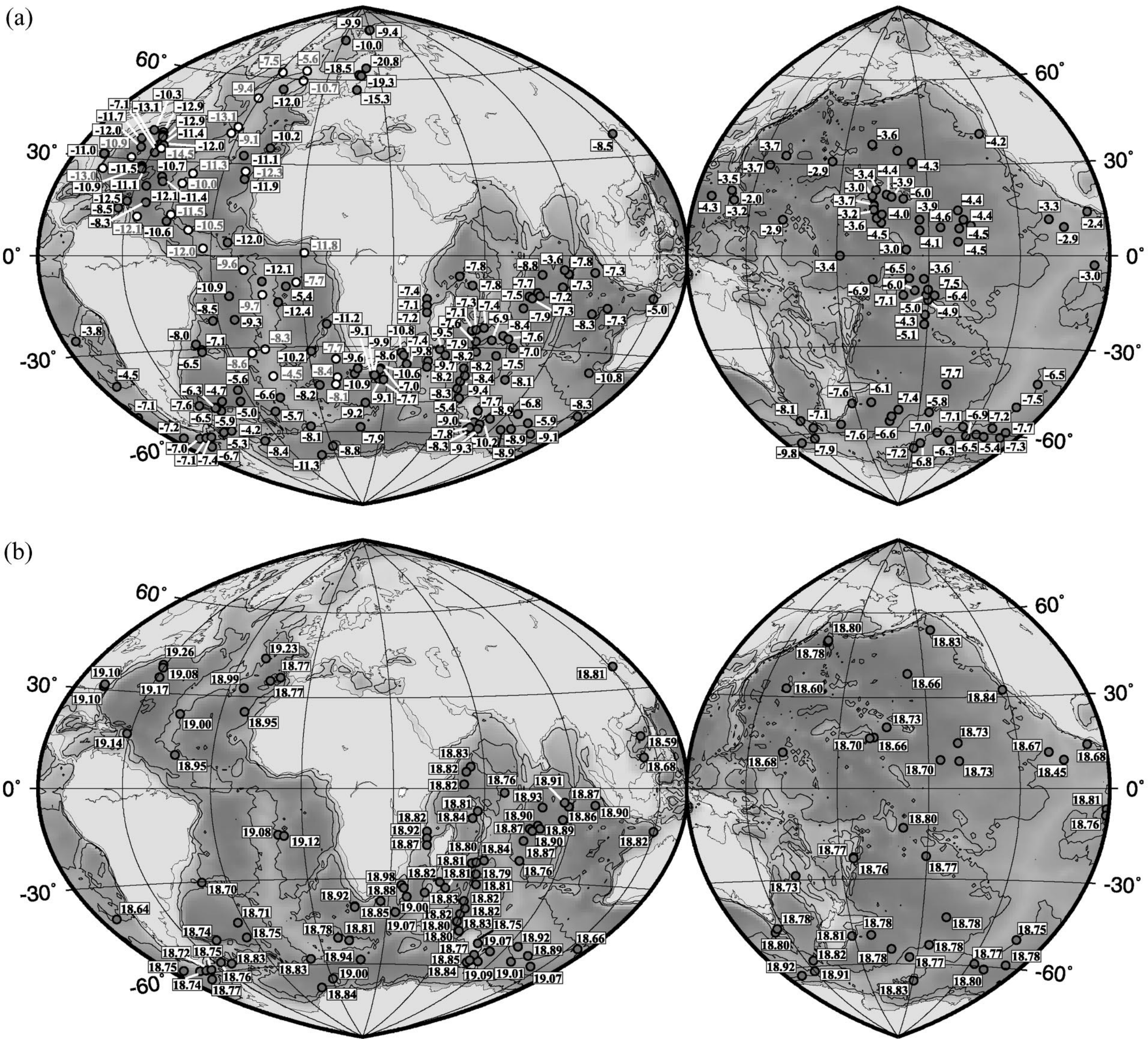


**Figure 9.** (a) Distribution of Nd isotope ratios in surface scrapings of ferromanganese crusts and nodules [*O'Nions et al.*, 1978; *Piepgras et al.*, 1979; *Goldstein and O'Nions*, 1981; *Elderfield et al.*, 1981; *Aplin et al.*, 1986/1987; *Futa et al.*, 1988; *Ben Othman et al.*, 1989; *Amakawa et al.*, 1991; *Albarède and Goldstein*, 1992; *Ling et al.*, 1997; *Burton et al.*, 1997; *Albarède et al.*, 1997, 1998; *O'Nions et al.*, 1998; *Abouchami et al.*, 1999; *Reynolds et al.*, 1999; *Frank et al.*, 1999b; *David et al.*, 2001]. The ratios are expressed as $\varepsilon_{Nd}$ units. The values labeled with a white circle and red numerals mark the Nd isotope results of studies of the ferromanganese coating of foraminfera in surface sediments [*Palmer and Elderfield*, 1985; *Rutberg et al.*, 2000]. (b) Distribution of Pb isotope ratios in surface scrapings of ferromanganese crusts and nodules [*O'Nions et al.*, 1978; *Ben Othman et al.*, 1989; *Abouchami and Goldstein*, 1995; *von Blanckenburg et al.*, 1996a; *Burton et al.*, 1997; *O'Nions et al.*, 1998; *Abouchami et al.*, 1999; *Reynolds et al.*, 1999; *Frank et al.*, 1999b; *Vlastélic et al.*, 2001]. Some hydrothermally influenced samples from near the mid-ocean ridges in the Indian Ocean [*Vlastélic et al.*, 2001] have not been included in Figure 9b.

reflection of the isotopic differences of the prevailing water masses and thus also water depth in the $\varepsilon_{Nd}$ signature of crusts from the Atlantic Ocean; for instance, crusts having grown from NADW have a lower $\varepsilon_{Nd}$ compared with those having grown from deeper waters (AABW) or shallower waters (AAIW) than the depth range of NADW ($\sim$ 1500–3500 m). A similar relationship between water depth and Pb isotope distribution in crusts from the Indian Ocean [*Vlastélic et al.*, 2001] and the Pacific [*Abouchami and Galer*, 1998] has also been suggested to be a consequence of isotopic differences between water masses.

### 5.3. Time Series Studies

[52] To date, trace metal isotope records (Pb, Nd, Hf) of 19 different ferromanganese crusts, dated by $^{10}Be/^{9}Be$, have been published (Figure 10, Table 2). Comparison of these time series shows that trace metals with

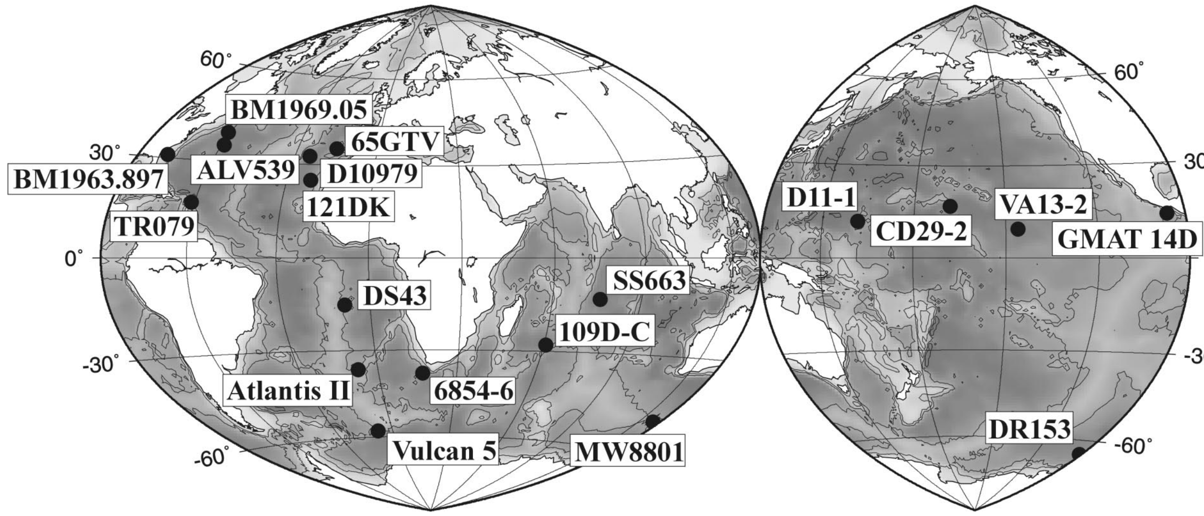


**Figure 10.** Locations of ferromanganese crusts for which trace metal isotope time series have been obtained.

oceanic residence times similar to the average global ocean mixing time, such as Nd [*Burton et al.*, 1997; *Ling et al.*, 1997; *O'Nions et al.*, 1998; *Abouchami et al.*, 1999; *Reynolds et al.*, 1999, *Frank et al.*, 1999b, 2002], Hf [*Lee et al.*, 1999; *Piotrowski et al.*, 2000; *David et al.*, 2001], and Be [*von Blanckenburg and O'Nions*, 1999], have generally retained the present provinciality in the deep ocean basins over the past up to 60 Myr (Figures 11a, 11c, 11d, and 12). In contrast, because of the much shorter oceanic residence time, the isotopes of Pb (Figures 11b and

**TABLE 2. Locations of Crusts With Published Radiogenic Isotope Time Series**

| *Cruise* | *Sample* | *Latitude* | *Longitude* | *Water Depth, m* | *Source of Isotope Data*[a] *Nd + Pb* | *Be* | *Thickness, mm* | *Average Growth Rate,*[b] *mm* $Myr^{-1}$ | *Maximum Age,*[c] *Myr* |
|---|---|---|---|---|---|---|---|---|---|
| | | | | *Atlantic Ocean* | | | | | |
| | BM1969.05 | 39°00′N | 60°57′W | 1829 | 1 | 3 | 130 | 1.62 | 60 |
| ALV539 | 2-1 | 35°36′N | 58°47′W | 2665 | 3 | 3 | 90 | 2.37 | 38 |
| | BM1963.897 | 30°58′N | 78°30′W | 850 | 8 | 8 | 38 | 4.5 | 8.5 |
| TR079 | D-14 | 16°55′N | 61.10′W | 2000 | 8 | 8 | 9.5 | 2.85 | 3 |
| SO83 | 65GTV | 35°20′N | 15°20′W | 1500 | 7 | | 38 | 4.5 | 8 |
| Discovery | D10979 | 32°36′N | 24°25′W | 5347–4867 | 8 | 8 | 15 | 2.3 | 8 |
| SO83 | 121DK | 24°53′N | 21°42′W | 2000 | 7 | | 38 | 3 | 13 |
| SO84 | DS43 | 15°09′S | 8°21′W | 1990–1966 | 8 | 8 | 15 | 1.56 | 9 |
| | | | | *Indian Ocean* | | | | | |
| Antipode | 109D-C | 27°58′S | 60°48′E | 5689–5178 | 3 | 3 | 30 | 1.60 | 14 |
| SS-XI | SS663 | 12°57′S | 76°06′E | 5250 | 3,6 | 6 | 67 | 2.80 | 26 |
| | | | | *Pacific Ocean* | | | | | |
| GMAT | 14D | 13°59′N | 96°08′W | 4000–3400 | 9 | 9 | 72 | 10.34 | 7 |
| VA13/2 | 237 KD | 09°25′N | 146°03′W | 4830 | 2 | 4 | 209 | 3.57 | 26 |
| F7-86-HW | CD29-2 | 16°42′N | 168°14′W | 2390–1970 | 2,5 | 2 | 105 | 2.10 | 55 |
| F10-89-CP | D11-1 | 11°39′N | 161°41′E | 1870–1690 | 2,5 | 2 | 147 | 2.53 | 58 |
| | | | | *Southern Ocean* | | | | | |
| Atlantis II | D4-1 | 36°23′S | 7°31′W | 2184 | 10 | 10 | 31 | 1.92 | 10 |
| Vulcan 5 | D34-42 | 57°47′S | 7°40′W | 3690–3900 | 10 | 10 | 15 | 6.14 | 3 |
| TBD463 | 6854-6 | 37°47′S | 16°55′E | 4517 | 10 | 10 | 33 | 3.86 | 7.5 |
| MW8801 | D18-1 | 50°03′S | 126°45′E | 3993 | 10 | 10 | 15 | 4.8 | 3 |
| BAS | DR153u/n | 64°58′S | 91°16′W | 3300–3150 | 10 | 10 | 6 | 0.7 | 6.5 |

[a]Sources are as follows: 1, *Burton et al.* [1997]; 2, *Ling et al.* [1997]; 3, *O'Nions et al.* [1998]; 4, *Segl et al.* [1984]; 5, *Christensen et al.* [1997]; 6, *Frank and O'Nions* [1998]; 7, *Abouchami et al.* [1999]; 8, *Reynolds et al.* [1999]; 9, *Frank et al.* [1999b]; 10, *Frank et al.* [2002].

[b]Average growth rates were derived from $^{10}Be/^{9}Be$ ratios.

[c] In cases where the ages of the bases of the crusts exceed 7–8 Myr, the maximum ages were calculated by extrapolating the growth rates derived from $^{10}Be$ concentrations in the upper sections of crust 121DK [*Abouchami et al.*, 1999] or by using Co chronometry for the others [*Frank et al.*, 1999a].

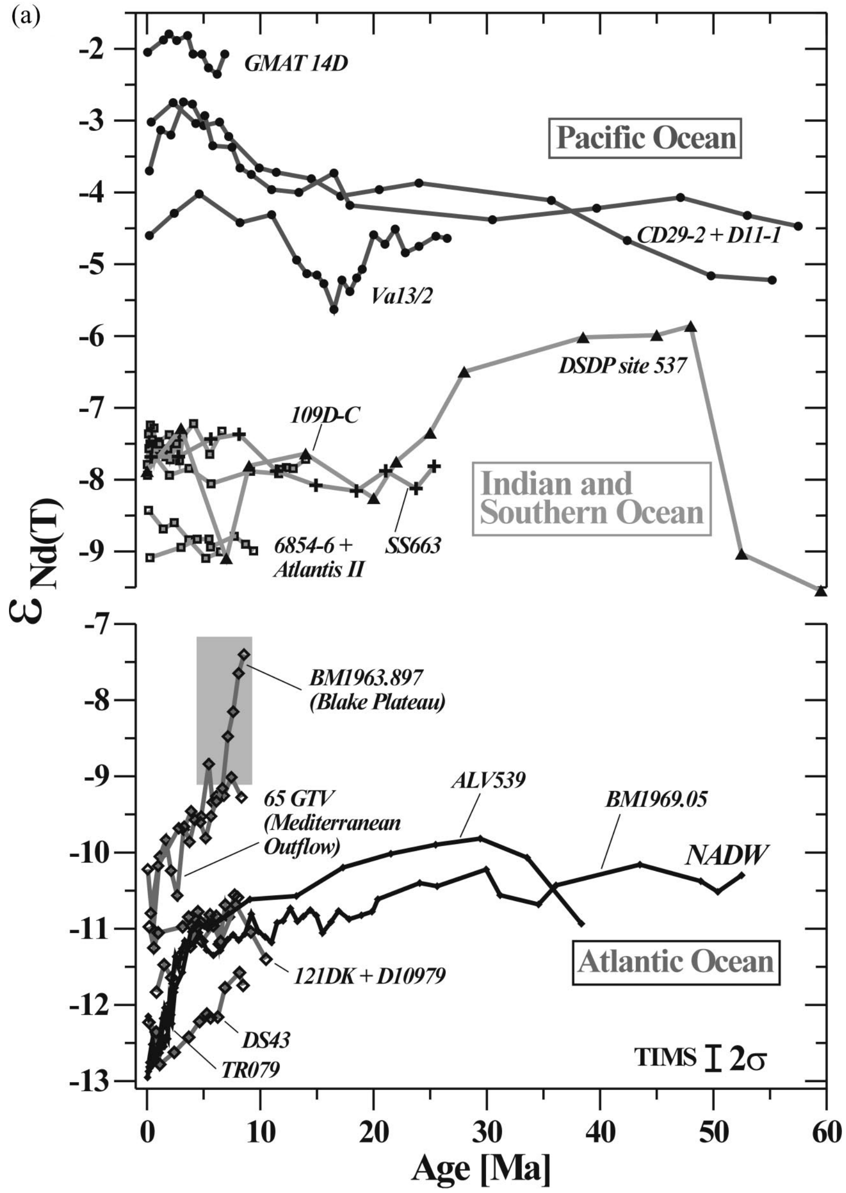


**Figure 11.** Overall comparison of deep-water isotope time series from all ocean basins for (a) Nd ($\varepsilon_{Nd}$), (b) Pb ($^{206}Pb/^{204}Pb$), (c) Hf ($\varepsilon_{Hf}$), and (d) Be ($^{10}Be/^{9}Be$). The data from the Pacific Ocean are marked by solid circles and blue lines; the data from the Indian Ocean are marked by crosses and green lines; the Southern Ocean data are marked by open squares and green lines; the data from the crusts having grown from NADW (BM1969.05, ALV539, TR079) are marked by black lines; and the other Atlantic Ocean records are marked by open diamonds and red lines. Error bars mark 2σ external reproducibilities of thermal ionization mass spectrometry (TIMS) and multiple-collector–inductively coupled plasma mass spectrometry (MC-ICPMS) measurements and can be assigned to the records from the respective publications for each crust. For Figure 11d, 2σ uncertainties of each individual measurement are given. Note that the *y* axes on this figure are discontinuous where there are overlaps between the data of the different ocean basins. The amount of overlap is marked by the green shadings.

12) have been strongly influenced by weathering of local source rocks, eolian, and riverine inputs, which are not as efficiently mixed in the ocean as in the case of Nd and Hf. Thus the Pb isotope time series show consistent patterns which are comparable with those of the Nd isotopes, but there are large overlaps between the isotopic signatures of the main ocean basins.

[53] The provinciality of the isotopic signatures has been most stable for Nd isotopes (Figure 11a), which only show an overlap between the data from the Atlantic sector of the Southern Ocean and the two shallowest crusts from the northern Atlantic Ocean for the period between 5 and 8 Ma. In the case of crust 65GTV (1500 m water depth) this reflects the continuous influence of Mediterranean Outflow Water (MOW) with its typical $\varepsilon_{Nd}$ value around −9.4 [*Spivack and Wasserburg*, 1988;

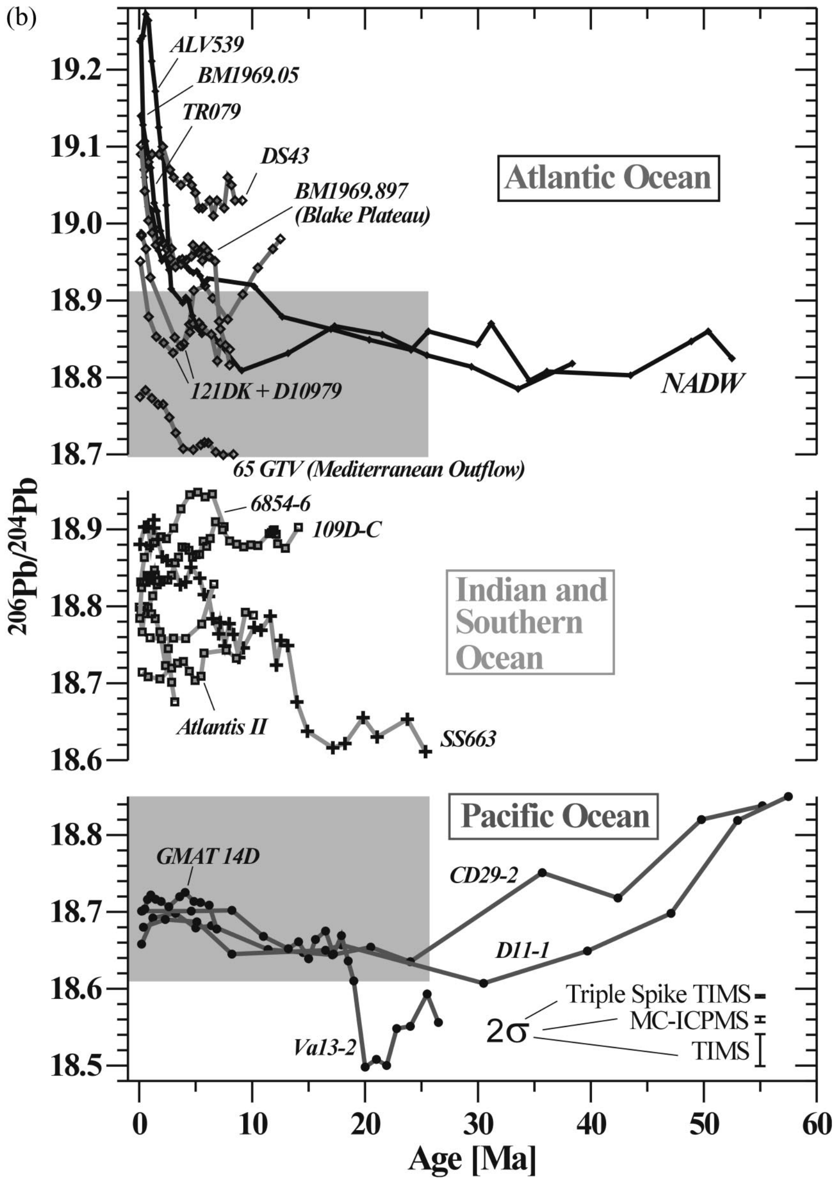


**Figure 11.** (continued)

*Abouchami et al.*, 1999]. The high Nd isotope values of crust BM1963.897 from the Blake Plateau (850 m water depth) for the past 5 Myr have been caused by admixture of water masses with relatively high $\varepsilon_{Nd}$ values from the Caribbean or from the dissolution of average continental dust, whereas the even higher values prior to 5 Ma probably reflect a contribution of surface and intermediate water masses from the Pacific Ocean prior to the closure of the Panama gateway (Figure 12) [*Reynolds et al.*, 1999; *Frank et al.*, 1999b] (see section 5.3.3). The records from the South Atlantic are in good agreement with a Nd isotope time series from the Rio Grande Rise obtained from ferromanganese oxide coatings [*Palmer and Elderfield*, 1986] (Figure 11a) and the central equatorial Pacific Ocean records agree well with Nd isotope records obtained from fish teeth [*Martin and Haley*, 2000]. The data reconstructed from the crusts are not, however, in good agreement with the reconstruction of the Nd isotope composition of Atlantic seawater as obtained from a combination of other discontinuous reservoirs such as phosphates, carbonates, or fish remains [*Shaw and Wasserburg*, 1985; *Staudigel et al.*, 1985; *Stille*, 1992; *Stille et al.*, 1996]. In view of the presently observed Nd isotope distribution in the Atlantic Ocean and its close relation to water depth and ocean water masses, this is, however, not surprising because, mostly, there is no information on water depth and thus potential water masses for these different locations [*Stille*, 1992; *Stille et al.*, 1996].

[54] The Hf and Be isotope records show considerable overlap between the Indian/Southern Ocean and Pacific Ocean records, whereas the data of the Atlantic Ocean and the Southern/Indian Ocean have stayed distinct from each other (Figures 11c and 11d). In the case of Be this is mainly explainable by the distinctly lower age of the Atlantic water masses, whereas for Hf the prove-

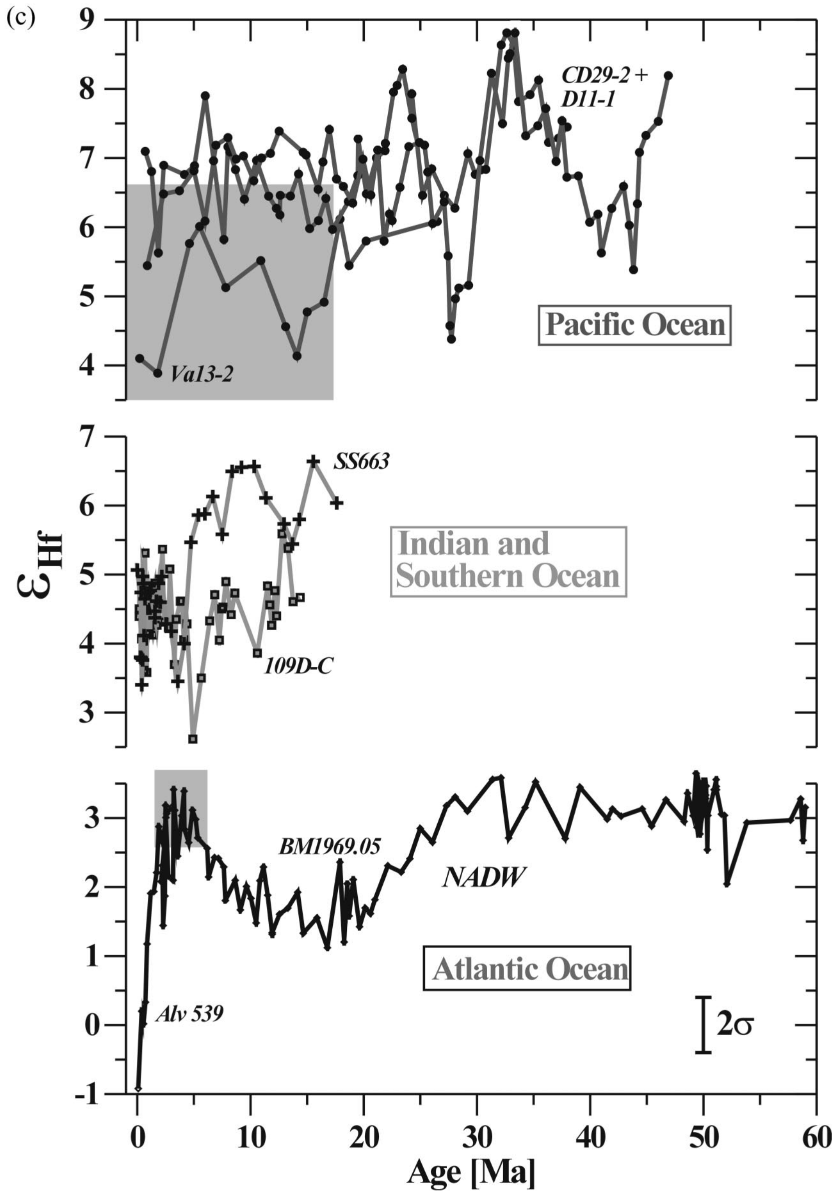


**Figure 11.** (continued)

nances of the source rocks combined with the difference in weathering regime in the North Atlantic area are mainly responsible for the persistent isotopic difference.

[55] All four isotope systems have in common, however, that there has been no overlap between the isotopic composition of the Atlantic and Pacific Oceans, although in the case of Pb isotopes, the values came quite close to each other for the periods between 50 and 60 Ma. This is probably the consequence of a more efficient mixing between the Atlantic and Pacific Oceans through the open seaway between North and South America at that time (see also section 5.3.5).

[56] Superimposed on the general provinciality, the isotope records of Nd, Hf, and Pb show pronounced trends over time, in particular over the past 15 Myr, some of which correlate basin-wide. The radiogenic isotope variations of the deep water of the past 60 Myr have thus predominantly been caused by either paleocirculation changes of the ocean, variations of inputs from the continents through weathering or provenance changes, or a combination of both and are discussed in more detail in the following sections (5.3.1–5.3.5). In general, the records show that the past 1 Myr has been the period of time with the most pronounced isotopic differences between the major ocean basins over the past 60 Myr. This is mainly a consequence of the distinct change in the isotopic composition of deep waters in the North Atlantic and will be discussed in more detail below (section 5.3.1).

[57] The influences of changes in ocean circulation and weathering processes have to be distinguished to facilitate the use of the radiogenic isotopes as paleocean tracers. Changes in weathering intensity and continental erosion have been the main factors controlling the long-

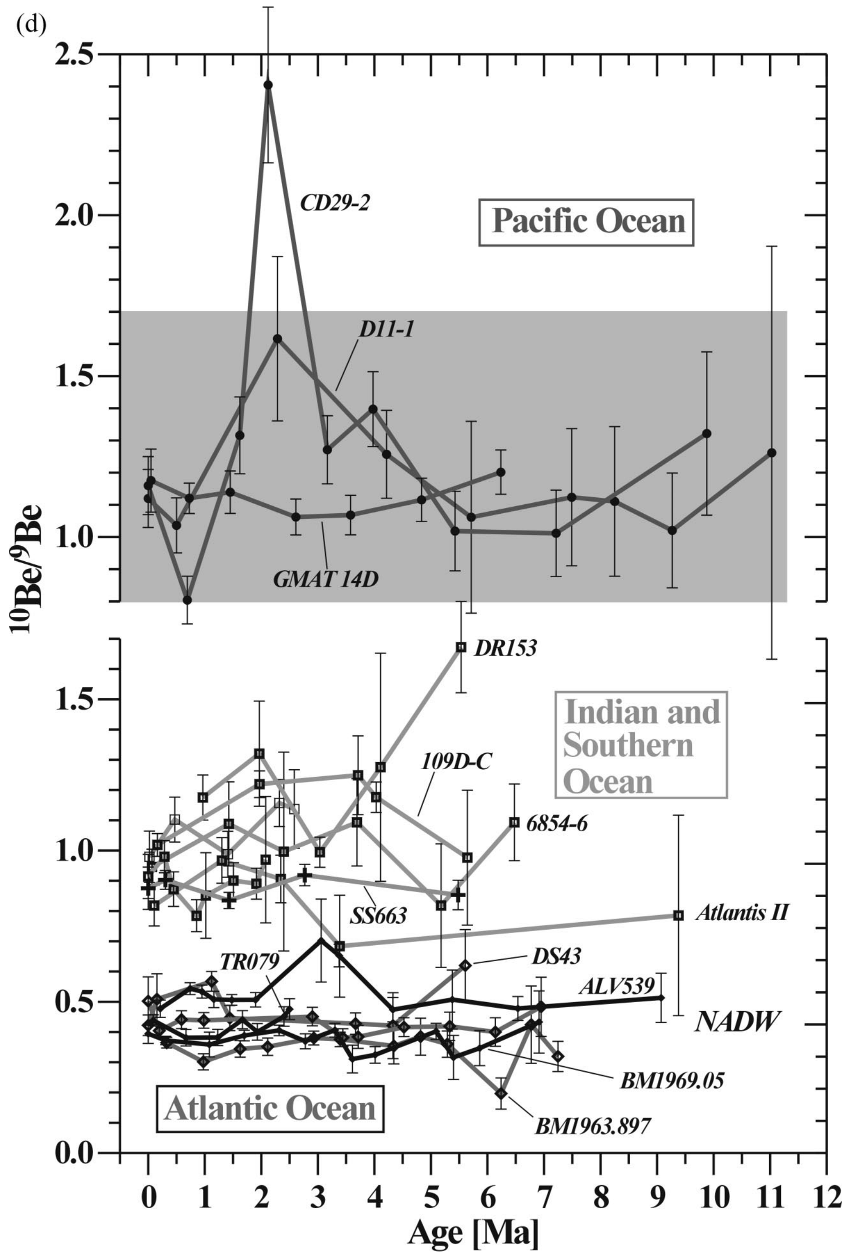


**Figure 11.** (continued)

term evolution of Sr and Os isotopes in the ocean, and it is thus obvious to compare these records to those of the potential paleocean tracers (Figures 6 and 11). It is immediately obvious that there are no clear relationships between them, which may have pointed to a common origin of the variations. For instance, in none of the Nd, Hf, or Pb isotope records can a long-term trend starting about 30 Ma be observed. The only records that resemble the Sr and Os records are the Pacific Nd isotope time series, which, however, have not continued to increase until the present day but started to decrease again for the past 3–5 Myr. If Himalayan erosion had played a major role for the Nd isotope evolution of the Pacific as has been suggested for Sr isotopes, the trend should point in the opposite direction because the Nd isotope signal of the eroded Himalayan material is very negative ($\varepsilon_{Nd} \sim -16$; see sections 5.3.4 and 5.3.5). The only clear indication for an influence of Himalayan erosion on deep-water radiogenic isotope composition is found in the local $^{208}Pb/^{206}Pb$ evolution of the deep Central Indian Ocean (crust SS663, see section 5.3.4.). It thus seems that the global trends in erosional input and weathering regime are not reflected by the Nd, Hf, and Pb isotope composition of the deep ocean. Clearly, more regional changes in either weathering and erosion processes or water mass circulation have been dominant, which is a consequence of the shorter oceanic residence time of Nd, Hf, and Pb compared with that of Os and Sr. In sections 5.3.1–5.3.5, results obtained from ferromanganese crusts for which a distinction between erosional/

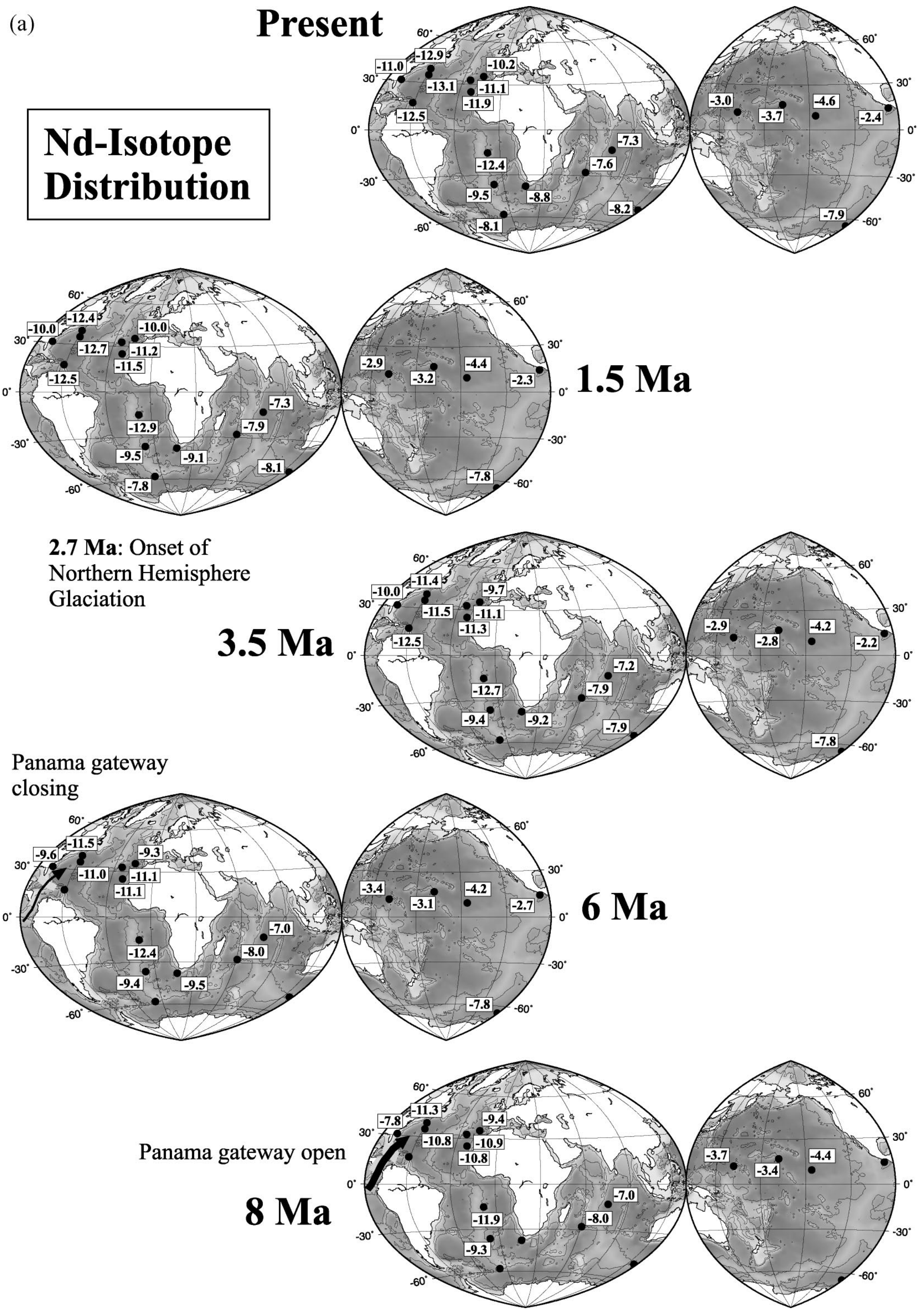


**Figure 12.** Time slice reconstructions of (a) the Nd and (b) the Pb isotope distributions in the global ocean for the periods 1.5 Ma, 3.5 Ma, 6 Ma, and 8 Ma, as derived from the available ferromanganese crust data [*Burton et al.*, 1997; *Ling et al.*, 1997; *O'Nions et al.*, 1998; *Frank and O'Nions*, 1998; *Abouchami et al.*, 1999; *Reynolds et al.*, 1999; *Frank et al.*, 1999b, 2001]. Note the open Panama gateway for the time slice maps at 8 Ma and the closing Panama gateway for the time slice at 6 Ma and the corresponding changes in the Pb and Nd isotope compositions at the shallow location on the Blake Plateau off Florida (crust BM1963.897). In addition, the stability of the Southern Ocean signals compared with the variations in the western North Atlantic after the onset of the Northern Hemisphere glaciation is noteworthy. In general, there was still a clear provinciality in isotope composition between the main ocean basins at 8 Ma, but the differences between the Atlantic and Pacific basins, particularly for Pb isotopes, were much less pronounced.

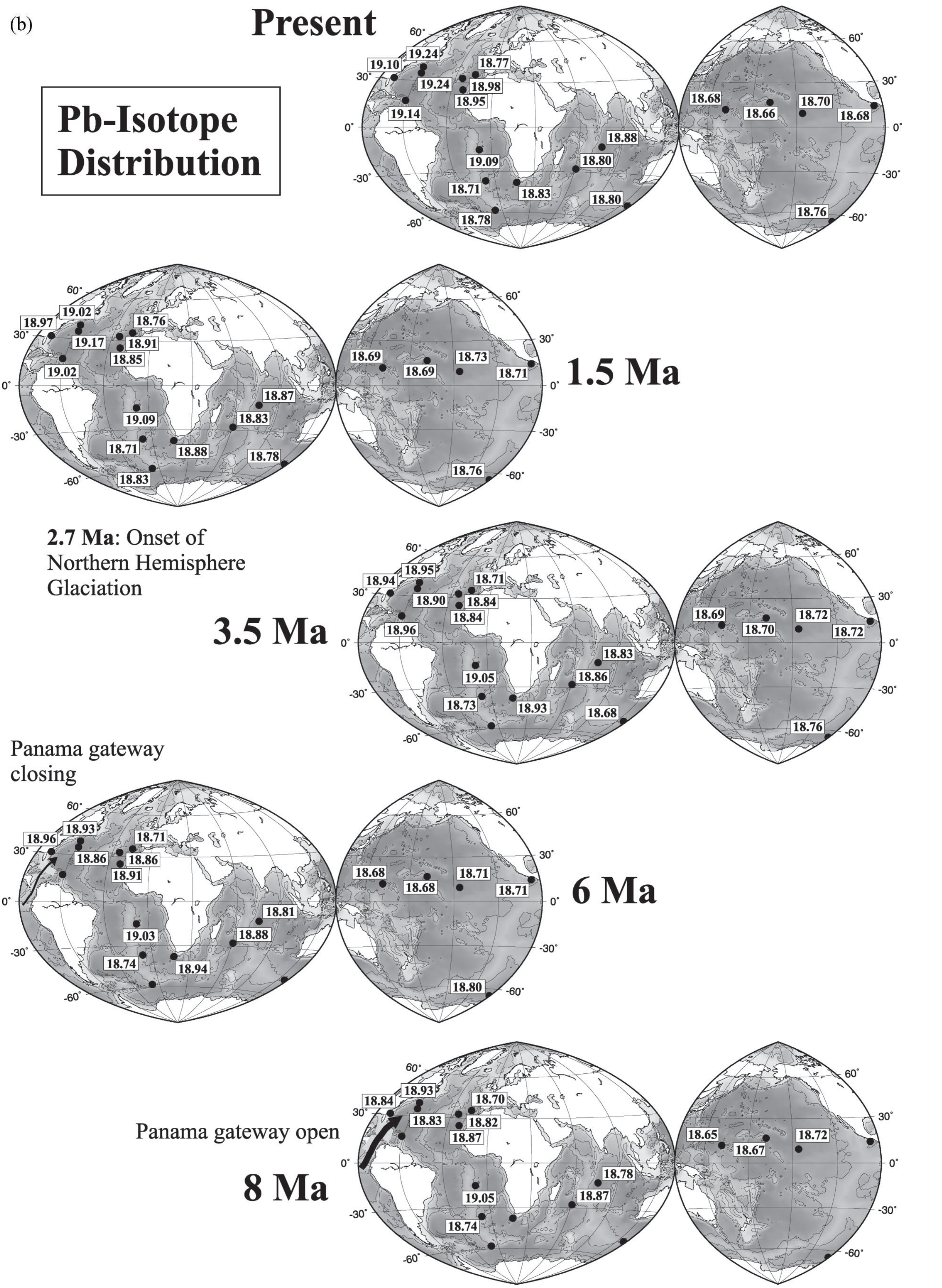


**Figure 12.** (continued)

weathering processes and variations in ocean circulation has been possible are discussed.

#### 5.3.1. Radiogenic Isotope Evolution of NADW in the North Atlantic Ocean

[58] NADW is produced in the North Atlantic Ocean, which makes this area one of the key locations controlling the global thermohaline circulation system and global climate. In the western North Atlantic, three crusts located within the flow path of present-day NADW (BM1969.05, ALV539, TR079) have recorded its radiogenic isotope evolution over the past up to 60 Myr (Figures 11 and 13). The most significant feature of these records is a relatively constant Pb and Nd isotope composition prior to about 3 Ma and a strong trend toward lower Nd isotope, $^{207}Pb/^{206}Pb$, and $^{208}Pb/^{206}Pb$ ratios and higher $^{206}Pb/^{204}Pb$ ratios afterward [*Burton et al.*, 1997, 1999a; *O'Nions et al.*, 1998; *Reynolds et al.*, 1999]. In the eastern Atlantic basin a similar pattern with a smaller amplitude (crust 121DK) has been ascribed to advection of NADW into the eastern Atlantic basin [*Abouchami et al.*, 1999]. A comparable decrease in the Hf isotope ratios in western North Atlantic crusts (BM1969.05 and ALV539) has been found over the same period [*Piotrowski et al.*, 2000; *van de Flierdt et al.*, 2002]. Prior to this the Hf isotopes in the one long record available for the western North Atlantic (BM1969.05) show a trough-like undulation starting at about 30 Ma with a broad minimum between ~12 and 23 Ma, which is not paralleled by the Pb and Nd isotope records and is not yet explained. From the patterns of these deep-water Nd, Hf, and Pb isotope records alone, it is not possible to decide whether changes in ocean circulation or changes in weathering regime on the continents have been the main cause for the observed variations over the past 3 Myr.

[59] Initially, the Nd isotope variations of NADW over the past 3 Myr (Figures 11, 12, and 13) were explained by an increasing contribution of deep water formed in the Labrador Sea [*Burton et al.*, 1997], which at present has a high Nd concentration and a very low $\varepsilon_{Nd}$ of –22, caused by weathering of Archean continental crust with values as low as $-40$ [*Stordal and Wasserburg*, 1986; *Hemming et al.*, 1998]. Consequently, even a small increase in the contribution of Labrador Seawater would lead to a decreased Nd isotope signal in NADW. In addition, it was initially argued that the final closure of the Panama gateway at about 3.5 Ma stopped the admixture of Pacific water masses with very radiogenic Nd (high $\varepsilon_{Nd}$) and at the same time strengthened NADW production, thus also suppressing the supply of water masses with a relatively high $\varepsilon_{Nd}$ from the southern Atlantic into the North Atlantic [*Burton et al.*, 1997]. These issues will be discussed in detail in sections 5.3.2 and 5.3.3, where it will be shown that it is unlikely that NADW production increased at the onset of Northern Hemisphere glaciation and that the closure of the Panama seaway for significant water mass exchange had already occurred at about 4.6–5 Ma.

[60] Recently, it has been shown that a change in weathering regime in the high northern latitudes was mainly responsible for the observed trace metal isotope changes. Nd isotope ratios have probably decreased owing to an increased amount of detrital input since the onset of Northern Hemisphere glaciation at about 2.7 Ma. Strongest evidence for a change in weathering regime comes from the Pb and Hf isotope records. *Von Blanckenburg and Nägler* [2001] demonstrated that the Pb isotope composition of dissolved Pb in the North Atlantic and Arctic Ocean has been dominated by the preferential release of radiogenic Pb ($^{206}Pb$, $^{207}Pb$, $^{208}Pb$) during weathering of rocks of the old continental shields of Canada and Greenland. Intense physical erosion such as during Northern Hemisphere glaciation favors the release of radiogenic Pb because of the continuous exposure of new rock surfaces and thus supposedly caused the observed variations in deep-water Pb isotope composition over the past 3 Myr (Figures 11b and 13). These processes are thus also responsible for the generally strong negative correlation between the $\varepsilon_{Nd}$ and $^{206}Pb/^{204}Pb$ time series and positive correlation between $\varepsilon_{Nd}$ and $^{207}Pb/^{206}Pb$ and $^{208}Pb/^{206}Pb$ in the Atlantic Ocean [*Frank and O'Nions*, 1998; *Frank et al.*, 1999a]. In contrast, the sign of correlation between the Nd and Pb isotopes is opposite in the equatorial Pacific Ocean, probably because there are no pronounced incongruent weathering effects on Pb isotopes in this regime of predominant chemical weathering. The dissolved Nd and Pb isotope composition in the Pacific Ocean more closely reflects the input sources such as the island arcs (section 5.3.5).

[61] Independent evidence corroborating the importance of a change in weathering regime in the North Atlantic after 3 Ma comes from the almost concomitant decrease in Hf isotope composition of NADW (Figure 11c). This decrease can only be explained by an enhanced contribution of unradiogenic (low $\varepsilon_{Hf}$) Hf hosted by zircons, which release some of their Hf during mechanical breakdown caused by enhanced physical erosion [*van de Flierdt et al.*, 2002]. The products of the enhanced mechanical weathering (with low $\varepsilon_{Hf}$ and $\varepsilon_{Nd}$ as well as radiogenic Pb isotope ratios) were supplied to NADW via the Baffin Bay by Labrador Sea water [*Vance and Burton*, 1999]. Additional support for a weathering-based explanation comes from Mn micronodules incorporated into sediment cores from the Arctic Ocean which have recorded variations in Nd and Pb isotopes of Arctic Ocean deep water over the past 5 Myr [*Winter et al.*, 1997]. These variations very closely resemble those of NADW but cannot have been caused by circulation changes in the Atlantic Ocean.

[62] In view of the pronounced change in the Nd, Hf, and Pb isotope composition over the past 2–3 Myr, one may expect a similar change in the $^{10}Be/^{9}Be$ ratios. The reason for this would be the increased input of $^{9}Be$ into

the ocean caused by enhanced weathering of the continental crust, whereas $^{10}Be$, which is supplied from the atmosphere, would at the same time remain unaffected. Such a change in the decay-corrected initial $^{10}Be/^{9}Be$ profiles is not observed (Figure 11d), but the ratios have remained constant within a small range [*von Blanckenburg and O'Nions*, 1999]. This appears to be an argument against the control of the observed patterns in the Nd isotopes by weathering [*Burton et al*., 1999a]. Further results indicate, however, that the surface water Nd isotope composition of the Labrador Sea experienced a similar general trend over the past 2.5 Myr as the deep NW Atlantic crusts [*Vance and Burton*, 1999]. It is thus more likely that the changes in detrital $^{9}Be$ supply were too small to cause a resolvable change in the deep-water $^{10}Be/^{9}Be$ ratio of the North Atlantic [*von Blanckenburg and O'Nions*, 1999; *von Blanckenburg and Nägler*, 2001]. Thus the constant initial $^{10}Be/^{9}Be$ ratios argue against significant overall circulation changes in the North Atlantic over the past 3 Myr but do not exclude changes on glacial-interglacial timescales, which cannot be resolved by the crust records.

[63] In summary, these lines of evidence strongly suggest that an increased input of detrital material released by enhanced physical erosion of the old continental landmasses of the Canadian Shield and Greenland associated with the onset of Northern Hemisphere glaciation was the most important factor controlling the changes in isotope composition of deep waters in both the North Atlantic and Arctic Ocean over the past 3 Myr.

#### 5.3.2. History of NADW Export Into the Southern Ocean

[64] From the reconstruction of the isotopic evolution of NADW in the North Atlantic alone, one cannot assess the strength of NADW production and the vigor of the global thermohaline circulation in the past. Analogous to approaches using $\delta^{13}C$ of benthic foraminifera (see section 1.2), an estimate of NADW export can be achieved from a comparison of the Nd isotope evolution of NADW and the Southern Ocean. The strength of the admixture of low $\varepsilon_{Nd}$ NADW to the Southern Ocean over time should be reflected by changes of the Southern Ocean deep-water Nd isotope composition because presently about 50% of the ACC water masses are derived from NADW.

[65] Nd isotope time series of five crusts in the South Atlantic and the Southern Ocean, however, display no resolvable variability over the past up to 14 Myr. They do not reflect the pronounced changes in Nd isotope composition over the past 3 Myr observed in the western North Atlantic [*Frank et al*., 2002] (Figure 14). A Nd isotope record obtained from ferromanganese coatings of foraminifera from a water depth of 2050 m on the Rio Grande Rise confirms this observation by showing the same range of values as the Southern Atlantic crust records over the past 14 Myr [*Palmer and Elderfield*, 1985] (Figure 11a). In addition, two glacial/interglacial records of Nd isotope variations obtained the same way at two locations in the deep Cape Basin [*Rutberg et al*., 2000] average exactly at the same values as the crust data from corresponding locations. This lends further support to the reliability of reconstructions of the deep-water radiogenic isotope composition from the authigenic fraction of marine sediments despite potential problems of Nd contributions from pore waters and the diagenetic mobility of Mn under reducing conditions.

[66] In view of the well-constrained export of low $\varepsilon_{Nd}$ NADW in the present-day Atlantic Ocean (Figure 5), the most likely explanation for these observations is a progressive decrease in overall NADW export into the Southern Ocean since the onset of Northern Hemisphere glaciation at about 3 Ma. This obviously coincided with the decrease in the $\varepsilon_{Nd}$ signature of NADW, which was caused by increased weathering intensity and detrital input into the North Atlantic in the course of Northern Hemisphere glaciation (section 5.3.1). Pb isotope data obtained from the same crusts similarly indicate a decrease in the export of typical NADW Pb isotope signature to the Southern Ocean over the past 3 Myr. This is in agreement with previous interpretations of the distribution of Pb isotopes in Mn-nodule surfaces [*Abouchami and Goldstein*, 1995; *Vlastélic et al*., 2001] and with modeling results [*Henderson and Maier-Reimer*, 2002] suggesting that, indeed, a significant NADW Pb isotope signature can be advected from the North Atlantic into the Southern Ocean. The short oceanic residence time of Pb and the strong influence of local contributions from continental weathering, however, prevent any quantitative estimates of the decrease in NADW export (Figure 14).

[67] A decrease in NADW export during the glacial periods of the late Quaternary has been identified from stable carbon isotope comparisons of North Atlantic and Pacific records [*Raymo et al*., 1990, 1992]. Nd isotope data recovered from the ferromanganese coating of foraminifera of glacial/interglacial Cape Basin sediments have recently been shown to reflect a greatly diminished NADW input into the Southern Ocean during glacial times [*Rutberg et al*., 2000] (Figure 15). The results of this Nd isotope record are entirely consistent with the carbon isotope record of the same sediment core, which also indicates a decreased glacial export of NADW [*Charles and Fairbanks*, 1992; *Charles et al*., 1996]. The Nd isotope record of this core is probably one of the most striking examples so far for the potential offered by radiogenic trace metal isotopes to reconstruct paleocirculation patterns.

[68] The new Nd isotope data from the Southern Ocean crusts now allow a semiquantitative estimate of the overall exchange between NADW and the main Southern Ocean deep-water mass CDW over the past 14 Myr. Such semiquantitative estimates are a valuable complementary addition to the carbon isotope approaches. Basic assumptions for this estimate are a

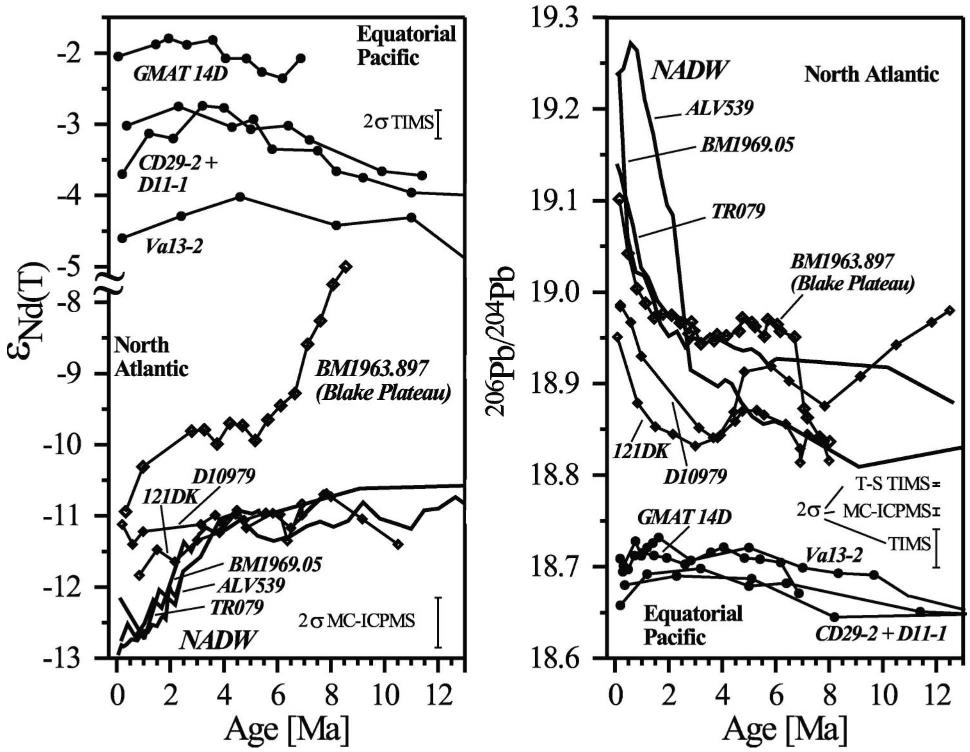


**Figure 13.** Comparison of Nd and Pb isotope time series from ferromanganese crusts in the North Atlantic Ocean [*Burton et al.*, 1997, 1999a; *O'Nions et al.*, 1998; *Abouchami et al.*, 1999; *Reynolds et al.*, 1999] and the equatorial Pacific [*Ling et al.*, 1997; *Abouchami et al.*, 1997; *Frank et al.*, 1999b] for the past 13 Myr. Error bars mark 2σ external reproducibilities of TIMS and MC-ICPMS measurements and can be assigned to the records from the respective publications for each crust. Symbols are the same as in Figure 11. Note the pronounced decrease in $\varepsilon_{Nd}$ and increase in $^{206}Pb/^{204}Pb$ in the western North Atlantic crusts (NADW: BM1969.05, ALV539, TR079) at about 3 Ma, which in the eastern north Atlantic basin is accompanied by a significant increase in $^{206}Pb/^{204}Pb$ and only a weak decrease in $\varepsilon_{Nd}$ (121DK, D10979). Also note the changes in $\varepsilon_{Nd}$ and $^{206}Pb/^{204}Pb$ between 5 and 8 Ma in crust BM1963.897, which have apparently been caused by a decrease in shallow water mass advection from the Pacific through the closing Panama gateway, and which are therefore not observed in the other deep basin isotope records from the Atlantic.

NADW-free Pacific-dominated end-member $\varepsilon_{Nd}$ of Southern Ocean deep water in the range of −4 to −6 and no systematic differences in Nd concentration between NADW and CDW. Simple mass balance of the Atlantic and Southern Ocean Nd isotope data then suggests that at the Walvis Ridge (location of crust Atlantis II), 45–55% of the water presently consists of NADW, which is in good agreement with estimates based on oceanographic [*Döös*, 1995] and water column Nd isotope data from the Southern Ocean [*Piepgras and Wasserburg*, 1982]. The time series data (Figures 11 and 14) indicate that the overall contribution of NADW to Southern Ocean water masses was between 15 and 35% higher at 3.5 Ma compared with the present [*Frank et al.*, 2002]. It is noted that this estimate of decreasing overall NADW export is also consistent with decreased NADW export during the glacial periods of the past 3 Myr because the ferromanganese crust samples always integrate over several glacial-interglacial cycles [*Albarède et al.*, 1997]. For the period between 14 Ma and 3.5 Ma the data indicate a continuous and strong export of a NADW-type water mass from the North Atlantic.

#### 5.3.3. Influence of the Panama Gateway Closure on Ocean Circulation

[69] Paleogeographic reorganizations either initiate or prevent water mass exchange between ocean basins with different trace metal isotope characteristics and should thus be mirrored by changes in deep-water isotope composition of the corresponding ocean basins. The most recent important paleogeographic event was the closure of the Panama gateway by the emergence of the land bridge between North and South America at ~3.5 Ma [*Keigwin*, 1982]. There is considerable debate as to when direct deep-water exchange between the Atlantic and Pacific Oceans was stopped because the paleogeography of the Caribbean region is complicated by the presence of several tectonic microplates. There is evidence for a shallow sill (1000 m) at 12 Ma [*Duque-Caro*, 1990] and a land bridge as early as 8 Ma [*Marshall*, 1985]. Faunal comparisons between Pacific and Caribbean deep-dwelling microorganisms suggest that the evolution of species in both basins did not occur in parallel after about 4.6 Ma. This suggests a cessation of deep-water exchange between the two oceans and is in

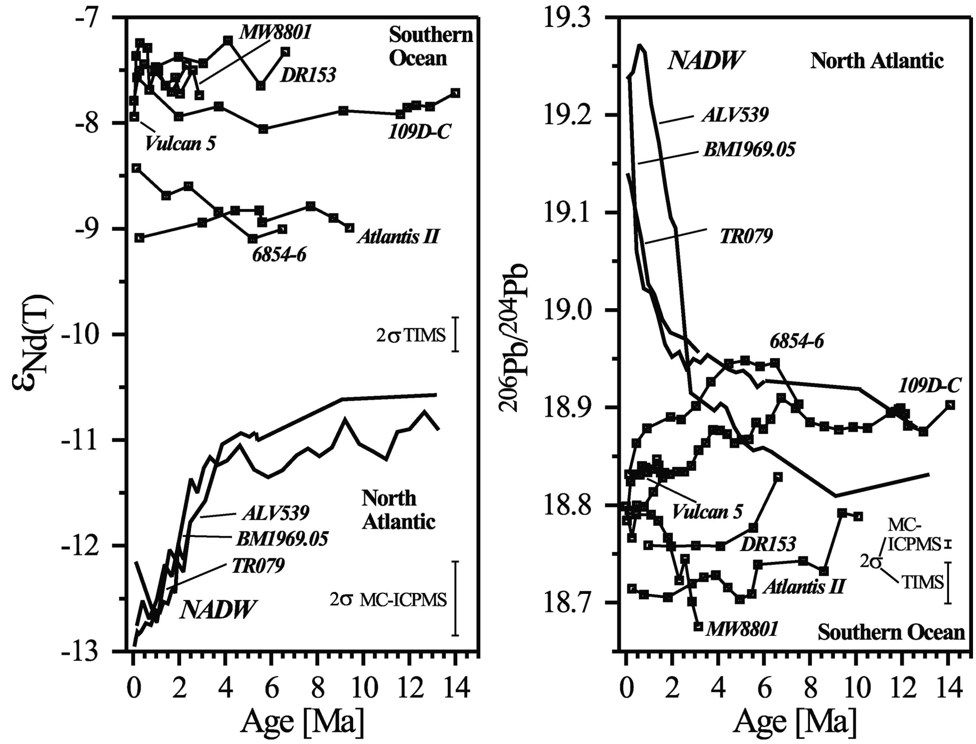


**Figure 14.** Comparison of Nd and Pb isotope time series obtained from ferromanganese crusts from the Southern Ocean [*Frank et al.*, 2001] and NADW in the western North Atlantic [*Burton et al.*, 1997, 1999; *O'Nions et al.*, 1998; *Reynolds et al.*, 1999]. Symbols are the same as in Figure 11. Error bars mark 2σ external reproducibilities of TIMS and MC-ICPMS measurements and can be assigned to the records from the respective publications for each crust.

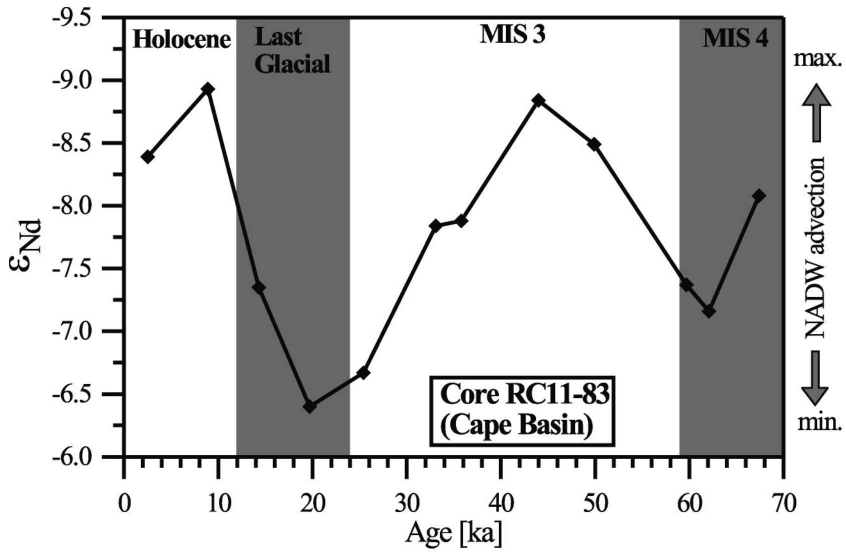


**Figure 15.** Nd isotope variations over the past 70 kyr as obtained from the authigenic Mn coating of particles in sediment core RC11-83 from the Cape Basin in the eastern Atlantic sector of the Southern Ocean [*Rutberg et al.*, 2000]. The shaded areas mark the glacial Marine Isotope Stages (MIS) 2 (last glacial) and 4. The $\varepsilon_{Nd}$ pattern of this core demonstrates that during glacial periods the deep water in the Cape Basin was dominated by Pacific-derived water with a more positive $\varepsilon_{Nd}$ signature, implying that the contribution of NADW with its much more negative $\varepsilon_{Nd}$ was substantially decreased (note the reversed scale of the *y* axis).

agreement with sedimentological results obtained from Caribbean and Pacific carbonate sediments [*Haug and Tiedemann*, 1998]. The consequences of the closure of the Panama gateway for the global thermohaline circulation and global climate have also been subject to divergent opinions. A causal relationship between closure of the Panama gateway and the approximately coinciding onset of Northern Hemisphere glaciation was inferred [*Stanley*, 1995], whereas others suggested that the Panama closure for deep-water exchange as early as 6 Ma inhibited the onset of Northern Hemisphere glaciation for several million years [*Berger and Wefer*, 1996]. Sedimentological results support an increase in NADW production rate coinciding with the closure for deep-water exchange at about 4.6 Ma [*Haug and Tiedemann*, 1998] and are in agreement with results obtained from carbon isotope comparisons of the deep Pacific and Atlantic basins [*Raymo et al.*, 1992; *Ravelo and Andreasen*, 2000].

[70] Reconstructions based on trace metal isotope records in ferromanganese crusts have recently shed new light on the consequences of Panama gateway closure for ocean circulation. Pacific deep-water crust (GMAT 14D), which recorded the Nd and Pb isotope composition close to Panama over the past 7 Myr, shows only a very small shift toward higher $\varepsilon_{Nd}$ values at 4.5 Ma and no change in Pb isotope composition [*Frank et al.*, 1999b] (Figure 13). Assuming this shift in Nd isotope values was caused by a stop of the admixture of North Atlantic Water masses across Panama, mass balance suggests that less than 5% Atlantic water contributed to Pacific deep water during the 3–4 Myr prior to complete closure of the Panama gateway.

[71] On the Atlantic side of Panama, a crust from a water depth of 850 m on Blake Plateau (BM1963.897) is now bathed in Gulf Stream water. This location was particularly sensitive to circulation changes induced by the closure of the Panama gateway because of the stopped inflow of shallower subsurface water masses with Pacific Nd ($\varepsilon_{Nd}$ $-2$ to $-4$) and Pb ($^{206}Pb/^{204}Pb \sim 18.7$) isotopic composition into the Atlantic. In addition, northward deviation of surface water masses originating from the South Atlantic which would have flowed into the Pacific prior to closure would result in similar changes for the Nd and Pb isotope composition of water masses on Blake Plateau. The isotope time series of the Blake Plateau crust shows two significant patterns for both Pb and Nd [*Reynolds et al.*, 1999]. At about 2–3 Ma the Nd and Pb isotopes show a shift comparable to the deeper western North Atlantic crusts [*Burton et al.*, 1997, 1999; *O'Nions et al.*, 1998; *Reynolds et al.*, 1999] (Figure 13). Following the interpretation given in section 5.3.1, this is probably a consequence of within-basin mixing of NADW, which is, for example, also evident in similar isotope patterns in two crusts from the eastern Atlantic Basin [*Abouchami et al.*, 1999].

[72] Prior to 3 Ma the water mass on the Blake Plateau shows an isotopic evolution that is not observed in other crusts located farther away from the Panama gateway in the North Atlantic. Over the period between ~8 and 5 Ma the Nd isotope composition decreased by 2.5 $\varepsilon_{Nd}$ units and $^{206}Pb/^{204}Pb$ increased from 18.83 to 18.97, with the change for the Pb isotopes having already been completed by 6.5 Ma. These patterns are interpreted as a progressive decrease in the advection of Pacific water masses into the Atlantic Ocean. The data suggest that the Panama gateway was already closed to deep and intermediate water mass exchange by ~5 Ma, in agreement with sedimentological evidence [*Haug and Tiedemann*, 1998]. This implies that the closure of the Panama gateway cannot have been the direct cause but rather only one of the prerequisites for the onset of the Northern Hemisphere glaciation [*Reynolds et al.*, 1999]. The immediate consequence of the Panama gateway closure for deep-water exchange at 4.6 Ma was thus early Pliocene climate warming rather than a major cooling.

[73] In summary, the radiogenic isotope record from the Blake Plateau is a good example for the potential of the radiogenic isotope records in paleoceanographic research in that it first documented changes in ocean circulation for the period between 8 and 5 Ma, and then from 3 Ma to present it has been influenced by changes of the weathering regime, similar to other crusts from different water depths in the North Atlantic basin.

#### 5.3.4. Radiogenic Isotope Evolution of Indian Ocean Deep Water and the Influence of Himalayan Uplift

[74] The Indian Ocean has been the sink for erosional products of Himalayan uplift over the past 30 Myr, as is evidenced by the sedimentary deposits of the Bengal and Indus fans. It may thus be expected that the dissolved trace metal isotopic composition of the Indian Ocean has also been influenced by Himalayan erosion products over this period of time as is suggested by Sr isotopes. An erosional signal from the Himalayas should be particularly pronounced during times of strongest uplift and thus maximum erosion, which probably started around 24 Ma [*Searle*, 1996].

[75] Nd isotope and $^{206}Pb/^{204}Pb$ records of crust SS663 from the deep Central Indian Ocean are compared with other crust records in Figure 11 [*O'Nions et al.*, 1998; *Frank and O'Nions*, 1998]. Over such long periods of time, factors such as subsidence and plate tectonic drift of the locations of the crusts have to be considered as potential causes for the observed isotopic trends of the ambient deep water. The location of crust SS663 from the central Indian Ocean has subsided by 2 km water depth from a location above the paleo-CCD in the Eocene to a water depth below the CCD at present. Growth of a ferromanganese crust at this location only started about 26 Ma, probably as a consequence of a higher deep-water oxygenation and decreased detrital sedimentation [*Banakar and Hein*, 2000]. In addition, the location of the crust moved about 2200 km northeast from its initial location during the past 53 Myr. These horizontal and vertical movements are obviously re-

flected by changes in the supply of detrital particles, growth structures, and major element geochemical composition of crust 55663 but have apparently not left any clear signal in its radiogenic isotope record.

[76] One of the most striking observations of the time series of this crust is the constancy of the Nd isotope composition in contrast to the marked change in Pb isotopes (Figures 11a and 11b). The Nd isotope data throughout this crust have been within the narrow range of present-day Indian Ocean deep water ($\varepsilon_{Nd} = -7.4$ to $-8$) [*Bertram and Elderfield*, 1993; *Albarède et al.*, 1997] for the past 26 Myr and suggest that the huge input of Himalayan weathering material with an $\varepsilon_{Nd}$ value of $-16 \pm 2$ [*Derry and France-Lanord*, 1996] did not significantly change the Nd isotope budget of the Indian Ocean deep water. In contrast, there was an increase of the $^{206}Pb/^{204}Pb$ from a low of 18.6 (similar to the deep Pacific) to a high around 18.9 at present. While this range is still intermediate between the Atlantic and Pacific Ocean data, an even more pronounced signal is observed for the time series of the $^{208}Pb/^{206}Pb$ ratio, which peaked between 20 and 8 Ma (Figure 16) at values even higher than the present Pacific. This signature has been attributed to Himalayan erosional input [*Frank and O'Nions*, 1998] mainly derived from the High Himalayan gneisses and leucogranites [*France-Lanord et al.*, 1993]. This is supported by an offset of the Pb isotope data of the Central Indian Ocean toward the Pb isotope composition of these rocks in Pb-Pb isotope space (Figure 17). This observation demonstrates the potential of the three radiogenic Pb isotopes that are derived from different sources and thus provide independent information on input processes and sources.

[77] The reason for the apparent decoupling of the seawater Pb and Nd isotope responses to Himalayan erosion remains somewhat speculative. One possible reason is that the Nd is retained more efficiently in the estuary of the Ganges and the sediments of the Bengal Fan than is Pb. An alternative explanation is that most of the Pb introduced by rivers into the Indian Ocean through Himalayan erosion is scavenged and deposited more efficiently than Nd proximal to the riverine sources, i.e., at the location of SS663. Nd is much less particle reactive, and the riverine Himalayan Nd may therefore be efficiently mixed with other water masses of different Nd isotope composition and advected into other ocean basins so that no particular signal of Himalayan erosion has been left in the deep northern Indian Ocean.

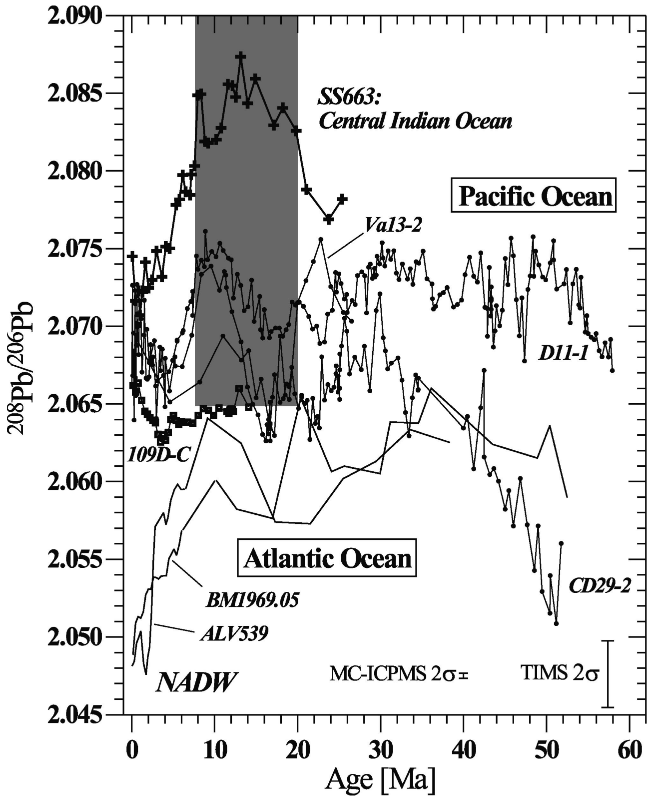


**Figure 16.** Time series of $^{208}Pb/^{206}Pb$ obtained from selected ferromanganese crusts in the Indian, Atlantic, and Pacific Oceans [*Ling et al.*, 1997; *Burton et al.*, 1997; *Christensen et al.*, 1997; *O'Nions et al.*, 1998; *Frank and O'Nions* 1998; *Reynolds et al.*, 1999; *Frank et al.*, 2001] modified after *Frank and O'Nions* [1998]. The most important feature is the broad peak of $^{208}Pb/^{206}Pb$ in crust SS663 (shaded ara), which is higher than any other deep-water data reconstructed from ferromanganese crusts so far. Symbols are the same as in Figure 11. Error bars mark 2σ external reproducibilities of TIMS and MC-ICPMS measurements and can be assigned to the records from the respective publications for each crust.

### 5.3.5. Radiogenic Isotope Evolution of the Equatorial Pacific Deep Water

[78] The equatorial Pacific Ocean is another example of the competition between ocean circulation changes and weathering inputs in controlling deep-water radiogenic isotope composition. Nd and Pb isotope records (and, to a lesser extent, Hf isotopes) derived from equatorial Pacific ferromanganese crusts show well-resolved and comparable patterns over the past 50–60 Myr. For Nd, there is a more or less steady increase from $\varepsilon_{Nd}$ values between $-5$ and $-4.5$ to maximum values around $-2.8$ at about 3–5 Ma in the two seamount crusts CD29-2 and D11-1 from water depths around 2000 m (Figure 11a). The rate of change in Nd isotopes was strongest between about 15–12 Ma and 5 Ma. After 3–5 Ma the trend reversed toward slightly lower $\varepsilon_{Nd}$ values [*Ling et al.*, 1997]. Applying the revised timescale given by *Frank et al.* [1999a], a third deep-water crust VA13/2 from the equatorial Pacific shows a very similar pattern over the past 26 Myr, but with a constant offset of about 1 $\varepsilon_{Nd}$ unit toward lower values, which is probably a reflection of a long-existing advection of AABW with its lower Nd isotope ratio into the deep central Pacific Ocean [*Ling et al.*, 1997]. A similar difference in $\varepsilon_{Hf}$ between deep crust VA13/2 and the other equatorial Pacific crusts is probably also related to the influence of AABW [*David et al.*, 2001]. A fourth crust, GMAT 14D, from deep waters

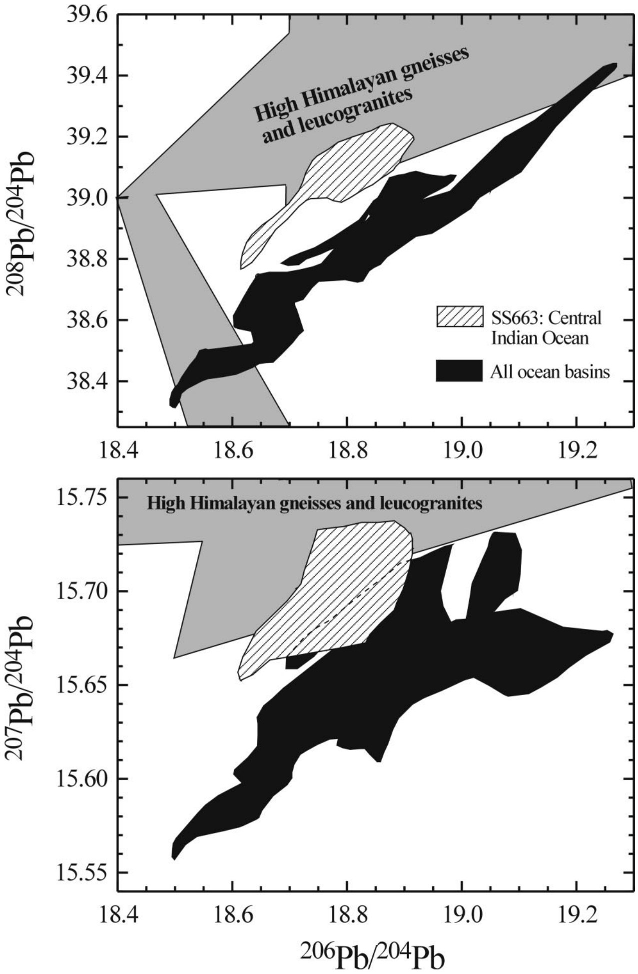


**Figure 17.** $^{207}Pb/^{204}Pb$ versus $^{206}Pb/^{204}Pb$ and $^{208}Pb/^{204}Pb$ versus $^{206}Pb/^{204}Pb$ ratios for available ferromanganese crust time series from the Atlantic, Pacific, and Indian Oceans updated after *Frank and O'Nions* [1998]. Sources are from *Burton et al.* [1997], *Ling et al.* [1997], *O'Nions et al.* [1998], *Frank and O'Nions* [1998], *Abouchami et al.* [1999], *Reynolds et al.* [1999], and *Frank et al.* [1999, 2002]. The arrays for the Himalayan gneisses and leucogranites are taken from *Vidal et al.* [1982] and the compilation by *Schärer et al.* [1990]. This kind of plot reveals mixing relationships between distinct end-member reservoirs. It can clearly be seen that, compared with the data of all other crusts available so far, it is only the data from the crust in the Central Indian Ocean which are significantly offset toward the field of High Himalayan gneisses and leucogranites, which supply most of the detritus found in the Bengal Fan. This obviously documents a contribution to the dissolved Pb in the deep central Indian Ocean by partial dissolution of this material.

close to Panama also shows a similar pattern as the others over the past 7 Myr but with a 1 $\varepsilon_{Nd}$ unit offset toward higher values (Figure 11a), providing evidence for some imprint of weathering products from the young nearby island arc rocks of Central America [*Frank et al.*, 1999b].

[79] The patterns of the Pb isotope time series obtained for these crusts by different analytical techniques also show a generally close agreement [*Ling et al.*, 1997; *Christensen et al.*, 1997; *Abouchami et al.*, 1997; *Frank et al.*, 1999b; *David et al.*, 2001] (Figure 11b). In particular, the patterns of the two high-resolution laser ablation MC-ICPMS Pb isotope profiles obtained on the two seamount crusts CD29-2 and D11-1 reveal close correspondence, despite the fact that they are separated by some 3000 km [*Christensen et al.*, 1997] (Figure 16). The high-resolution variability of the Pb isotope ratios seems to correlate with the deep-water oxygen isotope record and thus global climate and ice volume. *Christensen et al.* [1997] have also suggested that larger differences between the absolute values of the two Pb isotope records prior to about 30 Ma may indicate a weak circulation and water mass mixing in the Pacific basin for that period of time. After 30 Ma, Pb isotope records became very similar, indicating efficient mixing of Pb derived from various input sources in the Pacific Ocean despite its relatively short oceanic residence time (Figure 16). A similar interpretation was derived for Hf isotopes, which have apparently been very well mixed in the equatorial Pacific at water depths around 2000 m for the past 20 Myr [*Lee et al.*, 1999] (Figure 11c).

[80] The similar patterns of all four crusts suggests some common control for the changes in the Nd and Pb isotope composition of the entire equatorial Pacific Ocean. The continuous increase in Nd isotope composition over the past 15 Myr, particularly between 10 and 5 Ma, approximately coincides with the onset of deep-water production (AABW) around the Antarctic. One might expect that this circulation change also influenced the trace metal isotope composition of deep-water masses in the Pacific. Whereas the relatively small change in the $^{206}Pb/^{204}Pb$ time series over this period of time (Figure 11b) would be consistent with an increased contribution of AABW, the increase in Nd isotopes clearly goes the opposite way, which excludes this possibility. A more likely source for the observed long-term trend in the dissolved Pacific Nd isotope composition appears to be the evolution of the Pacific island arcs such as Indonesia and the subsequent weathering of these rocks with their very high $\varepsilon_{Nd}$ signature. This is in agreement with the inferred evolution of the Pacific island arc production rate in the past, which was relatively low between 15 and 8 Ma and has increased strongly afterward [*Kaiho and Saito*, 1994]. Earlier periods of high arc production rates between 35 and 15 Ma are not reflected by Nd isotope records, possibly as a function of lower total amounts of weathering products supplied to the ocean over this period. It has been shown that today REEs from tropical island arcs are very efficiently introduced into Pacific surface waters by riverine input and remobilization on the shelves [*Sholkovitz et al.*, 1999; *Lacan and Jeandel*, 2001]. For the dissolved Pb isotope composition of the Pacific, it has also been suggested that weathering of the Pacific island arcs may play an important role [*von Blanckenburg et al.*, 1996b].

[81] The coinciding small decrease in $\varepsilon_{Nd}$ and changes

in Pb isotope composition of Pacific deep waters at 3–5 Ma (Figures 11a, 11b, and 16) had (in the case of Nd) been attributed to advection of the pronounced isotopic changes within NADW (section 5.3.1) into the deep Pacific Ocean [*Ling et al.,* 1997; *Martin and Haley*, 2000]. In view of the previously published records (nearly invariant Nd isotope record from the Indian sector of the Southern Ocean [*O'Nions et al*., 1998] and, in particular, the new data from the Southern Ocean discussed in section 5.3.2 [*Frank et al*., 2002]), this is not a viable explanation because the NADW signal should have left its imprint on the isotope composition of the deep Southern Ocean on its way to the deep Pacific. This is not the case, probably as a consequence of the inferred decrease in NADW advection to the Southern Ocean. For Pb the oceanic residence time is too short to transfer a signal from the North Atlantic into the Pacific [*Henderson and Maier-Reimer*, 2002]. Alternatively, the small change in Nd and Pb isotope composition might be explained by an increased inflow of Southern Ocean water masses [*Abouchami et al*., 1999].

[82] Given that there was no decrease in island arc production over the past 3–5 Myr [*Kaiho and Saito*, 1994], the most likely explanation for the changes in Nd and Pb isotopes seems to be a change in eolian inputs, which have been suggested to be important factors in controlling the dissolved radiogenic isotope signal in the ocean [*Abouchami et al*., 1997; *Tachikawa et al*., 1999]. This is a reasonable interpretation in view of the fact that the eolian input into the Pacific derived from Asia increased by about an order of magnitude around 3 Ma [*Rea*, 1994], coinciding with the changes in dissolved Nd and Pb isotope composition of the deep Pacific Ocean. Changes in eolian dust supply and deposition prior to 5 Ma have probably been too small to influence the dissolved radiogenic isotope budget of the Pacific Ocean.

[83] Over the up to 60 Myr covered by the equatorial Pacific crusts the plate tectonic movement of their locations relative to the Pacific climate and wind belts and current systems may have had an influence on their radiogenic isotope evolution. An equatorial Pacific crust which has moved from a position at the equator to 25°N over the past ~80 Myr shows, for example, element compositional changes that have been related to the movement of the crust location relative to the Pacific trade wind zones [*McMurtry et al*., 1994]. The location of equatorial Pacific sediment core GPC3 has a similar paleopath and recorded clear Nd and Pb isotopic shifts of the deposited eolian dust caused by a change in dust source provenance from Northern America to Asia [*Pettke et al*., 2002]. Equatorial Pacific crusts with similar paleopaths, however, do not show clearly related shifts in their radiogenic isotope records [*Ling et al*., 1997; *Christensen et al*., 1997; *Lee et al*., 1999]. An increasing eolian influence from Asia should, for example, be reflected by a decrease in $\varepsilon_{Nd}$ over the past 20–30 Myr, whereas the opposite trend is observed.

[84] In summary, the available records from the equatorial Pacific Ocean suggest that changes in weathering sources and dust input rather than changes in ocean circulation have dominated the deep-water trace metal isotope composition over the past 30 Myr. Further records from the south and north Pacific are needed to verify this.

## 6. SUMMARY AND OUTLOOK

[85] Radiogenic isotope time series of the deep ocean provide important information for the reconstruction of paleocirculation patterns as a consequence of paleoclimatic or paleogeographic changes, changing inputs due to changes in weathering regimes, weathering intensity, or mountain uplift. These different factors have to be distinguished in order to extract reliable information on distinct processes. For the reconstruction of changes in regime and intensity of weathering, this has been successful in three example areas. In the deep North Atlantic, radiogenic isotope records have mainly varied as a function of weathering changes associated with the onset of Northern Hemisphere glaciation. In the Indian Ocean a Pb isotope time series has obviously recorded the intensity of Himalayan erosion. In the equatorial Pacific Ocean, changes in the erosional input associated with the evolution of the island arcs have mainly controlled the radiogenic isotope variability. In contrast, a shallow North Atlantic record from Blake Plateau documented changes in ocean circulation related to the closure of the Panama gateway, and a comparison of the radiogenic isotope evolution of the Southern Ocean with that of NADW documented a decrease in the intensity of NADW export to the Southern Ocean over the past 3 Myr. These and other studies have resulted in a greatly improved understanding of the main input sources and the processes controlling the oceanic distribution of the dissolved signatures originating from these sources.

[86] To reconstruct past circulation patterns of the oceans on timescales of millions of years, there are a number of interesting key areas from which ferromanganese crust–based studies could provide additional valuable information. Provided that suitable crust material can be found, this includes the timing and the oceanographic consequences of the opening of the Drake Passage or the closure of the Indonesian gateway, or the evolution of mass exchange through oceanic fracture zones of mid-ocean ridges, which should be highly sensitive to circulation changes. In addition, there is a lack of long-term Pacific time series which are not from equatorial regimes.

[87] With the advance of methods to extract the trace metal isotope information from the authigenic fraction of pelagic marine sediments, the future of radiogenic isotopes as paleoceanographic proxies lies mainly in applications to changes on much shorter timescales such as glacial/interglacial or even decadal or centennial instabilities of the ocean and their causes and responses to

abrupt climate change. Pelagic sediments have the advantage of a much better time control and availability of study material from almost everywhere in the ocean, which should provide more quantitative estimates on past water mass exchange. In addition, information on changes in weathering regimes and erosional inputs can be extracted from the detrital fraction of the same material.

[88] Future work should also include a more detailed study of the input mechanisms in key areas (such as the Ganges and Brahmaputra estuaries or high-latitude rivers and estuaries), which are close to those of the most pronounced isotopic changes of the deep ocean. In addition, a more detailed study of the eolian input and the processes that make this material available for the dissolved radiogenic isotope budget of the ocean is needed in order to better quantify the importance of this source and its local distribution.

[89] Such parameterization will enable more detailed and better constrained modeling of the present and past oceanic behavior of radiogenic isotopes, which will improve the understanding of the relevant processes in the ocean. Together, such studies will allow better constrained applications of radiogenic isotopes as tracers in oceanography and paleoceanography.

[90] **ACKNOWLEDGMENTS.** I would like to thank F. von Blanckenburg for numerous discussions about the use of trace metal isotopes in the ocean and for critical comments on the manuscript. R. K. O'Nions, A. N. Halliday, B. Reynolds, N. Whiteley, N. Belshaw, K. David, T. van de Flierdt, and J. R. Hein are thanked for many discussions. The paper benefited greatly from reviews of H. Elderfield and L. Derry and constructive comments of the editor T. Torgersen. I would like to thank the Swiss Science Foundation for support. Much of the work presented was carried out during support by a grant within the Training and Mobility through Research network program "The Marine Record of Continental Tectonics and Erosion" of the European Union.

Tom Torgersen was the Editor responsible for this paper. He thanks one anonymous cross-disciplinary reviewer and one anonymous technical reviewer.

## REFERENCES

Abouchami, W., and S. J. G. Galer, The provinciality of Pb isotopes in Pacific Fe-Mn deposits, *Min. Mag.*, *62A*, 1–2, 1998.

Abouchami, W., and S. L. Goldstein, A lead isotopic study of Circum-Antarctic manganese nodules, *Geochim. Cosmochim. Acta*, *59*, 1809–1820, 1995.

Abouchami, W., S. L. Goldstein, S. J. G. Galer, A. Eisenhauer, and A. Mangini, Secular changes of lead and neodymium in central Pacific seawater recorded by a Fe-Mn crust, *Geochim. Cosmochim. Acta*, *61*, 3957–3974, 1997.

Abouchami, W., S. J. G. Galer, and A. Koschinsky, Pb and Nd isotopes in NE Atlantic Fe-Mn crusts: Proxies for trace metal paleosources and paleocean circulation, *Geochim. Cosmochim. Acta*, *63*, 1489–1505, 1999.

Albarède, F., and S. L. Goldstein, World map of Nd isotopes in sea-floor ferromanganese deposits, *Geology*, *20*, 761–763, 1992.

Albarède, F., S. L. Goldstein, and D. Dautel, The neodymium isotopic composition of manganese nodules from the Southern and Indian Oceans, the global oceanic neodymium budget, and their bearing on deep ocean circulation, *Geochim. Cosmochim. Acta*, *61*, 1277–1291, 1997.

Albarède, F., A. Simonetti, J. D. Vervoort, J. Blichert-Toft, and W. Abouchami, A Hf-Nd isotopic correlation in ferromanganese nodules, *Geophys. Res. Lett.*, *25*, 3895–3898, 1998.

Alleman, L. Y., A. J. Véron, T. M. Church, A. R. Flegal, and B. Hamelin, Invasion of the abyssal North Atlantic by modern anthropogenic lead, *Geophys. Res. Lett.*, *26*, 1477–1480, 1999.

Amakawa, H., J. Ingri, A. Masuda, and H. Shimizu, Isotopic compositions of Ce, Nd and Sr in ferromanganese nodules from the Pacific and Atlantic Oceans, the Baltic and Barents Seas and the Gulf of Bothnia, *Earth Planet. Sci. Lett.*, *105*, 554–565, 1991.

Amakawa, H., D. S. Alibo, and Y. Nozaki, Nd isotopic composition and REE pattern in the surface waters of the eastern Indian Ocean and its adjacent seas, *Geochim. Cosmochim. Acta*, *64*, 1715–1727, 2000.

Andersson, P., R. Dahlqvist, J. Ingri, and Ö. Gustafsson, The isotopic composition of Nd in a boreal river: A reflection of selective weathering and colloidal transport, *Geochim. Cosmochim. Acta*, *65*, 521–527, 2001.

Aplin, A., A. Michard, and F. Albarède, $^{143}Nd/^{144}Nd$ in Pacific ferromanganese encrustations and nodules, *Earth Planet. Sci. Lett.*, *81*, 7–14, 1986/1987.

Archer, D., A. Winguth, D. Lea, and N. Mahowald, What caused the glacial/interglacial atmospheric $p$CO$_2$ cycles?, *Rev. Geophys.*, *38*, 159–189, 2000.

Asmus, T., M. Frank, C. Koschmieder, N. Frank, R. Gersonde, and A. Mangini, Variations of biogenic particle flux in the southern Atlantic section of the Subantarctic Front during the late Quaternary: Evidence from sedimentary $^{231}Pa_{ex}$ and $^{230}Th_{ex}$, *Mar. Geol.*, *159*, 63–78, 1999.

Banakar, V. K., and D. V. Borole, Depth profiles of $^{230}Th_{excess}$, transition metals and mineralogy of ferromanganese crusts of the Central Indian basin and implications for paleoceanographic influence on crust genesis, *Chem. Geol.*, *94*, 33–44, 1991.

Banakar, V.K., and J.R. Hein, Growth response of a deep-water ferromanganese crust to evolution of the Neogene Indian Ocean, *Mar. Geol.*, *162*, 529–540, 2000.

Barker, P.F., and J. Burrell, The opening of Drake Passage, *Mar. Geol.*, *25*, 15–34, 1977.

Barrett, T. J., P. N. Taylor, and J. Lugowski, Metalliferous sediments from DSDP Leg 92: The East Pacific Rise transect, *Geochim. Cosmochim. Acta*, *51*, 2241–2253, 1987.

Bayon, G., C. R. German, R. M. Boella, J. A. Milton, R. N. Taylor, and R. W. Nesbitt, An improved method for extracting marine sediment fractions and its application to Sr and Nd isotopic analysis, *Chem. Geol*, in press, 2002.

Belshaw, N. S., R. K. O'Nions, and F. von Blanckenburg, A SIMS technique for $^{10}Be/^{9}Be$ measurement in environmental materials, *Int. J. Mass Spectrom. Ion Phys.*, *142*, 55–67, 1995.

Belshaw, N. S., P. A. Freedman, R. K. O'Nions, M. Frank, and Y. Guo, A new variable dispersion double-focussing plasma mass spectrometer with performance illustrated for Pb-isotopes, *Int. J. Mass. Spectrom.*, *181*, 51–58, 1998.

Ben Othman, D., W. M. White, and P. J. Patchett, The geochemistry of marine sediments, island arc magma genesis, and crust mantle recycling, *Earth Planet. Sci. Lett.*, *94*, 1–21, 1989.

Berger, W. H., and G. Wefer, Expeditions into the past: Paleoceanographic studies in the South Atlantic, in *The South Atlantic: Present and Past Circulation*, edited by W.H. Berger et al., pp. 363–410, Springer-Verlag, New York, 1996.

Bertram, C. J., and H. Elderfield, The geochemical balance of the rare earth elements and neodymium isotopes in the oceans, *Geochim. Cosmochim. Acta*, *57*, 1957–1986, 1993.

Bollhöfer, A., A. Eisenhauer, N. Frank, D. Pech, and A. Mangini, Thorium and uranium isotopes in a manganese nodule from the Peru basin determined by alpha sectrometry and thermal ionization mass spectrometry (TIMS): Are manganese supply and growth related to climate?, *Geol. Rundsch.*, *85*, 577–585, 1996.

Bout-Roumazeilles, V., G. Davies, and L. Labeyrie, Nd-Sr-Pb evidence of glacial-interglacial variations in clay provenance and transport in the North Atlantic Ocean, *Min. Mag.*, *62A*, 1443–1444, 1998.

Boyle, E. A., Cadmium: Chemical tracer of deepwater paleoceanography, *Paleoceanography*, *3*, 471–489, 1988.

Boyle, E. A., Cadmium and $\delta^{13}C$ paleochemical ocean distributions during the stage 2 glacial maximum, *Annu. Rev. Earth Planet. Sci.*, *20*, 245–287, 1992.

Boyle, E. A., S. D. Chapnick, G. T. Shen, and M. P. Bacon, Temporal variability of lead in the western North Atlantic, *J. Geophys. Res.*, *91*, 8573–8593, 1986.

Broecker, W. S., The great ocean conveyor, *Oceanography*, *4*, 79–89, 1991.

Broecker, W. S., and T. H. Peng, Tracers in the sea, report, Lamont-Doherty Geol. Obs., Palisades, N. Y., 1982.

Broecker, W. S., T. H. Peng, S. Trumbore, G. Bonani, and W. Wölfli, The distribution of radiocarbon in the glacial ocean, *Global Biochem. Cycles*, *4*, 103–117, 1990.

Bruland, K. W., Trace elements in sea-water, in *Chemical Oceanography*, vol. 8, edited by J.P. Riley and R. Chester, pp. 175–220, Academic, San Diego, Calif., 1983.

Burton, K. W., and D. Vance, Glacial-interglacial variations in the neodymium isotope composition of seawater in the Bay of Bengal recorded by planktonic foraminifera, *Earth Planet Sci. Lett.*, *176*, 425–441, 2000.

Burton, K. W., H.-F. Ling, and R. K. O'Nions, Closure of the Central American Isthmus and its effect on deep-water formation in the North-Atlantic, *Nature*, *386*, 382–385, 1997.

Burton, K. W., D.-C. Lee, J. N. Christensen, A. N. Halliday, and J. R. Hein, Actual timing of neodymium isotopic variations recorded by Fe-Mn crusts in the western North Atlantic, *Earth Planet Sci. Lett.*, *171*, 149–156, 1999a.

Burton, K. W., B. Bourdon, J.-L. Birck, C. J. Allègre, and J. R. Hein, Osmium isotope variations in the oceans recorded by Fe-Mn crusts, *Earth Planet Sci. Lett.*, *171*, 185–197, 1999b.

Charles, C. D., and R. G. Fairbanks, Evidence from Southern Ocean sediments for the effect of North Atlantic Deep Water flux on climate, *Nature*, *355*, 416–419, 1992.

Charles, C. D., J. Lynch-Stieglitz, U. S. Ninnemann, and R. G. Fairbanks, Climate connections between the hemisphere revealed by deep-sea sediment core/ice core correlations, *Earth Planet Sci. Lett.*, *142*, 19–27, 1996.

Chen, J. H., G. J. Wasserburg, K. L. Von Damm, and J. M. Edmond, The U-Th-Pb systematics in hot springs on the East Pacific Rise at 21°N and Guayamas Basin, *Geochim. Cosmochim. Acta*, *50*, 2467–2479, 1986.

Chow, T. J., and C. C. Patterson, The occurrence and significance of Pb isotopes in pelagic sediments, *Geochim. Cosmochim. Acta*, *26*, 263–308, 1962.

Christensen, J. N., A. N. Halliday, L. V. Godfrey, J. R. Hein, and D. K. Rea, Climate and ocean dynamics and the lead isotopic records in Pacific ferromanganese crusts, *Science*, *277*, 913–918, 1997.

Claude-Ivanaj, C., A. W. Hofmann, I. Vlastélic, and A. Koschinsky, Recording changes in ENADW composition over the last 340 ka using high precision lead isotopes in a Fe-Mn crust, *Earth Planet Sci. Lett.*, *188*, 73–89, 2001.

Cochran, J. K., T. McKibbin-Vaughan, M. M. Dornblaser, D. Hirschberg, H.D. Livingstone, and K.O. Buesseler, $^{210}Pb$ scavenging in the North Atlantic and North Pacific Oceans, *Earth Planet Sci. Lett.*, *97*, 332–352, 1990.

Curry, W. B., and G. P. Lohmann, Reduced advection into Atlantic Ocean deep eastern basins during last glacial maximum, *Nature*, *308*, 317–324, 1983.

Curry, W. B., J. C. Duplessy, L. D. Labeyrie, D. Oppo, and L. Kallel, Quaternary deep-water circulation changes in the distribution of $\delta^{13}C$ of deep water $\Sigma CO_2$ between the last glaciation and the Holocene, *Paleoceanography*, *3*, 317–342, 1988.

David, K., M. Frank, R. K. O'Nions, N. S. Belshaw, J. W. Arden, and J. R. Hein, The Hf isotope composition of global seawater and the evolution of Hf isotopes in the deep Pacific Ocean from Fe-Mn crusts, *Chem. Geol.*, *178*, 23–42, 2001.

Derry, L. A., and C. France-Lanord, Neogene Himalayan weathering history and river $^{87}Sr/^{86}Sr$: Impact on the marine Sr record, *Earth Planet. Sci. Lett.*, *142*, 59–74, 1996.

Dia, A., B. Dupré, and C. J. Allègre, Nd isotopes in Indian Ocean sediments used as tracer of supply to the ocean and circulation paths, *Mar. Geol.*, *103*, 349–359, 1992.

Döös, K., Interocean exchange of water masses, *J. Geophys. Res.*, *100*, 13,499–13,514, 1995.

Duce, R.A., et al., The atmospheric input of trace species to the world ocean, *Global Biochem. Cycles*, *5*, 193–259, 1991.

Duque-Caro, H., Neogene stratigraphy, paleoceanography and paleobiogeography in northwest South America and the evolution of the Panama seaway, *Palaeogeogr. Palaeoclimatol. Palaeoecol.*, *77*, 203–234, 1990.

Edmond, J. M., Himalayan tectonics, weathering processes, and the strontium isotope record in marine limestones, *Science*, *258*, 1594–1597, 1992.

Eisenhauer, A., K. Gögen, E. Pernicka, and A. Mangini, Climatic influences on the growth rates of Mn crusts during the late Quaternary, *Earth Planet. Sci. Lett.*, *109*, 25–36, 1992.

Elderfield, H., and J. M. Gieskes, Sr isotopes in interstitial waters of marine carbonate sediments, *Nature*, *300*, 493–497, 1982.

Elderfield, H., and E. R. Sholkovitz, Rare elements in pore waters of reducing near shore sediments, *Earth Planet. Sci. Lett.*, *82,* 280–288, 1987.

Elderfield, H., C. J. Hawkesworth, M. J. Greaves, and S. E. Calvert, Rare earth element geochemistry of oceanic ferromanganese nodules and associated sediments, *Geochim. Cosmochim. Acta*, *45*, 513–528, 1981.

Elderfield, H., R. Upstill-Goddard, and E. R. Sholkovitz, The rare earth elements in rivers, estuaries, and coastal seas and their significance to the composition of ocean waters, *Geochim. Cosmochim. Acta*, *54*, 971–991, 1990.

Erel, Y., Y. Harlavan, and J. D. Blum, Lead isotope systematics of granitoid weathering, *Geochim. Cosmochim. Acta*, *58*, 5299–5306, 1994.

Fagel, N., C. Innocent, R. K. Stevenson, and C. Hillaire-Marcel, Deep circulation changes in the Labrador Sea since the Last Glacial Maximum: New constraints from Sm-Nd data on sediments, *Paleoceanography*, *14*, 777–788, 1999.

France-Lanord, C., L. A. Derry, and A. Michard, Evolution of the Himalaya since Miocene time: Isotopic and sedimentologic evidence from the Bengal Fan, in *Himalayan Tectonics*, edited by P.J. Treloar and M. Searle, *Geol. Soc. London Spec. Publ.*, *74*, 603–621, 1993.

Frank, M., and R. K. O'Nions, Sources of Pb for Indian Ocean ferromanganese crusts: A record of Himalayan erosion?, *Earth Planet. Sci. Lett.*, *158*, 121–130, 1998.

Frank, M., R.K. O'Nions, J. R. Hein, and V. K. Banakar, 60 Ma records of major elements and Pb-Nd isotopes from hydrogenous ferromanganese crusts: Reconstruction of seawater paleochemistry, *Geochim. Cosmochim. Acta*, *63*, 1689–1708, 1999a.

Frank, M., B. C. Reynolds, and R. K. O'Nions, Nd and Pb isotopes in Atlantic and Pacific water masses before and after closure of the Panama gateway, *Geology*, *27*, 1147–1150, 1999b.

Frank, M., N. Whiteley, S. Kasten, J. R. Hein, and R. K. O'Nions, North Atlantic Deep Water export to the Southern Ocean over the past 14 Myr: Evidence from Nd and Pb isotopes in ferromanganese crusts, *Paleoceanography 17*(2), 10.1029/2000PA000606, 2002.

Futa, K., Z. E. Peterman, and J. R. Hein, Sr and Nd isotopic variations in ferromanganese crusts from the Central Pacific: Implications for age and source provenance, *Geochim. Cosmochim. Acta*, *52*, 2229–2233, 1988.

Galer, S. J. G., Optimal double and triple spiking for high precision lead isotopic measurement, *Chem. Geol.*, *157*, 255–274, 1999.

Ganachaud, A., and C. Wunsch, Improved estimates of global ocean circulation, heat transport and mixing from hydrographic data, *Nature*, *408*, 453–457, 2000.

German, C. R., G. P. Klinkhammer, J. M. Edmond, A. Mitra, and H. Elderfield, Hydrothermal scavenging of rare-earth elements in the ocean, *Nature*, *345*, 516–518, 1990.

Godfrey, L. V., W. M. White, and V. J. M. Salters, Dissolved zirconium and hafnium distributions across a shelf break in the NE Atlantic, *Geochim. Cosmochim. Acta*, *60*, 3995–4006, 1996.

Godfrey, L. V., D.-C. Lee, W. F. Sangrey, A. N. Halliday, V. J. M. Salters, J.R. Hein, and W.M. White, The Hf isotopic composition of ferromaganese nodules and crusts and hydrothermal manganese deposits: Implications for seawater Hf, *Earth Planet. Sci. Lett.*, *151*, 91–105, 1997.

Goldstein, S. J., and S. B. Jacobsen, The Nd and Sr isotopic systematics of river water dissolved material: implications for the sources of Nd and Sr in seawater, *Chem. Geol.*, *66*, 245–272, 1987.

Goldstein, S. J., and S. B. Jacobsen, Rare earth elements in river waters, *Earth Planet. Sci. Lett.*, *89*, 35–47, 1988.

Goldstein, S. L., and R. K. O'Nions, Nd and Sr isotopic relationships in pelagic clays and ferromanganese deposits, *Nature*, *292*, 324–327, 1981.

Goldstein, S. L., R. K. O'Nions, and P. J. Hamilton, A Sm-Nd isotopic study of atmospheric dusts and particulates from major river systems, *Earth Planet. Sci. Lett.*, *70*, 221–236, 1984.

Gordon, A. L., Interocean exchange of thermocline water, *J. Geophys. Res.*, *91*, 5037–5046, 1986.

Greaves, M. J., H. Elderfield, and E. R. Sholkovitz, Aeolian sources of rare earth elements to the Western Pacific Ocean, *Mar. Chem.*, *68*, 31–38, 1999.

Grousset, F. E., P. E. Biscaye, A. Zindler, J. Prospero, and R. Chester, Neodymium isotopes as tracers in marine sediments and aerosols: North Atlantic, *Earth Planet. Sci. Lett.*, *87*, 367–378, 1988.

Halbach, P., M. Segl, D. Puteanus, and A. Mangini, Co-fluxes and growth rates in ferromanganese deposits from central Pacific seamount areas, *Nature*, *304*, 719–722, 1983.

Halliday, A. N., J. P. Davidson, P. Holden, R. M. Owen, and A. M. Olivarez, Metalliferous sediments and the scavenging residence time of Nd near hydrothermal vents, *Geophys. Res. Lett.*, *19*, 761–764, 1992.

Haq, B. U., Paleogene paleoceanography: Early Cenozoic oceans revisited, *Oceanol. Acta*, *4*, 71–82, 1981.

Harada, K., and S. Nishida, Biostratigraphy of some marine manganese nodules, *Nature*, *260*, 770–771, 1976.

Haug, G. H., and R. Tiedemann, Influence of Panamanian isthmus formation on Atlantic Ocean thermohaline circulation, *Nature*, *393*, 673–676, 1998.

Hemming, S. R., W. S. Broecker, W. D. Sharp, G. C. Bond, R. H. Gwiazda, J. F. McManus, M. Klas, and I. Hajdas, Provenance of Heinrich layers in core V28-82, northeastern Atlantic: $^{40}Ar/^{39}Ar$ ages of ice-rafted hornblende, Pb isotopes in feldspar grains, and Nd-Sr-Pb isotopes in the fine sediment fraction, *Earth Planet. Sci. Lett.*, *164*, 317–333, 1998.

Henderson, G., and K. W. Burton, Using ($^{234}U/^{238}U$) to assess diffusion rates of isotope tracers in ferromanganese crusts, *Earth Planet. Sci. Lett.*, *170*, 169–179, 1999.

Henderson, G., and E. Maier-Reimer, Advection and removal of $^{210}Pb$ and stable Pb isotopes in the oceans: A general circulation model study, *Geochim. Cosmochim. Acta*, *66*, 257–272, 2002.

Hodell, D. A., P. A. Mueller, and J. R. Garrido, Variations in the strontium isotopic compositions of seawater during the Neogene, *Geology*, *19*, 24–27, 1991.

Igel, H., and F. von Blanckenburg, Lateral mixing and advection of reactive isotopes in ocean basins: Numerical modeling, *Geochem. Geophys. Geosys.*, vol. 1, paper number 1999GC000003, [10,402 words, 15 figures, 3 tables, 2 movies], Dec. 13, 1999.

Ingri, J., A. Widerlund, M. Land, Ö. Gustafsson, P. Andersson, and B. Öhlander, Temporal variations in the fraction of the rare earth elements in a boreal river: The role of colloidal particles, *Chem. Geol.*, *166*, 23–45, 2000.

Innocent, C., N. Fagel, and C. Hillaire-Marcel, Sm-Nd isotope systematics in deep-sea sediments: Clay-size versus coarser fractions, *Mar. Geol.*, *168*, 79–87, 2000.

Ito, T., A. Usui, Y. Kajiwara, and T. Nakano, Strontium isotopic compositions and paleoceanographic implication of fossil manganese nodules in DSDP/ODP cores, Leg 1-126, *Geochim. Cosmochim. Acta*, *62*, 1998.

Jeandel, C., Concentration and isotopic composition of Nd in the Southern Atlantic Ocean, *Earth Planet. Sci. Lett.*, *117*, 581–591, 1993.

Jeandel, C., J. K. Bishop, and A. Zindler, Exchange of neodymium and its isotopes between seawater and small and large particles in the Sargasso Sea, *Geochim. Cosmochim. Acta*, *59*, 535–547, 1995.

Jeandel, C., D. Thouron, and M. Fieux, Concentrations and isotopic compositions of neodymium in the eastern Indian Ocean and Indonesian Straits, *Geochim. Cosmochim. Acta*, *62*, 2597–2607, 1998.

Jones, C. E., A. N. Halliday, D. K. Rea, and R. M. Owen, Neodymium isotopic variations in North Pacific modern silicate sediment and the insignificance of detrital REE contributions to seawater, *Earth Planet. Sci. Lett.*, *127*, 55–66, 1994.

Jones, C. E., A. N. Halliday, D. K. Rea, and R. M. Owen, Eolian inputs of lead into the North Pacific, *Geochim. Cosmochim. Acta*, *64*, 1405–1416, 2000.

Joshima, M., and A. Usui, Magnetostratigraphy of hydrogenetic manganese crusts from Northwestern Pacific seamounts, *Mar. Geol.*, *146*, 53–62, 1998.

Kadko, D., and L. H. Burckle, Manganese nodule growth rates determined by fossil diatom dating, *Nature*, *287*, 725–726, 1980.

Kaiho, K., and S. Saito, Oceanic crust production and climate during the last 100 Myr, *Terra Nova*, *6*, 376–384, 1994.

Keigwin, L. D., Isotopic paleoceanography of the Carribbean and East Pacific: Role of Panama uplift in late Neogene time, *Science*, *217*, 350–352, 1982.

Kennett, J. P., Cenozoic evolution of Antarctic glaciation, the

Circum-Antarctic Ocean, and their impact on global paleoceanography, *J. Geophys. Res.*, *82*, 3843–3860, 1977.
Koschinsky, A., and P. Halbach, Sequential leaching of marine ferromanganese precipitates: Genetic implications, *Geochim. Cosmochim. Acta*, *59*, 5113–5132, 1995.
Krishnaswami, S., B. L. K. Somayajulu, and W. S. Moore, Dating of manganese nodules using beryllium-10, in *Ferromanganese Deposits on the Ocean Floor*, edited by D.R. Horn, pp. 117–121, Natl. Sci. Found., Washington, D. C., 1972.
Ku, T. L., A. Omura, and P. S. Chen, $^{10}$Be and U-series isotopes in manganese nodules from the central north Pacific, in *Marine Geology and Oceanography of the Pacific Manganese Nodule Province*, edited by J.L. Bishoff and Z. Piper, pp. 791–814, Plenum, New York, 1979.
Ku, T. L., L. Kusakabe, C. I. Measures, J. R. Southon, J. S. Vogel, D. E. Nelson, and S. Nakaya, Be isotope distribution in the western north Atlantic: A comparison to the Pacific, *Deep Sea Res.*, *37*, 795–808, 1990.
Kusakabe, M., T. L. Ku, J. R. Southon, J. S. Vogel, D. E. Nelson, C. I. Measures, and Y Nozaki, Distribution of $^{10}$Be and $^{9}$Be in the Pacific Ocean, *Earth Planet. Sci. Lett.*, *82*, 231–240, 1987.
Lacan, F., and C. Jeandel, Tracing Papua New Guinea imprint on the central Equatorial Pacific Ocean using neodymium isotopic compositions and Rare Earth Element patterns, *Earth Planet. Sci. Lett.*, *186*, 497–512, 2001.
Lao, Y., R. F. Anderson, W. S. Broecker, S. E. Trumbore, H. J. Hofmann, and W. Wölfli, Transport and burial rates of $^{10}$Be and $^{231}$Pa in the Pacific Ocean during the Holocene period, *Earth Planet. Sci. Lett.*, *113*, 173–189, 1992.
Lear, C. H., H. Elderfield, and P. A. Wilson, Cenozoic deep-sea temperatures and global ice volumes from Mg/Ca in benthic foraminiferal calcite, *Science*, *287*, 269–272, 2000.
Lee, D.-C., A. N. Halliday, J. R. Hein, K. W. Burton, J. N. Christensen, and D. Günther, Hafnium isotope stratigraphy of ferromanganese crusts, *Science*, *285*, 1052–1054, 1999.
Levasseur, S., J.-L. Birck, and C. J. Allègre, Direct measurement of femtomoles of osmium and $^{187}$Os/$^{186}$Os ratio in seawater, *Science*, *282*, 272–274, 1998.
Levasseur, S., J.-L. Birck, and C. J. Allègre, The osmium riverine flux and the oceanic mass balance of osmium, *Earth Planet. Sci. Lett.*, *174*, 7–23, 1999.
Levitus, S., Climatological atlas of the world ocean, *NOAA Prof. Pap.*, *13*, 1–173, 1982.
Ling, H.-F., K. W. Burton, R. K. O'Nions, B. S. Kamber, F. von Blanckenburg, A. J. Gibb, and J. R. Hein, Evolution of Nd and Pb isotopes in Central Pacific seawater from ferromanganese crusts, *Earth Planet. Sci. Lett.*, *146*, 1–12, 1997.
Macdonald, A. M., and C. Wunsch, An estimate of global ocean circulation and heat fluxes, *Nature*, *382*, 436–439, 1996.
Manheim, F. T., Marine Cobalt Resources, *Science*, *232*, 600–608, 1986.
Manheim, F. T., and C. M. Lane-Bostwick, Cobalt in ferromanganese crusts as a monitor of hydrothermal discharge on the Pacific sea floor, *Nature*, *335*, 59–62, 1988.
Marchal, O., R. Francois, T. Stocker, and F. Joos, Ocean thermohaline circulation and sedimentary $^{231}$Pa/$^{230}$Th ratio, *Paleoceanography*, *15*, 625–641, 2000.
Marshall, L. G., Geochronology and land-mammal biochronology of the trans-American faunal interchange, in *The Great American Biotic Interchange*, edited by F.G. Stehli and S.D. Webb, pp. 49–85, Plenum, New York, 1985.
Martin, E. E., and B. A. Haley, Fossil fish teeth as proxies for sea water Sr and Nd isotopes, *Geochim. Cosmochim. Acta*, *64*, 835–847, 2000.
McKelvey, B. A., and K. J. Orians, The determination of dissolved zirconium and hafnium from seawater using isotope dilution inductively coupled plasma mass spectrometry, *Mar. Chem.*, *60*, 245–255, 1998.
McMurtry, G. M., D. L. VonderHaar, A. Eisenhauer, J. J. Mahoney, and H.-W. Yeh, Cenozoic accumulation history of a Pacific ferromanganese crust, *Earth Planet. Sci. Lett.*, *125*, 105–118, 1994.
Measures, C. I, T. L. Ku, S. Luo, J. R. Southon, X. Xu, and M. Kusakabe, The distribution of $^{10}$Be and $^{9}$Be in the South Atlantic, *Deep Sea Res., Part I*, *43*, 987–1009, 1996.
Miller, K. G., R. G. Fairbanks, and G. S. Mountain, Tertiary oxygen isotope synthesis sea level history, and continental margin erosion, *Paleoceanography*, *2*, 1–19, 1987.
Morton, J. L., and N. H. Sleep, A mid-ocean ridge thermal model: Constraints on the volume of axial hydrothermal heat flux, *J. Geophys. Res.*, *90*, 11,345–11,353, 1985.
Nowell, G. M., P. D. Kempton, S. R. Noble, J. G. Fitton, A. D. Saunders, J. J. Mahoney, and R. N. Taylor, High precision Hf isotope ratio measurements of MORB and OIB by thermal ionisation mass spectrometry: Insights into the depleted mantle, *Chem. Geol.*, *149*, 211–233, 1998.
Nozaki, Y., J. Thompson, and K. K. Turekian, The distribution of $^{210}$Pb and $^{210}$Po in the surface waters of the Pacific Ocean, *Earth Planet. Sci. Lett.*, *32*, 304–312, 1976.
Öhlander, B., J. Ingri, M. Land, and H. Schöberg, Change of Sm-Nd isotope composition during weathering of till, *Geochim. Cosmochim. Acta*, *64*, 813–820, 2000.
O'Nions, R. K., S. R. Carter, R. S. Cohen, N. M. Evensen, and P. J. Hamilton, Pb, Nd, and Sr isotopes in oceanic ferromanganese deposits and ocean floor basalts, *Nature*, *273*, 435–438, 1978.
O'Nions, R. K., M. Frank, F. von Blanckenburg, and H.-F. Ling, Secular variation of Nd and Pb isotopes in ferromanganese crusts from the Atlantic, Indian and Pacific Oceans, *Earth Planet. Sci. Lett.*, *155*, 15–28, 1998.
Oxburgh, R., Variations in the osmium isotope composition of sea water over the past 200,000 years, *Earth Planet. Sci. Lett.*, *159*, 183–191, 1998.
Oxburgh, R., Residence time of osmium in the ocean, *Geochem. Geophys. Geosyst.*, vol. 2, Paper number 2000GC000104 [8551 words, 4 figures, 1 table, 1 appendix table], June 21, 2001.
Palmer, M. R., and J. M. Edmond, The strontium isotope budget of the modern ocean, *Earth Planet. Sci. Lett.*, *92*, 11–26, 1989.
Palmer, M. R., and H. Elderfield, Variations in the Nd isotopic composition of foraminifera from Atlantic Ocean sediments, *Earth Planet. Sci. Lett.*, *73*, 299–305, 1985.
Palmer, M. R., and H. Elderfield, Rare earth elements and neodymium isotopes in ferromanganese oxide coatings of Cenozoic foraminifera from the Atlantic Ocean, *Geochim. Cosmochim. Acta*, *50*, 409–417, 1986.
Paytan, A., M. Kastner, E. E. Martin, J. D. Macdougall, and T. Herbert, Marine barite as a monitor of seawater strontium isotope composition, *Nature*, *366*, 445–449, 1993.
Paytan, A., M. Kastner, D. Campbell, and M. H. Thiemens, Sulfur isotopic composition of Cenozoic seawater sulfate, *Science*, *282*, 1459–1462, 1998.
Pegram, W. J. and K. K. Turekian, The osmium isotopic composition change of Cenozoic sea water as inferred from a deep-sea core corrected for meteoritic contributions, *Geochim. Cosmochim. Acta*, *63*, 4053–4058, 1999.
Pegram, W. J., S. Krishnaswami, G. Ravizza, and K. K. Turekian, The record of seawater $^{187}$Os/$^{186}$Os variation through the Cenozoic, *Earth Planet. Sci. Lett.*, *113*, 569–576, 1992.
Pettke, T., A. N. Halliday, and D. K. Rea, Cenozoic evolution of Asian climate and sources of Pacific seawater Pb and Nd derived from eolian dust of sediment core LL44-GPC3, *Paleoceanography,* 10.1029/2001PA000673, in press, 2002.

Peucker-Ehrenbrink, B., and G. Ravizza, The marine osmium isotope record, *Terra Nova*, *12*, 205–219, 2000.

Peucker-Ehrenbrink, B., G. Ravizza, and A.W. Hofmann, The marine $^{187}Os/^{186}Os$ record of the past 80 million years, *Earth Planet. Sci. Lett.*, *130*, 155–167, 1995.

Piepgras, D. J., and S. B. Jacobsen, The isotopic composition of neodymium in the North Pacific, *Geochim. Cosmochim. Acta*, *52*, 1373–1381, 1988.

Piepgras, D. J., and G. J. Wasserburg, Neodymium isotopic variations in seawater, *Earth Planet. Sci. Lett.*, *50*, 128–138, 1980.

Piepgras, D. J., and G. J. Wasserburg, Isotopic composition of neodymium in waters from the Drake Passage, *Science*, *217*, 207–214, 1982.

Piepgras, D. J., and G. J. Wasserburg, Influence of the Mediterranean outflow on the isotopic composition of neodymium in waters of the north Atlantic, *J. Geophys. Res.*, *88*, 5997–6006, 1983.

Piepgras, D. J., and G. J. Wasserburg, Rare earth transport in the western North Atlantic inferred from isotopic observations, *Geochim. Cosmochim. Acta*, *51*, 1257–1271, 1987.

Piepgras, D. J., G. J. Wasserburg, and E. J. Dasch, The isotopic composition of Nd in different water masses, *Earth Planet. Sci. Lett.*, *45*, 223–236, 1979.

Piotrowski, A. M., D.-C. Lee, J. N. Christensen, K. W. Burton, A. N. Halliday, J.R. Hein, and D. Günther, Changes in erosion and ocean circulation recorded in the Hf isotopic compositions of North Atlantic and Indian Ocean ferromanganese crusts, *Earth Planet. Sci. Lett.*, *181*, 315–325, 2000.

Pomies, C., and G. R. Davies, Neodymium isotopes in modern foraminifera from the Indian Ocean: Assessment of the use of Nd isotope composition of foraminifera as a tracer for paleo-oceanic circulation changes, paper presented at 10th Annual V. M. Goldschmidt Conference, Geochem. Soc., Oxford, England, Sept. 3–8, 2000.

Puteanus, D., and P. Halbach, Correlation of Co concentration and growth rate: A method for age determination of ferromanganese crusts, *Chem. Geol.*, *69*, 73–85, 1988.

Ravelo, A. C., and D. H. Andreasen, Enhanced circulation during a warm period, *Geophys. Res. Lett.*, *27*, 1001–1004, 2000.

Ravizza, G., Variations of the $^{187}Os/^{186}Os$ ratios of seawater over the past 28 million years as inferred from metalliferous carbonates, *Earth Planet. Sci. Lett.*, *118*, 335–348, 1993.

Ravizza, G., and K. K. Turekian, The osmium isotopic composition of organic-rich marine sediments, *Earth Planet. Sci. Lett.*, *110*, 1–6, 1992.

Ravizza, G., R. N. Norris, J. Blusztajn, and M.-P. Aubry, An osmium isotope excursion associated with the late Paleocene thermal maximum: Evidence of intensified chemical weathering, *Paleoceanography*, *16*, 155–163, 2001.

Raymo, M. E., and W. F. Ruddiman, Tectonic forcing of late Cenozoic climate, *Nature*, *359*, 117–122, 1992.

Raymo, M. E., W. F. Ruddiman, N. J. Shackleton, and D. W. Oppo, Evolution of Atlantic-Pacific $\delta^{13}C$ gradients over the last 2.5 m.y., *Earth Planet. Sci. Lett.*, *97*, 353–368, 1990.

Raymo, M. E., D. Hodell, and E. Jansen, Response of deep ocean circulation to initiation of northern hemisphere glaciation (3–2 Ma), *Paleoceanography*, *7*, 645–672, 1992.

Rea, D. K., The paleoclimatic record provided by eolian deposition in the deep sea: The geologic history of wind, *Rev. Geophys.*, *32*, 159–195, 1994.

Rehkämper, M., M. Schönbächler, and C. Stirling, Multiple collector ICP-MS: Introduction to instrumentation, measurement techniques and analytical capabilities, *Geostand. Neswl.*, *25*, 23–40, 2001.

Revel, M., M. Cremer, F. E. Grousset, and L. Labeyrie, Grain-size and Sr-Nd isotopes as tracer of paleo-bottom current strength, Northeast Atlantic Ocean, *Mar. Geol.*, *131*, 233–249, 1996.

Reynolds, B. C., M. Frank, and R. K. O'Nions, Nd- and Pb-isotope time series from Atlantic ferromanganese crusts: Implications for changes in provenance and paleocirculation over the last 8 Myr, *Earth Planet. Sci. Lett.*, *173*, 381–396, 1999.

Richter, F. M., D. B. Rowley, and D. J. DePaolo, Sr isotope evolution of seawater: The role of tectonics, *Earth Planet. Sci. Lett*., *109*, 11–23, 1992.

Rutberg, R. L., S. R. Hemming, and S. L. Goldstein, Reduced North Atlantic Deep Water flux to the glacial Southern Ocean inferred from neodymium isotope ratios, *Nature*, *405*, 935–938, 2000.

Sarnthein, M., K. Winn, S. J. A. Jung, J.-C. Duplessy, L. Labeyrie, H. Erlenkeuser, and C. Ganssen, Changes in east Atlantic deepwater circulation over the last 30,000 years: Eight time-slice reconstructions, *Paleoceanography*, *9*, 209–267, 1994.

Schärer, U., P. Copeland, M. Harrison, and M. P. Searle, Age, cooling history, and origin of post-collisional leucogranites in the Karakoram Batholith: A multi-system isotope study, *J. Geol.*, *98*, 233–251, 1990.

Schaule, B. K., and C. C. Patterson, Lead concentrations in the north Pacific: Evidence for global anthropogenic perturbations, *Earth Planet. Sci. Lett.*, *54*, 97–116, 1981.

Schlosser, P., G. Bönisch, M. Rhein, and R. Bayer, Reduction of deepwater in the Greenland sea during the 1980's: Evidence from tracer data, *Science*, *251*, 1054–1056, 1991.

Schmitz, W. J., On the interbasin-scale thermohaline circulation, *Rev. Geophys.*, *33*, 151–173, 1995.

Searle, M., Cooling history, erosion, exhumation and kinematics of the Himalaya-Karakoram-Tibet orogenic belt, in *The Tectonics of Asia*, edited by A. Yin and T. M. Harrison, pp. 110–137, Cambridge Univ. Press, New York, 1996.

Segl, M., et al., $^{10}Be$ dating of a manganese crust from Central North Pacific and implications for oceanic paleocirculation, *Nature*, *309*, 540–543, 1984.

Segl, M., A. Mangini, J. Beer, G. Bonani, M. Suter, W. Wölfli, and C. Measures, $^{10}Be$ in the Atlantic Ocean, a transect at 25°N, *Nucl. Instrum. Methods Phys. Res. Sect. B*, *5*, 332–334, 1987.

Sharma, M., D. A. Papanastassiou, and G. J. Wasserburg, The concentration and isotopic composition of osmium in the oceans, *Geochim. Cosmochim. Acta*, *61*, 3287–3299, 1997.

Sharma, M., G. J. Wasserburg, A. W. Hofmann, and G. J. Chakrapani, Himalayan uplift and osmium isotopes in ocean and rivers, *Geochim. Cosmochim. Acta*, *63*, 4005–4012, 1999.

Sharma, M., G. J. Wasserburg, A. W. Hofmann, and D. A. Butterfield, Osmium isotopes in hydrothermal fluids from the Juan de Fuca Ridge, *Earth Planet. Sci. Lett.*, *179*, 139–152, 2000.

Sharma, P., and B. L. K. Somayajulu, $^{10}Be$ dating of large manganese nodules from world oceans, *Earth Planet. Sci. Lett.*, *59*, 235–244, 1982.

Shaw, H. F., and G. J. Wasserburg, Sm-Nd in marine carbonates and phosphates: Implications for Nd isotopes in seawater and crustal ages, *Geochim. Cosmochim. Acta, 49*, 503–518, 1985.

Shen, G. T., and E. A. Boyle, Thermocline ventilation of anthropogenic lead in the western North Atlantic, *J. Geophys. Res.*, *93*, 15,715–15,732, 1988.

Shimizu, H., K. Tachikawa, A. Masuda, and Y. Nozaki, Cerium and Nd isotope ratios and REE patterns in seawater from the North Pacific ocean, *Geochim. Cosmochim. Acta*, *58*, 323–333, 1994.

Sholkovitz, E. R., H. Elderfield, R. Szymczak, and K. Casey,

Island weathering: River sources of rare earth elements to the Western Pacific Ocean, *Mar. Chem.*, *68*, 39–57, 1999.
Spero, H. J., J. Bijma, D. W. Lea, and B. E. Bemis, Effect of seawater carbonate concentration on foraminiferal carbon and oxygen isotopes, *Nature*, *390*, 497–500, 1997.
Spivack, A. J., and G. J. Wasserburg, Neodymium isotopic composition of the Mediterranean outflow and the eastern North Atlantic, *Geochim. Cosmochim. Acta*, *58*, 2767–2773, 1988.
Stanley, S. M., New horizons for paleontology with two examples: The rise and fall of the Cretaceous Supertethys and the cause of the modern Ice Age, *J. Paleontol.*, *69*, 999–1007, 1995.
Staudigel, H., P. Doyle, and A. Zindler, Sr and Nd systematics of fish teeth, *Earth Planet. Sci. Lett.*, *76*, 45–56, 1985.
Stille, P., Nd-Sr evidence for dramatic changes of paleocurrents in the Atlantic ocean during the past 80 m.y., *Geology*, *20*, 387–390, 1992.
Stille, P., and H. Fischer, Secular variation in the isotopic composition of Nd in Tethys seawater, *Geochim. Cosmochim. Acta*, *54*, 3139–3145, 1990.
Stille, P., M. Steinmann, and S.R. Riggs, Nd isotope evidence for the evolution of the paleocurrents in the Atlantic and Tethys Oceans during the past 180 Ma, *Earth Planet. Sci. Lett.*, *144*, 9–19, 1996.
Stordal, M. C., and G. J. Wasserburg, Neodymium isotopic study of Baffin bay water: Sources of REE from very old terranes, *Earth Planet. Sci. Lett.*, *77*, 259–272, 1986.
Suter, M., Accelerator mass-spectrometry: Fascinating applications and their technical challenges, *Nucl. Instrum. Meth. Phys. Res.*, *Sect. B*, *64*, 361–369, 1992.
Tachikawa, K., C. Jeandel, and B. Dupré, Distribution of rare earth elements and neodymium isotopes in settling particulate material of the tropical Atlantic Ocean (EUMELI site), *Deep Sea Res., Part I*, *44*, 1769–1792, 1997.
Tachikawa, K., C. Jeandel, and M. Roy-Barman, A new approach to the Nd residence time in the ocean: The role of atmospheric inputs, *Earth Planet. Sci. Lett.*, *170*, 433–446, 1999.
Turner, D. R., M. Whitfield, and A. G. Dickson, Equilibrium speciation of dissolved components in freshwater and seawater at 25°C and 1 atm pressure, *Geochim. Cosmochim. Acta*, *45*, 855–881, 1981.
Vance, D., and K. W. Burton, Neodymium isotopes in planktonic foraminifera: A record of the response of continental weathering and ocean circulation rates to climate change, *Earth Planet. Sci. Lett.*, *173*, 365–379, 1999.
van de Flierdt, T., M. Frank, D.-C. Lee, and A. N. Halliday, Glacial weathering and the hafnium isotope composition of seawater, *Earth Planet. Sci. Lett.*, *198*, 167–175, 2002.
Veizer, J., et al., $^{87}Sr/^{86}Sr$, $\delta^{13}C$ and delta $\delta^{18}O$ evolution of Phanerozoic seawater, *Chem. Geol.*, *161*, 59–88, 1999.
Vennemann, T. W., and E. Hegner, Oxygen, strontium, and neodymium isotope composition of fossil shark teeth as a proxy for the palaeoceanography and paleoclimatology of the Miocene northern Alpine Paratethys, *Palaeogeogr., Palaeoclimat., Palaoecol.*, *142*, 107–121, 1998.
Vervoort, J. D, P. J. Patchett, J. Blichert-Toft, and F. Albarède, Relationships between Lu-Hf and Sm-Nd isotopic systems in the global sedimentary system, *Earth Planet. Sci. Lett.*, *168*, 79–99, 1999.
Vidal, P., A. Cocherie, and P. LeFort, Geochemical investigation of the origin of the Manaslu leucogranite (Himalaya, Nepal), *Geochim. Cosmochim. Acta*, *46*, 2279–2292, 1982.
Vlastélic, I., W. Abouchami, S. J. G. Galer, A. W. Hofmann, and C. Claude-Ivanaj, Geographic control on Pb isotopic distribution and sources in Indian Ocean Fe-Mn deposits, *Geochim. Cosmochim. Acta*, *65*, 4303–4319, 2001.
von Blanckenburg, F., Tracing past ocean circulation?, *Science*, *286*, 1862–1863, 1999.
von Blanckenburg, F., and H. Igel, Lateral mixing and advection of reactive isotopes in ocean basins: Observations and mechanisms, *Earth Planet. Sci. Lett.*, *169*, 113–128, 1999.
von Blanckenburg, F., and T. F. Nägler, Weathering versus circulation-controlled changes in radiogenic isotope tracer composition of the Labrador Sea and Northern Atlantic Deep Water, *Paleoceanography*, *16*, 424–434, 2001.
von Blanckenburg, F., and R. K. O'Nions, Response of beryllium and radiogenic isotope ratios in Northern Atlantic Deep Water to the onset of northern hemisphere glaciation, *Earth Planet. Sci. Lett.*, *167*, 175–182, 1999.
von Blanckenburg, F., R. K. O'Nions, N. S. Belshaw, A. Gibb, and J. R. Hein, Global distribution of beryllium isotopes in deep ocean water as derived from Fe-Mn crusts, *Earth Planet. Sci. Lett.*, *141*, 213–226, 1996a.
von Blanckenburg, F., R. K. O'Nions, and J. R. Hein, Distribution and sources of pre-anthropogenic lead isotopes in deep ocean water from Fe-Mn crusts, *Geochim. Cosmochim. Acta*, *60*, 4957–4936, 1996b.
Weissel, J. K., and D. E. Hayes, Magnetic anomalies in the southeast Indian Ocean, in *Antarctic Oceanology II: The Australian-New Zealand Sector*, *Antarctic Res. Ser.*, vol. 19, edited by D.E. Hayes, AGU, Washington, D. C., 1972.
White, W. M., P. J. Patchett, and D. Ben Othman, Hf isotope ratios of marine sediments and Mn nodules: Evidence for a mantle source of Hf in seawater, *Earth Planet. Sci. Lett.*, *79*, 46–54, 1986.
Winter, B., C. M. Johnson, and D. L. Clark, Strontium, neodymium and lead isotope variations of authigenic silicate sediment components from the Late Cenozoic Arctic Ocean: Implications for sediment provenance and the source of trace metals in sea water, *Geochim. Cosmochim. Acta*, *61*, 4181–4200, 1997.
Woodhouse, O. B., G. E. Ravizza, K. K. Falkner, P. J. Statham, and B. Peucker-Ehrenbrink, Osmium in sea water: Concentration and isotopic composition vertical profiles in the eastern Pacific ocean, *Earth Planet. Sci. Lett.*, *173*, 223–233, 1999.
Woodruff, F., and S. Savin, Miocene deepwater oceanography, *Paleoceanography*, *4*, 87–140, 1989.
Xu, X., Geochemical studies of beryllium isotopes in marine and continental natural systems, Ph.D. thesis, 315 pp., Univ. of South. Calif., Los Angeles, 1994.
Yu, E. F., R. Francois, and M. P. Bacon, Similar rates of modern and last-glacial ocean thermohaline circulation inferred from radiochemical data, *Nature*, *379*, 689–694, 1996.
Zachos, J., M. Pagani, L. Sloan, E. Thomas, and K. Billups, Trends, rhythms, and aberrations in global climate 65 Ma to present, *Science*, *292*, 686–693, 2001.

---

M. Frank, Department of Earth Sciences, Institute for Isotope Geology and Mineral Resources, Eidgenössische Technische Hochschule, ETH Zentrum, NO F51.3, Sonneggstrasse 5, CH-8092 Zürich, Switzerland. (frank@erdw.ethz.ch)